Optimization of energy recovery in an industrial wastewater treatment plant

Feldman, Hannah

Publication date:
2018

Document Version
Publisher's PDF, also known as Version of record

Optimization of energy recovery in an industrial wastewater treatment plant

Hannah Feldman

PhD Thesis

October 2018

DTU Chemical Engineering
Department of Chemical and Biochemical Engineering

Technical University of Denmark

Optimization of energy recovery in an industrial wastewater treatment plant

PhD Thesis

Hannah Feldman

Department of Chemical and Biochemical Engineering
Technical University of Denmark

Supervisors
Krist V. Gernaey
Xavier Flores-Alsina
Gürkan Sin
Kasper Kjellberg
Ulf Jeppsson

novozymes

Address: Process and Systems Engineering Center (PROSYS)

Department of Chemical and Biochemical Engineering

Technical University of Denmark

Building 229

Dk-2800 Kgs. Lyngby

Denmark

Phone: +45 4525 2800

Web: www.kt.dtu.dk/forskning/prosys

Print: STEP

DTU Chemical Engineering
Department of Chemical and Biochemical Engineering

Preface

This project was carried out at the Process and Systems Engineering Centre (PROSYS) at the Technical University of Denmark, in collaboration with the wastewater treatment plant at Novozymes. During the duration of my PhD I have been lucky to be able to work together with many different people across universites and industry.

I would like to thank Krist V. Gernaey for giving me the opportunity to do this project and for the guidance along the way. Collaborating with many people can give many different opinions, and I could count on you for support when needed. To Xavier Flores-Alsina, for all the help, discussions and feedback. I am very grateful for all the time you have spent on working on the models with me. To Ulf Jeppsson, for the thorough reading of all my abstracts and articles.

At Novozymes a lot of people were involved in my work in one way or another. I would like to thank Kasper Kjellberg for providing the opportunity to do experimental work on site, and also for the constructive feedback and fruitful discussions. It was a great experience to be able to apply my work in an industrial setting. A lot of discussions were together with Sille Bendix Larsen, whose input was of great value. I would also like to thank all of the operators at the wastewater treatment plant, who were always there to help when needed. I would also like to thank Karin Nikolajsen for reading all my articles, posters and presentations.

I am grateful for all the support from Damien Batstone, who welcomed me in his group for my external stay and has given me a lot of helpful feedback throughout the project. His knowledge on modelling and anaerobic processes really accelerated my work during the external stay.

From DTU I would like to thank all my friends for the discussions, both work-related or otherwise, encouragement for when things weren't going as planned,

and of course all the fun times. Furthermore, I would like to express my thanks to CISV and Lyngby-Taarbæk Harmonieorkester for including me from the beginning.

Finally, I would like to thank my friends and family for their support over the years. I would especially like to thank Philip, who has always believed in me.

Abstract

Biogas production from wastewater is seen as a sustainable way to recover energy. Anaerobic digestion processes convert the organic material in wastewater to biogas, which can subsequently be converted to electricity and heat. The focus of this project is to optimize the energy recovery in an industrial wastewater treatment plant. The main objective is to study how mathematical models can be used for the description and analysis of processes, and subsequently be explored for the optimization of the reactor performance.

The anaerobic digester under study is a granular sludge reactor, where the biomass is present in the form of granules. This leads to high-rate conditions and can be a challenge to model, due to the decoupling of hydraulic and sludge retention time. To this end, two separate models based on the Anaerobic Digestion Model No. 1 (ADM1) were developed: i) A flow + reactor model (Model I), reaching high biomass concentrations by recycling the biomass back into the reactor through an artificial loop, and ii) a granular sludge model (Model II), where the reactions take place within a biofilm.

Both models were calibrated with two separate datasets of three weeks each. The datasets contain extensive measurements of COD, nitrogen, sulfur and phosphorus species, as well as measurements of biogas production and mineral composition. Mass balances verified the quality of the measurements, and an influent fractionation was performed.

Model I was applied for optimization of the process conditions, where it was found that lowering the pH had a positive effect on the chemical dosage to the reactor and did not lead to reduced energy recovery. This strategy was succesfully applied to the full-scale reactor. Simulation results furthermore revealed that while removing sulfur compounds from the influent increased the energy recovery, the gain was

less than the removal cost. Long-term simulations were performed with Model II, where precipitation within the granules was taken into account. It was shown that precipitation can have detrimental effects on the process performance on the long-term, due to the competition for space between precipitates and biomass within the granules. The implementation of both models indicated that the choice of model type depends on the desired output. Model I can be implemented when the model output should be the impact of influent conditions on the biogas production or effluent concentrations, whereas Model II can be used when the biomass affects the output due to for example precipitation kinetics or mass transfer limitations.

The impact of an increased loading rate was one of the optimization strategies that was studied, as the loading is limited by nitrogen removal. An evaluation was made on the potential implementation of the anammox process as an alternative nitrogen removal method post-anaerobic digestion, indicating significant experimental and modelling work is still needed.

Resumé

Fremstilling af biogas fra spildevand udgør en bæredygtig metode til at genvinde energi. Den anaerobe fermenteringsproces omdanner spildevandets organiske materiale til biogas, som efterfølgende kan omdannes til elektricitet og varme. Fokus for nærværende projekt er at optimere energiudbyttet i et industrielt spildevandsanlæg. Hovedformålet er at undersøge, hvorledes matematiske modeller kan udnyttes i beskrivelsen og analysen af processerne, og herefter udnyttes til optimering af bioreaktorens ydelse.

Den anaerobe fermenteringsreaktor, der undersøges, er en reaktor med granulær slam, hvor biomassen forefindes i en biofilm i granulerne. Den type reaktor fører til høje massetransport og reaktions-hastigheder, hvilket kan være en udfordring at simulere med en matematisk model. For at adressere dette er der udviklet to forskellige model-versioner af Anaerobic Digestion Model No. 1 (ADM1): i) En flow- og reaktormodel (Model I), hvor høj biomassekoncentration opnås ved at recirkulere biomassen tilbage til reaktoren via et simuleret loop, og ii) En model baseret på biomassegranulat (Model II), hvor reaktionerne foregår i en biofilm.

Begge modeller blev kalibreret efter to uafhængige datasæt, svarende til 3 ugers drift per datasæt. Datasættene indeholder detaljerede målinger af COD, nitrogen-, svovl- og fosforforbindelser samt målinger af biogas produktion og mineraler. Kvaliteten af begge datasæt er verificeret via massebalancer, og målingerne lavet på det indkommende spildevand blev brugt til at lave en fraktionering af spildevandets sammensætning.

Model I blev anvendt til optimering af procesbetingelser, hvor det viste sig at pH-sænkning udviste positiv effekt ved at mindske doseringen af kemikalier til bioreaktoren og i øvrigt ikke medførte reduktion i energiudbytte. Denne strategi blev også anvendt på den fuld-skala reaktor. Simuleringsresultaterne afslørede, at fjernelse

af svovlforbindelser fra reaktorfødestrømmen medførte et forbedret energiudbytte, men at værdien af det højere udbytte ikke fuldt kan kompensere for omkostningerne forbundet med at fjerne svovlforbindelserne. Langtidssimulering blev udført med Model II under hensyn til effekten fra udfældning i granulerne. Det blev demonstreret, at udfældning kan have en langsigtet negativ effekt på reaktionshastigheden som følge af indbyrdes konkurrence om reaktionsvolumen i granulerne i mellem udfældningsprodukterne og selve biomassen.

Effekten af at øge spildevand flowet var en af de optimeringsstrategier, der blev undersøgt, idet bioreaktor load er begrænset af trinnet til fjernelse af nitrogen. En evaluering af anammox processen som mulig alternativ metode til nitrogenfjernelse efter den anaerobe fermentor indikerer at betydeligt eksperimentelt- og modelleringsarbejde stadig udestår.

Contents

Nomenclature

Symbol	Definition	Unit
Roman symbols		
A_b	Total biofilm area	m^2
A_k	Area of the sphere at point *k*	m^2
C	Carbon	-
C_{SI}	Carbon content of S_I	$kmolC\,(kgCOD)^{-1}$
C_{XI}	Carbon content of X_I	$kmolC\,(kgCOD)^{-1}$
Ca^{2+}	Calcium measurements	$g\,m^{-3}$
$Ca_3(PO_4)_2$	Tricalcium phosphate	-
$CaCO_3$	Calcium carbonate	-
CaO	Quicklime	-
CH_4	Methane production measurements	$m^3\,d^{-1}$
Cl^-	Chloride measurements	$g\,m^{-3}$
CO_2	Carbon dioxide production measurements	$m^3\,d^{-1}$
COD	Chemical Oxygen Demand	-
COD_{sol}	Soluble COD measurements	$g\,m^{-3}$
COD_{part}	Particulate COD measurements	$g\,m^{-3}$
COD_T	Total COD measurements	$g\,m^{-3}$
#D	Dataset for model testing	-
Et-OH	Ethanol measurements	$g\,m^{-3}$
Fe^{x+}	Iron (II/III) measurements	$g\,m^{-3}$
ΔG	Gibbs free energy	J
G_{CH4}	Methane production rate (gas)(ADM1)	$m^3\,d^{-1}$
G_{CO2}	Carbon dioxide production rate (gas)(ADM1)	$m^3\,d^{-1}$
G_{H2}	Hydrogen production rate (gas)(ADM1)	$m^3\,d^{-1}$
G_{H2S}	Hydrogen sulfide production rate (gas)(ADM1)	$m^3\,d^{-1}$
G - L	Gas liquid separation unit	-

Continued on next page

Continued from previous page

Symbol	Definition	Unit
H	Hydrogen	-
H_2S	Hydrogen sulfide production rate	$m^3\,d^{-1}$
$H_xPO_4^{3-x}$	Phosphate measurements	$g\,m^{-3}$
K^+	Potassium measurements	$g\,m^{-3}$
K_{hyd}	Hydrolysis rate	d^{-1}
K_I	Inhibition constant	$kgCOD\,d^{-1}$
K_m	Maximum specific uptake rate	d^{-1}
K_s	Half-saturation constant	$kgCOD\,d^{-1}$
L	Biofilm thickness	m
$L_{boundary}$	Thickness of the boundary layer	m
L_{max}	Maximum biofilm thickness	m
LCFA	Long chain fatty acids	$g\,m^{-3}$
M	Mixing section	-
Mg^{2+}	Magnesium measurements	$g\,m^{-3}$
N	Nitrogen	-
N_{aa}	Nitrogen content of amino acids	$kmolN\,(kgCOD)^{-1}$
$N_biofilm$	Number of layers within the biofilm	-
N_bulk	Bulk layer	-
n_g	Number of granules	-
N_{pr}	Nitrogen content of proteins	$kmolN\,(kgCOD)^{-1}$
N_{SI}	Nitrogen content of S_I	$kmolN\,(kgCOD)^{-1}$
N_{XI}	Nitrogen content of X_I	$kmolN\,(kgCOD)^{-1}$
N_2	Nitrogen gas	-
Na^+	Sodium measurements	$g\,m^{-3}$
NaOH	Sodium hydroxide	-
NH_x	Ammonium/ammonia measurements	$g\,m^{-3}$
NO_2	nitrite measurements	$g\,m^{-3}$
NO_3	nitrate measurements	$g\,m^{-3}$
O	Oxygen	-
O_2	Oxygen	-
P	Phosphorus	-
ΔP	Pressure difference	atm
P_{bac}	Phosphorus content of bacteria	$kmolP\,(kgCOD)^{-1}$
PHA	Polyhydroxyalkanoate	-
pK_a	Acid dissociation constant	-

Continued on next page

Continued from previous page

Symbol	Definition	Unit
P_{li}	Phosphorus content of lipids	$kmolP\,(kgCOD)^{-1}$
R	Universal gas constant	$L\,atm\,mol^{-1}\,K^{-1}$
R1	Expanded sludge bed section of the reactor	-
R2	Polishing section of the reactor	-
$r_{biomass}$	Rate of biomass growth	$g\,m^{-3}\,d^{-1}$
$r_{organic}$	Rate of organic growth	$g\,m^{-3}\,d^{-1}$
$r_{precipitation}$	Rate of precipitation	$g\,m^{-3}\,d^{-1}$
S	Sulfur	-
S_I	Inert soluble compound (model)	$kg\,m^{-3}$
SO_x^{2-}	Sulfate/sulfite measurements	$g\,m^{-3}$
S_{aa}	Amino acids (ADM1)	$kgCOD\,m^{-3}$
S_{ac}	Total acetic acid (ADM1)	$kgCOD\,m^{-3}$
$S_{biomass}$	S content in biomass (ADM1)	$kmolS\,(kgCOD)^{-1}$
S_{bu}	Total butyric acid (ADM1)	$kgCOD\,m^{-3}$
S_{ca}	Calcium (ADM1)	$kmol\,m^{-3}$
S_{CH4}	Methane (liquid) (ADM1)	$kgCOD\,m^{-3}$
S_{cl}	Chloride (ADM1)	$kmol\,m^{-3}$
S_{COD}	soluble COD (ADM1)	$kgCOD\,m^{-3}$
S_{eth}	Ethanol (ADM1)	$kgCOD\,m^{-3}$
S_{fa}	Fatty acids (ADM1)	$kgCOD\,m^{-3}$
S_{H2}	Hydrogen (liquid) (ADM1)	$kgCOD\,m^{-3}$
S_{IC}	Inorganic carbon (liquid) (ADM1)	$kmol\,m^{-3}$
S_{IN}	Inorganic nitrogen (ADM1)	$kmol\,m^{-3}$
S_{IP}	Inorganic phosphorus (ADM1)	$kmol\,m^{-3}$
S_{IS}	Inorganic total sulfides (ADM1)	$kmol\,m^{-3}$
S_K	Potassium (ADM1)	$kmol\,m^{-3}$
S_{Mg}	Magnesium(ADM1)	$kmol\,m^{-3}$
S_{Na}	Sodium (ADM1)	$kmol\,m^{-3}$
S_{pro}	Total propionic acid (ADM1)	$kgCOD\,m^{-3}$
S_{prot}	Sulfur content in proteins (ADM1)	$kmolS\,(kgCOD)^{-1}$
S_{su}	Sugars (ADM1)	$kgCOD\,m^{-3}$
S_{va}	Total valeric acid (ADM1)	$kgCOD\,m^{-3}$
S_{VFA}	Volatile fatty acids (ADM1)	$kgCOD\,m^{-3}$
T	Temperature	Kelvin
t_f	assumed time until steady state	days

Continued on next page

Continued from previous page

Symbol	Definition	Unit
TN	Total nitrogen measurements	$g\,m^{-3}$
TP	Total phosphorus measurements	$g\,m^{-3}$
u_D	Detachment rate from the biofilm surface	$m\,d^{-1}$
u_F	Net growth rate of the particulate species	$m\,d^{-1}$
V	Volume	m^3
V_{gas}	Gas volume in the bioreactor	m^3
V_{liq}	Liquid volume in the bioreactor	m^3
VFA	Volatile fatty acids measurements	$g\,m^{-3}$
X_{aa}	Acidogens (ADM1)	$kgCOD\,m^{-3}$
X_{ac}	Acetate degraders (ADM1)	$kgCOD\,m^{-3}$
X_{bio}	Biomass (ADM1)	$kgCOD\,m^{-3}$
X_{c4}	Butyrate and valerate degraders (ADM1)	$kgCOD\,m^{-3}$
X_{ch}	Carbohydrates (ADM1)	$kgCOD\,m^{-3}$
X_{EtOH}	Ethanol degraders (ADM1)	$kgCOD\,m^{-3}$
X_{fa}	Acidogens (ADM1)	$kgCOD\,m^{-3}$
X_{H2}	Hydrogenotrophic methanogens (ADM1)	$kgCOD\,m^{-3}$
X_I	Inert particulate organics (ADM1)	$kgCOD\,m^{-3}$
$X_{inorganic}$	Particulate inorganic matter(ADM1)	$kgCOD\,m^{-3}$
X_{li}	Lipids (ADM1)	$kgCOD\,m^{-3}$
X_{met}	Methanogens (ADM1)	$kgCOD\,m^{-3}$
X_{org}	Particulate organic material (ADM1)	$kgCOD\,m^{-3}$
X_{pr}	Proteins (ADM1)	$kgCOD\,m^{-3}$
X_{pro}	Propionate degraders (ADM1)	$kgCOD\,m^{-3}$
X_{su}	Acidogens (ADM1)	$kgCOD\,m^{-3}$
X_{SRB}	Sulfate reducing bacteria (ADM1)	$kgCOD\,m^{-3}$
$X_{SRB,H2}$	hydrogenotrophic sulfate reducing bacteria (ADM1)	$kgCOD\,m^{-3}$
z	Radial distance within the biofilm	m
Z_i	Chemical species concentration of species i (algebraic variable of physico-chemical module)	$kmol\,m^{-3}$
Greek symbols		
$\rho_{biofilm}$	Biofilm density	$kgTSS\,m^{-3}$
Abbreviations		
AD	Anaerobic digestion	

Continued on next page

Continued from previous page

Symbol	Definition	Unit
ADM1	Anaerobic digestion model no. 1	
AFRBR	Anaerobic fluidized bed reactor	
AnAOB	Anaerobic ammonium oxidizing bacteria	
AOB	Aerobic oxidizing bacteria	
ASM	Activated sludge model	
BSM	Benchmark simulation model	
CANR	Complete autotrophic nitrogen removal	
CAPEX	Capital expenditures	
CFD	Computational fluid dynamic	
CSTR	Continuous stirred tank reactor	
DA	Degree of acidification	
DAMO	Denitrifying anaerobic methane oxidizing bacteria	
DO	Dissolved oxygen	
EGSB	Expanded granular sludge bed	
HB	Heterotrophic bacteria	
HRT	Hydraulic retention time	
IC	Internal circulation	
IRR	Internal rate of return	
ISS	Inorganic suspended solids	
MET	Methanogens	
MOB	Methane oxidizing bacteria	
NOB	Nitrite oxidizing bacteria	
NPV	Net present value	
ODE	Ordinary differential equation	
PAO	Phosphate accumulating organisms	
PAT	Pre-acidification tank	
PCF	Physico-chemical framework	
PDE	Partial differential equations	
PHA	Polyhydroxyalkanoates	
RPI	Reactor performance index	
RSS	Residual sum of squares	
RT	Recirculation tank	
SBR	Sequential batch reactor	
SI	Saturation index	
SMA	Specific methanogenic activity	

Continued on next page

Continued from previous page

Symbol	Definition	Unit
SOB	Sulfide oxidizing bacteria	
SRB	Sulfate reducing bacteria	
SRT	Solids retention time	
TSS	Total suspended solids	
UASB	Upflow anaerobic sludge blanket	
VSS	Volatile suspended solids	
WWTP	Wastewater treatment plant	

1 Introduction

1.1 Energy recovery

Energy is necessary for modern day life. Communication, safety, economics, production and everyday appliances are some examples that need a continuous supply of energy in the form of heat or electricity. Traditional energy sources are for example derived from oil, gas or coal and are unsustainable. When being used, they release carbondioxide into the atmosphere (IPCC, 1996), and the supply is limited (Dalgaard et al., 2001). Furthermore, as there is a high dependency on energy, the availability of oil and gas go hand in hand with economic and political power in a region (Healy and Barry, 2017).

Due to the above-mentioned issues, local recovery of energy is desired. One of the sources that is high in organic matter, and thus has a considerable energy potential, is wastewater. The organic material in wastewater must be removed, as it will otherwise lead to pollution of the environment. Removal of organics can be done by the activated sludge process. This process removes both the nitrogen and organic material from the wastewater. However, in that case the organics are needed for nitrogen removal and no/limited energy can be recovered depending on the COD:N ratio in the wastewater. Another process to remove organic material is through anaerobic digestion. This process does recovery energy in the form of heat and electricity by producing methane (biogas). In this case, there is no nitrogen removal, which is a large contributor to eutrophication of rivers and lakes (Howarth and Marino, 2006). In order to maintain efficient energy recovery from anaerobic digestion, the nitrogen must be removed in an alternative way. Autotrophic nitrogen removal is capable of removing nitrogen without the need of organics. The next sections will go further into detail about these two wastewater treatment processes. In the rest of the thesis, organics will be referred to as chemical oxygen

demand (COD), which is a term used in the wastewater sector to group together different organic and inorganic compounds that can be oxidized.

1.2 Anaerobic digestion

As mentioned previously, anaerobic digestion (AD) converts organics to biogas (mainly carbon dioxide + methane). The methane of the biogas can be converted to heat and electricity. This is a naturally occuring process, and while it is believed bath water in Assyria in the 10th Century B.C. was heated by biogas (Bond and Templeton, 2011), in the modern world the technology was first introduced for wastewater treatment in India in 1897 (Abbasi et al., 2012). Since then, the technology has been developed significantly, and today there is wide variety of AD technologies available for both municipal and industrial wastewater (van Lier et al., 2001).

1.2.1 Process pathway

The conversion of organics to methane and carbondioxide is not a one-step process. On the contrary, many different types of micro-organsims are involved and live in symbiosis (Figure 1.1). First of all, particulate COD in the form of proteins, lipids and carbohydrates is hydrolyzed to sugars, amino acids and long chain fatty acids. This process is carried out by fermentative bacteria. Subsequently, acidogens convert the previously mentioned compounds to volatile fatty acids (VFA; acetate, butyrate, propionate, valerate). Acetogens convert the VFA to hydrogen (H_2) and carbondioxide (CO_2), as well as acetate (from butyrate, propionate and valerate). Finally, methanogens can produce methane (CH_4) and CO_2 from either hydrogen and carbondioxide, or acetate (Gujer and Zehnder, 1983).

1.2.2 High-rate AD technologies

The suitability of a specific AD technology is dependent on the type of wastewater and the loading rate. A distinction must be made between municipal and industrial wastewater, as well as solid waste and liquid waste. While municipal wastewater treatment plants have to operate with loading peaks during daily operation (day/night), industrial treatment plants have fluctuating wastewater characteristics, which depend on the production scheme of the factory upstream. Process parameters that can be a challenge to traditional processes are high loading rates, variable pH (Fang and Liu, 2002), influent degradability (Astals et al., 2013) and non-standard N:COD and P:COD ratios (Punal et al., 2000). Furthermore, indus-

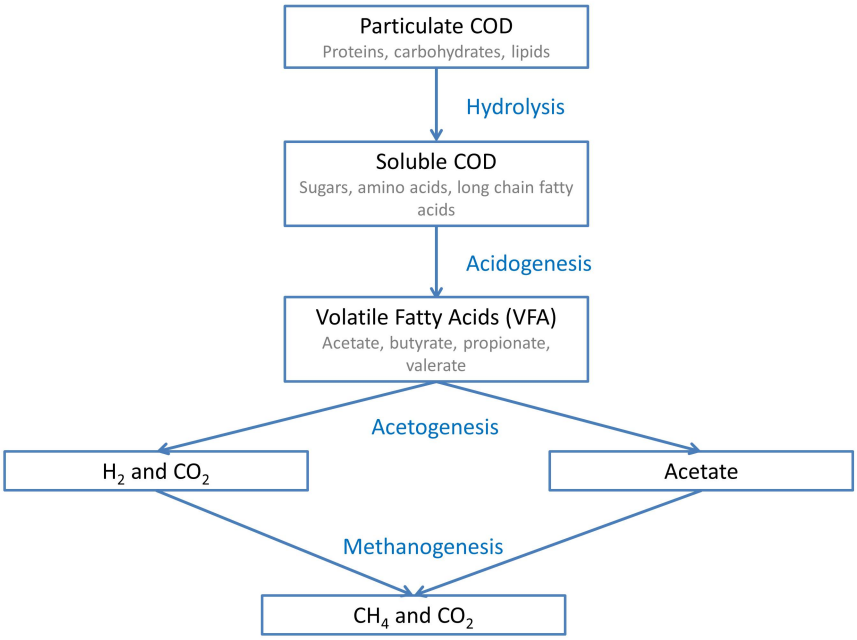

Figure 1.1. Schematic representation of the reactions taking place in an anaerobic digester.

trial wastewaters can contain high concentrations of metals, anions and cations, as well as sulfate. While metals and sulfate can be inhibitory to the process and decrease the energy recovery (Chen et al., 2008), the presence of anions and cations can lead to precipitation and cause not only decrease of methanogenic activity, but also cementation inside the reactor (van Langerak et al., 1998, 2000). This will have catastrophic effects on the reactor performance. All of these factors need to be taken into account when designing a new reactor.

The anaerobic digestion technologies available can be distuingished into two main groups: i) conventional systems, and ii) high-rate systems. Conventional systems are generally used for the digestion of sludge. High-rate systems retain the biomass inside the reactor, and can therefore run under high loading rates by decoupling the sludge retention time and hydraulic retention time (van Lier et al., 2015). Of the high-rate systems, the most frequently applied technology used to be the upflow anaerobic sludge blanket (UASB) reactor, which has also given rise to systems such

as the expanded granular sludge bed (EGSB) and internal circulation (IC) reactors. The number of applications for the latter two reactor types is increasing (van Lier, 2008). All three reactor types retain the biomass by granule formation.

The UASB gets its name from the description of the process. The influent wastewater is fed at the bottom and flows upwards in the anaerobic reactor where the biomass is settled in a sludge bed. In the EGSB, effluent recirculation is combined with a tall reactor to generate a high superficial velocity (Seghezzo et al., 1998). This, as the name of the reactor indicates, expands the sludge bed, optimizing the biomass to wastewater contact. The internal circulation reactors have a self-controlling mechanism to maintain a high flow rate. The degree of internal circulation is dependent on the COD loading rate, and subsequentally the amount of biogas produced. More detail on the IC reactor can be found in Chapter 2, as it is the technology this study focuses on. A list of commercial applications of high-rate AD technologies has been published in 2008 by van Lier (2008).

1.3 Autotrophic nitrogen removal

Conventional nitrogen removal is achieved through the activated sludge process (Figure 1.2). Ammonium (NH_4) is converted to nitrite (NO_2) by ammonium oxidizing bacteria (AOB). AOB need oxygen (O_2) to perform this conversion. Nitrite is subsequently converted to nitrate (NO_3) by nitrite oxidizing bacteria (NOB), and finally nitrogen gas (N_2) by heterotrophic denitrifying bacteria. The conversion of nitrite to nitrate needs oxygen, while the last step to nitrogen gas needs COD. The activated sludge process is therefore high in oxygen consumption, and thus energy consuming by means of aeration. An alternative way to remove the nitrogen is through autotrophic nitrogen removal (Mulder et al., 1995). In this process, the first step is carried out by AOB. However, anaerobic ammonium oxidizing bacteria (anammox or AnAOB) are able to use the nitrite as electron acceptor to directly produce nitrogen gas from ammonium. This bypasses the rest of the conventional nitrogen cycle (Figure 1.2).

1.3.1 Advantages of autotrophic nitrogen removal

The main advantages of autotrophic nitrogen removal over conventional nitrogen removal in the activated sludge process are:

- Lower energy consumption, due to the reduced need of oxygen (Van Hulle et al., 2010).

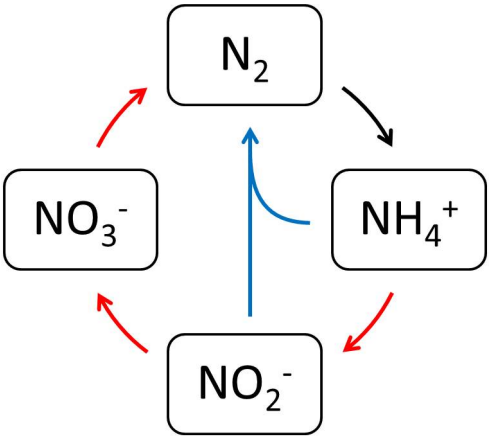

Figure 1.2. The nitrogen cycle. The traditional activated sludge process is represented by the red arrows. The autotrophic nitrogen removal process is represented by the blue arrows.

- Lower biomass yield, because anammox are slow growing organisms (Suneethi et al., 2014). This reduces the cost of sludge disposal.
- No COD needed for nitrogen removal (Zhao et al., 2015), so this can be redirected to anaerobic digestion to increase the energy recovery of the wastewater treatment plant.

1.3.2 Technologies

The first autotrophic nitrogen removal reactor was built in 2002 in Rotterdam, The Netherlands (van der Star et al., 2007). Since then, a wide variety of reactors with different operational schemes and biomass retention types has been developed by different companies and universities. While initially the two-stage process was developed, where partial nitritation and autotrophic nitrogen removal are separated from each other, current development favours one-stage technologies. Here the whole process takes place in one reactor instead of two.

One-stage technologies are often favoured, due to the lower space occupation and capital expenditures (CAPEX) investment (Cao et al., 2017). Sludge retention is desired and can be achieved by growing the bacteria on carriers, such as in the ANITA Mox process from Veolia Water Technologies. The first full-scale ANITA Mox plant was developed at Sjölunda, Sweden (Christensson et al., 2013). This plant now also functions as a seeding producer for new plants, where approximately 3-15

% of the added plastic carriers contain an anammox biofilm.

Another method for sludge retention is through the application of a granular sludge reactor. A commonly used granular sludge reactor is the upflow anaerobic sludge blanket (UASB) reactor (Xing et al., 2014). Granules can be seen as a type of biofilm, where anaerobic, anoxic, and aerobic conditions are present. Instead of growth of a biofilm on a plastic carrier, granules consist only of biomass, in which constant competition between different species occurs. Heterotrophic bacteria (HB) compete with AOB and NOB for dissolved oxygen, while NOB, anammox and HB compete for nitrite (Vangsgaard et al., 2012). Paques has patented the continuous granular ANAMMOX® process, in which biomass retention results in high conversion rates.

The last method for sludge retention discussed here is by means of the sequential batch reactors. The Deammonification (DEMON®) technology is the most used sequential batch reactor (SBR) system, with 80 % of all SBR systems being the DEMON® configuration (Lackner et al., 2014). The first implementation of this process was in Strass, Austria (Wett, 2006). The biomass in an SBR is present as suspended sludge. An issue with suspended sludge is that wash-out takes place when the HRT is unstable.

1.3.3 Discussion on available technologies

The technologies are diverse in application, biomass growth and retention, as well as in control methods. Choosing the right application for a process is dependent on the type of wastewater, loading rates and investment potential. Since the first installation in 2002, which is a two-stage reactor, the one-stage reactor has gained in popularity. As of 2014, 88 % of the installations are one-stage. While most installations are SBR, granular sludge systems treat the highest amount of nitrogen per unit reactor volume (Lackner et al., 2014). For this reason, part of the thesis will look into the application of a one-stage anammox process, and more specifically a granular sludge reactor.

1.4 Mathematical modelling of wastewater treatment plants

The application of mathematical models to wastewater treatment plants is beneficial for elucidating the reactions taking place inside a reactor, evaluating reactor performance and important process parameters and finally process optimization. While it is possible to find this information through lab- and pilot-scale studies,

experimental work is energy, materials and time intensive (Batstone and Keller, 2003). To overcome these issues with mathematical models, these should be fast and robust to simulate many different scenarios within a certain time-frame.

The first platform for mathematical models for wastewater treatment plants that was relatively easy to use in terms of computer power needed and model complexitiy was the Activated Sludge Model No. 1 (ASM1), developed in in 1986 by the International Association on Water Pollution Research and Control (IAWPRC) task group. Over the years model extensions were added to increase the number of processes the ASM1 could describe. Additionally, this increased the model complexity.

The ASM platform has also given rise to models for different applications, such as anaerobic digestion and autotrophic nitrogen removal. While these processes are inherently different, the models follow the set-up of the ASM, and therefore allow for plant-wide modelling of wastewater treatment plants.

1.4.1 Anaerobic Digestion Model No. 1 (ADM1)

The anaerobic digester in this study will be simulated with the Anaerobic Digestion Model No. 1 (ADM1). This model was published in 2002 by an IWA task group (Batstone et al., 2002a), combining many different models to one generic model. In 2006, Rosen and Jeppsson published the implementation of ADM1 within the IWA Benchmark Simulation Model No. 2 (BSM2), which gives a full overview of all equations and mass balances of the model (Rosen and Jeppsson, 2006).

1.4.1.1 Extensions

Since the publication of the ADM1 numerous extensions have been developed. These can be divided into two parts: 1) the extension of reactions happening on a biological and/or chemical level, and 2) the extension of the applications of the ADM1 to fit with numerous reactor designs. The following sections will focus on the first type, extensions of biological and chemical processes. An overview on the application of ADM1 on biofilm systems is given in Chapter 3 (flow and reactor models) and Chapter 5 (biofilm models).

Sulfate

Just one year after the publication of the ADM1, Fedorovich et al. (2003) published the ADM1 extension with sulfate reduction processes. This extension is important for anaerobic digesters where a signficant amount of sulfate enters the reactor.

Sulfate is reduced by sulfate reducing bacteria (SRB), which compete with VFA degraders and methanogens for carbon source and hydrogen. A by-product of sulfate reduction is hydrogen sulfide (H_2S), which is toxic to bacteria. Consequently, the impact of influent sulfate on anaerobic digestion is a reduced biogas production and subsequently energy production by 1) loss of carbon source and hydrogen to sulfate reduction instead of methane production, and 2) reduced methanogenic activity due to sulfide inhibition. Several implementations of sulfur conversion processes have since been published (Flores-Alsina et al., 2016). Some major differences between the extension published by Fedorovich et al. (2003) and later implementations, such as Batstone (2006) and Flores-Alsina et al. (2016) is the type of sulfate reducing bacteria present that compete for electrons. While Fedorovich et al. (2003) takes into account SRB using organic acids as well as hydrogen as electron source, Batstone (2006) states that at low S:COD ratios it can be assumed only hydrogen consuming SRB are present. In the case of high strength and sulfate-rich wastewater, it can be assumed that hydrogen is depleted and SRB take up organic acids instead (Barrera et al., 2015). Flores-Alsina et al. (2016) also take into account iron conversion from Fe^{3+} to Fe^{2+} with either hydrogen or hydrogen sulfide as electron donor (Solon et al., 2015b).

Phosphorus

Phosphorus accumulating organisms (PAO) can store phosphorus in the form of polyphosphates when oxygen is present. In the presence of VFA, PAO are capable of degrading polyphosphates to polyhydroxyalkanoates (PHA). In the ADM1 model extension no growth and polyphosphate production is assumed, as conditions are anaerobic (Flores-Alsina et al., 2016).

Ion speciation/pairing

The extension published by Flores-Alsina et al. (2015) describes physico-chemical processes for ion speciation and pairing, as well as pH variations. This implementation can be used to predict the pH in a system, as well as be coupled with the precipitation model discussed below.

Precipitation kinetics

Minerals in wastewater have the potential to precipitate inside the reactor. One of the main contributors to precipitation is the carbonate produced within the reactor, which precipitates with calcium to limestone (calcium carbonate) (Kazadi Mbamba et al., 2015b). If the influent contains high concentrations of phosphate, magnesium and ammonium, there is a chance of struvite production. Kazadi Mbamba

et al. (2015a,b) developed an extension to the ADM1 to account for precipitation kinetics.

Ethanol
The equations for ethanol production and degradation in anaerobic digestion of glucose were published already in 1997 by Kalyuzhnyi (Kalyuzhnyi, 1997). However, these equations were not part of the initial ADM1. The choice of omitting ethanol was made because this alcohol degrades to acetate relatively easily, and concentrations in most anaerobic digesters will be low (Batstone et al., 2002a). Peiris et al. (2006) included the ethanol equations in the ADM1, as the digestion product they were aiming for (hydrogen) had been reported to have significant concentrations of ethanol as by-product.

1.4.1.2 Applications

Due to the many states and conversion processes present in the ADM1, the model is applicable to a wide variety of wastewater treatment industries. Shang et al. (2005) implemented the ADM1 to a full-scale municipal anaerobic digester treating sewage sludge and had good biogas production predictions of no more than 10 % deviation with the data. Implementations on traditional chinese medicine wastewater (Chen et al., 2009), co-digestion of olive mill wastewater and olive mill solid waste (Boubaker and Ridha, 2008), pig slurry (Girault et al., 2011), opium alkaloids effluent (Dereli et al., 2010) and grass silage (Koch et al., 2010; Wichern et al., 2009) resulted in good fits between model outputs and data. However, in all these cases, the wastewater was taken from the full-scale plant and fed to a lab- or pilot-scale reactor.

While there are many implementations of the ADM1 reported for lab- and pilot-scale data for industrial processes, full-scale implementation is more rare. Often, wastewater from a full-scale plant is taken and experiments on a smaller scale are performed to be able to monitor all model states. While model implementation on lab- and pilot-scale can be a useful indication for process performance, it does not mean that the model can be directly upscaled to full-scale for process control or optimization strategies. The controlled environment of a lab reactor cannot be replicated on full-scale.

Some examples of industrial applications show-case the benefit of model implementation directly on full-scale. Batstone and Keller (2003) applied the ADM1 to two industrial cases. In the first case study the aim was to simulate the influence of

a pH decrease on calcium carbonate precipitation within the reactor (precipitation was unwanted). A cost analysis was made on the results to make a final recommendation. In this case, the cost analysis is not something that can be tested in smaller scale first, because it is not certain that you can upscale the chemical dosing for pH control. Another full-scale implementation of the ADM1 can be found in Elaiuy et al. (2018), in which the ADM1 is cross validated to describe a large-scale covered in-ground anaerobic reactor treating sugarcane vinasse.

1.4.2 Complete Autotrophic Nitrogen Removal (CANR) model

The first one-stage model to describe the Complete Autotrophic Nitrogen Removal (CANR) process in a biofilm was published by Koch et al. (2000). The model is a relatively simple stoichiometric kinetic model describing AOB, NOB and AnAOB processes. No heterotrophic bacteria were taken into account, as it was assumed no COD was present in the influent. Furthermore, this model assumes the nitrogen content of biomass to be zero. Hao et al. (2002) expanded on this model by including ammonium consumption for biomass growth, in order to close the nitrogen mass balances. All subsequent models discussed further contain the stoichiometric and kinetic equations presented by Koch et al. (2000) and Hao et al. (2002).

Over the years, the model has become increasingly more complex by the addition of additional reactions or increased biofilm complexity. Volcke et al. (2010) implemented a biofilm model on granular scale. The amount of granules in the reactor is dependent on the reactor volume and the granule size, which is a fixed parameter. This model does not include heterotrophic biomass, inhibition of nitrite and ammonium, as the concentrations for which inhibition of these compounds takes place is relatively high. The competition between heterotrophic biomass and anammox was included by Mozumder et al. (2013), while Corbalá-Robles et al. (2016) included the inhibition for both nitrite and ammonium.

The implementation of the previous two models was done in Aquasim. A Matlab implementation was developed by Vangsgaard et al. (2012). The model includes nitrite inhibition, heterotrophic competition, as well as external mass transfer limitations. This last addition has not been included in previous versions of the CANR model. The external mass transfer of a compound is dependent on the diffusivity of the soluble compound in water divided by the thickness of the mass transfer boundary layer. This means that the larger the boundary layer, the smaller the mass transfer coefficient, and thus the larger the external mass transfer limitation. In practice, a larger boundary layer results in a smaller flux of soluble compounds

passing into the granule. In other words, conversion rates could be limited by this factor and including it gives a more comlete description of the physico-chemical properties of granules.

1.5 Objectives of the PhD study

The aim of this project is to optimize the energy recovery in the industrial wastewater treatment plant at Novozymes A/S (Kalundborg, Denmark). The project is divided in two parts.

In the first part, the anaerobic digester producing biogas is evaluated (Chapter 2) and studied through mathematical models (Chapters 3 and 5). These models are used to evaluate different scenarios to increase the biogas production, while keeping the costs into account (Chapters 4 and 6). The main research questions that are aimed to be answered are as follows:

- Can we use mathemetical models to describe, analyze and evaluate an industrial full-scale anaerobic digester?
- Is there a choice in what type of model (hydraulic or granular) can be used?
- Can the developed models be used for process optimization?
  - What impact does the influent sulfate and process pH have on the reactor performance?
  - Does removing the CO_2 from the external recycle flow have a significant impact?
  - What is the impact of the addition of a reject water stream (high COD and high mineral content)?

The second part of this thesis evaluates the potential of removing nitrogen through the anammox process. This will reduce the COD removal associated with the reduction of nitrogen, and this COD can subsequently be redirected to the anaerobic digester, thus increasing energy recovery. While this part was planned to consist of a pilot-scale study and a mathematical model describing the pilot-plant, unforeseen circumstances made it so this is not a part of this thesis. Instead, Chapter 7 consists of an outlook on what experimental and modelling work is needed to study the impact that the composition of the anaerobic digester influent will have on the nitrogen removal efficiency of the anammox process. Furthermore, an economic evaluation based on literature values is presented to illustrate what parameters are

needed from the pilot plant and the model to increase the reliability and accuracy of the economic analysis.

Finally an overall conclusion and perspective is presented in Chapter 8, which includes a discussion of the impact this work could have on academia and industry.

Part I

Anaerobic digestion

2 Reactor performance and influent characterization of the anaerobic digester

Chapter 2 describes the industrial anaerobic digester on which this study is based. The reactor configuration is explained, and the reactor performance is analysed based on the data from two measurement campaigns. An influent characterization is performed and finally used to generate a high frequency influent for dynamic modelling. The chapter is partly based on the following articles:

Feldman, H., Flores-Alsina, X., Kjellberg, K., Jeppsson, U., Batstone, D.J. and Gernaey K.V. (2018). Model-based optimization of a full-scale industrial high rate anaerobic bioreactor. *Biotechnology and Bioengineering*, **115**(11), 2726-2739.

Feldman, H., Flores-Alsina, X., Kjellberg, K., Jeppsson, U., Batstone, D.J. and Gernaey K.V. (2017). Modelling an industrial anaerobic granular reactor using a multi-scale approach. *Water Research*, **126**, 488-500.

2.1 Reactor configuration

The plant under study is a BIOPAQ®IC reactor (Paques, the Netherlands; Figure 2.1), which is comprised of four parts with a total liquid volume (V_{liq}) of 1963 m^3 and gas volume (V_{gas}) of 213 m^3. These sections are: i) mixing section (M); ii) expanded sludge bed (R1); iii) polishing section (R2); and, iv) gas-liquid separator (G – L).

The wastewater enters the reactor at the mixing section. Here it is mixed together with the treated wastewater from the top of the reactor, which partly flows down through the downer. This fraction is internally controlled based on the gas production, i.e. the more gas produced, the more water flows downwards. In other words,

when the loading rate of COD to the reactor is increased, a higher gas production is expected, and thus a higher internal circulation which results in a higher dilution of the influent. This is a self-controlling method to keep the COD loading inside the reactor close to constant.

The water flows upwards from the mixing section to R1, where a high biomass concentration converts most of the COD into biogas. The biomass is present in the form of granules and these granules together form an expanded sludge bed. Next, the biogas produced is collected in the lower separation module and flows upwards through the riser to G – L at the top of the reactor. In this section the water and biogas are separated.

The water from R1 flows to the upper compartment (R2), which contains a lower biomass concentration. In this section the rest of the organic material is transformed into biogas. Due to the lower COD concentration, the biogas upflow to G – L is lower, resulting in settling of the biomass. Again biogas is separated in G – L, which leaves the reactor at the top and the polished effluent leaves through the effluent pipe (see Figure 2.1 for details). The effluent is led to a recirculation tank (RT), where a fraction of the effluent is mixed with influent wastewater. This increases the flow rate to the IC reactor from 3 460 $m^3 d^{-1}$ to 12 720 $m^3 d^{-1}$, without increasing the loading of organic compounds to the reactor.

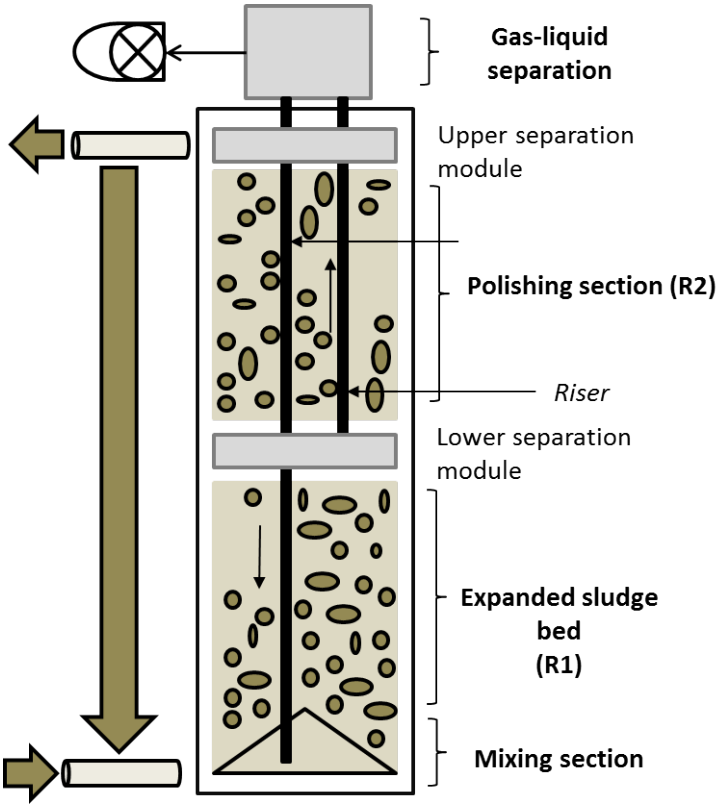

Figure 2.1. Schematics of the BIOPAQ®IC reactor (Feldman et al., 2017).

2.2 Data collection

Two (#D1 and #D2) different data sets corresponding to two operational periods (25.01.2016 to 11.02.2016 and 28.08.2016 to 19.09.2016, respectively) were collected. Daily measurements of the influent and effluent are available of nutrients (N, P), COD, different types of S forms (SO_4^{2-}, H_2S) and minerals and ions (Na^+, K^+, Ca^{2+}, Mg^{2+}, Cl^-), as well as continuous measurements of pH, flow rate, VFA and alkalinity. Furthermore, gas flow rate and fractions (CH_4 and CO_2) are available from continuous monitoring. H_2S fractions are measured daily. Analyses are done using Standard Methods (APHA et al., 2012). Average values for the measurements can be found in Table 2.1, where it is apparent that #D2 has a higher loading rate than #D1. This is caused by the addition of reject water, which originates from the sludge line in the wastewater treatment plant. The sludge that is treated is a 1:1 mixture of biomass from enzyme production in the upstream part of the factory and waste activated sludge. Lime (CaO) is used as a stabilization agent during sludge

Table 2.1. Average influent characteristics of operational periods for #D1 and #D2 (Feldman et al., 2017).

Compound/ratio	#D1	#D2	Unit
Flow rate	3461	4976	$m^3\,d^{-1}$
VFA	3.96	5.06	$kgCOD\,m^{-3}$
COD_T	11.3	10.8	$kgCOD\,m^{-3}$
COD_{sol}	9.47	7.71	$kgCOD\,m^{-3}$
COD_{part}	1.81	3.11	$kgCOD\,m^{-3}$
COD_{sol}/COD_{part} ratio	5.23	2.48	-
NH_4	0.22	0.35	$kgN\,m^{-3}$
TN	0.50	0.76	$kgN\,m^{-3}$
PO_4	0.051	0.015	$kgP\,m^{-3}$
TP	0.10	0.16	$kgP\,m^{-3}$
SO_4	0.27	0.22	$kgS\,m^{-3}$
Ca^{2+}	0.32	0.60	$kg\,m^{-3}$
TSS	0.94	2.0	$kg\,m^{-3}$
S:COD	0.026	0.027	$kgS\,kgCOD^{-1}$
pH	7.03	7.2	-

treatment, which means that the reject water has an alkaline pH. Furthermore, additional COD, mainly in particulate form, is present in this wastewater line. Finally, the water has a high mineral content.

2.3 Mass balances

In order to analyze the measurements, mass balances are set up to check that all compounds are correctly measured. These mass balances are subsequently necessary for the influent characterization (section 2.4), which uses some of the principles reported in Nopens et al. (2009). All mass balance data can be found in Table A.1 in the appendices.

2.3.1 Chemical Oxygen Demand (COD)

The COD concentrations in the influent are similar for #D1 and #D2 Table (2.1). However, due to the increased loading rate in #D2, there is a significant increase in COD loading from 1626 $kgCOD\,h^{-1}$ in #D1 to 2228 $kgCOD\,h^{-1}$ in #D2 (Figure 2.2). This constitutes an increase of 37 %. This increase is not observed in the methane production, which increased by 12 % from #D1 to #D2, because the biodegradability of the influent is higher in #D1, where 74 % of the total COD was converted to CH_4, while this was only 60 % for #D2. The ratio of soluble COD over particulate COD in the influent is 5.23 for #D1 and 2.48 for #D2. This decrease is due to the

addition of reject water in #D2, which increases the amount of particulate COD entering the reactor. However, this increase is assumed to be mainly in the form of inert material (X_I, which increases from 10 % of the particulate material in #D1 to 78 % in #D2).

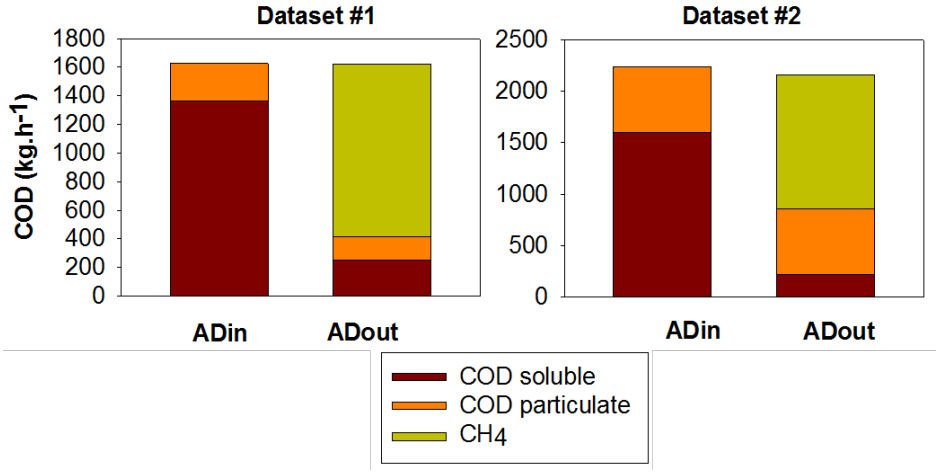

Figure 2.2. Bar charts of the COD balances of Dataset #1 and Dataset #D2 of the influent (AD_{in}) and effluent (AD_{out}).

2.3.2 Nitrogen

The nitrogen balances (Figure 2.3) close for #D1 and #D2 with a gap of 11.2 % and 8.8 %, respectively. The soluble ammonium (S_{NH4}) concentrations are higher in the effluent than the influent in both datasets, due to the hydrolysis of proteins inside the reactor. Consequently, the amount of particulate nitrogen, which is mainly in the form of proteins, has lowered in the effluent. The soluble nitrogen that is not attributed to ammonium or nitrate (negligible concentrations) is assumed to be in the form of amino acids ($N_{organic,soluble}$).

2.3.3 Phosphorus

Measuring particulate phosphorus in the effluent deemed to be unrepresentative for the complete sample taken. Due to the fact that the effluent contained large particles containing phosphorus components, making representative dilutions for measuring was not possible. Therefore concentrations are assumed in order to close the mass balances (Figure 2.4). In #D1 it is assumed that phosphorus enters the reactor as either soluble P ($H_XPO_4^{3-X}$) or organic particulate P (lipids). However,

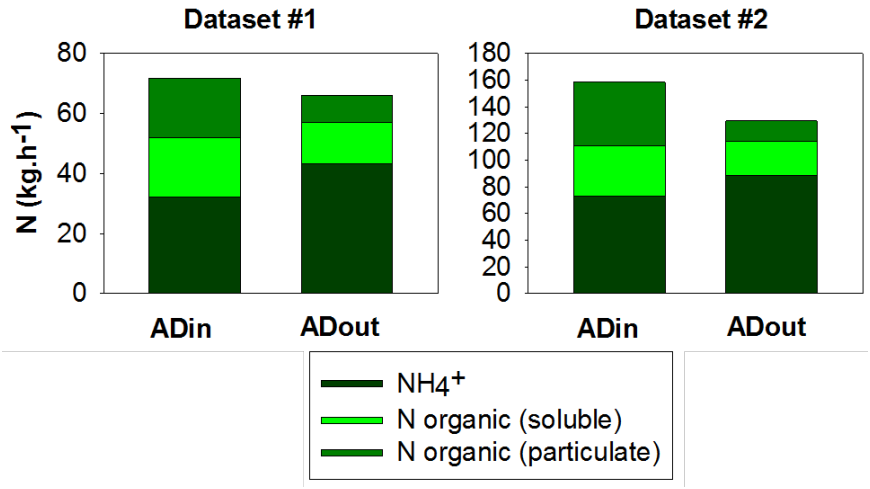

Figure 2.3. Bar charts of the elemental N balances of Dataset #1 and Dataset #D2 of the influent (AD_{in}) and effluent (AD_{out}).

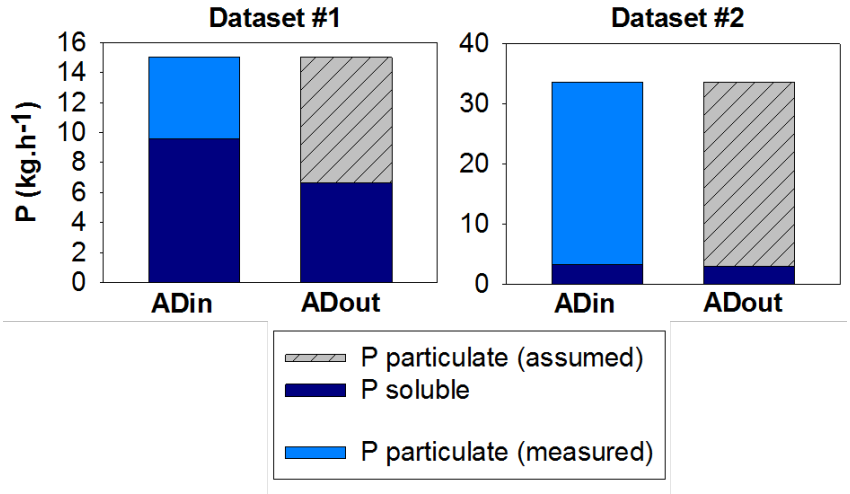

Figure 2.4. Bar charts of the elemantal P balances of Dataset #1 and Dataset #D2 of the influent (AD_{in}) and effluent (AD_{out}).

for #D2 the addition of reject water with high mineral content, meant that 56 % of the influent particulate phosphorus was present as precipitates ($P_{inorganic,P}$).

2.3.4 Sulfur

The SO_x^{2-} reduction was between 50 and 60 % for both datasets, while the effluent ratio SO_x^{2-}/H_xS^{2-x} was 0.8 for #D1 and 1.0 for #D2. Part of the influent S is bound to proteins, which is released upon hydrolysis. 9 % and 18 % of the influent S in #D1 and #D2, respectively, is in the form of dissolved H_xS^{2-x}. At the same time, the SO_x^{2-} concentration is 16.6 % lower in #D2 than in #D1, resulting in an influent SO_x^{2-}/H_xS^{2-x} ratio of 9.9 and 4.5 for #D1 and #D2, respectively. See Figure 2.5 for details.

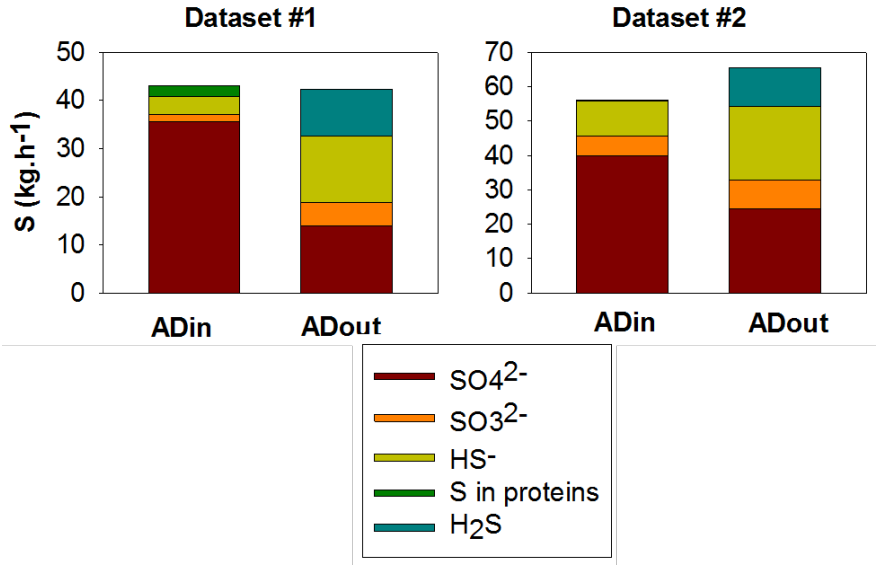

Figure 2.5. Bar charts of the elemental S balances of Dataset #1 and Dataset #2 of the influent (AD_{in}) and effluent (AD_{out}).

2.4 Influent fractionation

The fractionation of the influent is important to determine the different states that are needed for the ADM1. The fractionation is done on both the particulate COD and soluble COD and takes the mass balances of the different species into account. Figure 2.6 gives an overview of the influent fractionation for both #D1 and #D2.

2.4.1 Particulate COD

As reported in Nopens et al. (2009), the particulate COD is divided directly into carbohydrates (X_{ch}), proteins (X_{pr}), lipids (X_{li}) and inerts (X_I). The calcluation of

proteins and lipids was based on the elemental content of nitrogen and phosphorus respectively (Nopens et al., 2009). As such, the particulate nitrogen that was not attributed to X_I (N_{XI}) (0.00429 kmolN/kgCOD) is assumed to be part of X_{pr}, based on the nitrogen content of proteins. Equation 2.1 describes the calculation of X_{pr}.

$$X_{pr} = \frac{TN_{particulate} - N_{XI}}{N_{pr}} \tag{2.1}$$

The phosphorus content of lipids and the concentration of organic particulate P was used to determine X_{li} according to Equation 2.2. It is assumed no carbohydrates are present. See Table 3.1 in Chapter 3 for details about the nitrogen and phosphorus content of proteins and lipids, respectively.

$$X_{li} = \frac{TP_{particulate}}{P_{li}} \tag{2.2}$$

It is assumed that 10 % and 78 % of the particulate COD is present in the form of X_I, for #D1 and #D2 respectively. These percentages are based on closing the mass balance for $COD_{particulates}$, which follows the following equation.

$$COD_{particulate} = X_{pr} + X_{li} + X_I \tag{2.3}$$

2.4.2 Soluble COD

The soluble COD is divided into sugars (S_{su}), amino acids (S_{aa}), fatty acids (S_{fa}), volatile fatty acids (VFA; butyrate, valerate, propionate, acetate), ethanol (S_{eth}) and inerts (S_I). As for carbohydrates, it is assumed no sugars are present in the influent. These assumptions are based on the fact that the wastewater originates from fermentation processes, where the production schedules are planned to use up all the sugars. Furthermore, a pre-acidification tank prior to the anaerobic digester would degrade any remaining sugars. VFA was monitored online and fractionated offline, and measurements are available for the ethanol concentration. S_{aa} is calculated based on the organic soluble nitrogen concentration and the nitrogen content of amino acids (Equation 2.4). S_I is estimated from effluent $COD_{soluble}$ (8 % in #D1 and 3 % in #D2) according to Equation 2.5 The remaining soluble COD is allocated to S_{fa}.

$$S_{aa} = \frac{N_{soluble,organic}}{N_{aa}} \tag{2.4}$$

$$S_I = S_{COD} - S_{eth} - S_{VFA} - S_{aa} \tag{2.5}$$

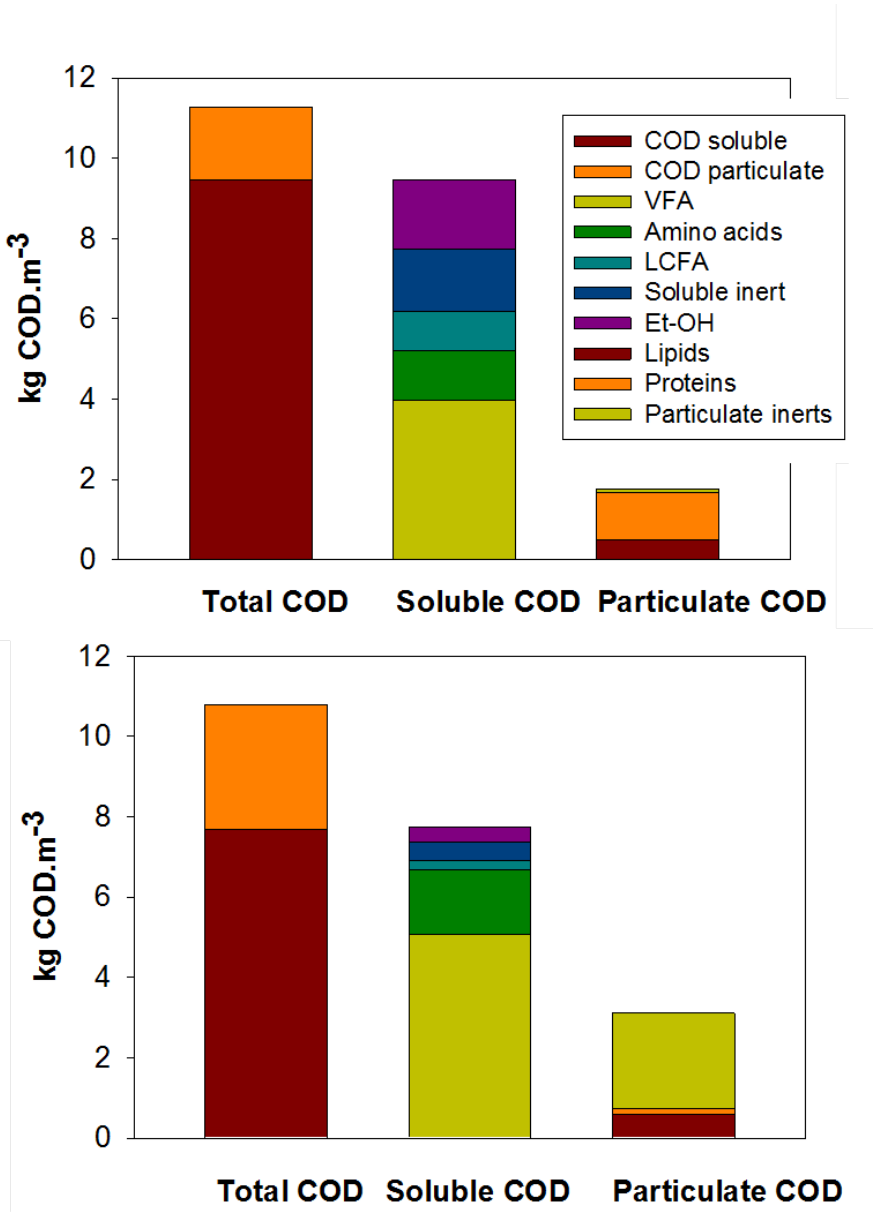

Figure 2.6. Influent fractionation for COD compounds for Dataset #1 and Dataset #2 (Feldman et al., 2018).

2.5 Dynamic modelling of influent data

2.5.1 Method

High frequency influent data is reproduced from the measured data, based on the BSM2 influent generator (Gernaey et al., 2011). While the BSM2 influent generator is developed for urban wastewater, it can also be applied to industrial systems. The model blocks for flow generation (FLOW), compounds generation (POLLUTION) and sewer network (TRANSPORT) are used to reproduce the wastewater dynamics. Specific (daily/weekly) industry-type defined profiles (FLOW, POLLUTION), which are continuously measured online, are scaled to an average of 1. The resulting values are then multiplied with the offline daily measurements, in order to generate a dynamic influent for all states. Based on the available measurements, the BSM2 influent generator provides: 1) additional influent dynamics; 2) increased data frequency; and, 3) a more realistic and complete picture of how the WWTP might perform under a wide range of disturbances (Flores-Alsina et al., 2014; Snip et al., 2016).

2.5.2 Results

Figure 2.7 illustrates that the BSM2 influent generator is able to reproduce flow rate and pollution (VFAs, COD, N, P and S) trends for the two studied data sets (#D1 and #D2). Simulation results demonstrate that the assumed specific user-defined profiles can produce influent data with high frequency. The generated plots show some additional daily (day 15 #D1 and day 13 #D2) and weekly variations (day 7 in #D1 and day 8 #D2), the effect of cleaning equipment within the production site (day 15 in #D1) and shutting down the reactor (day 4 and 11 in #D2), which was not originally available for all the influent measurements. It is important to highlight that the averages of the generated data series equal the measured values summarized in Table 2.1.

2.6 Discussion

This chapter has described the configuration of the anaerobic digester under study, as well as the reactor performance and influent and effluent characteristics. The influent characterization is an important part of any model. The quality of the collected data and the translation to model parameters will have a significant impact on the results and reliability of a model (Parker, 2005).

The mass balances and influent fractionation from the two collected datasets (#D1

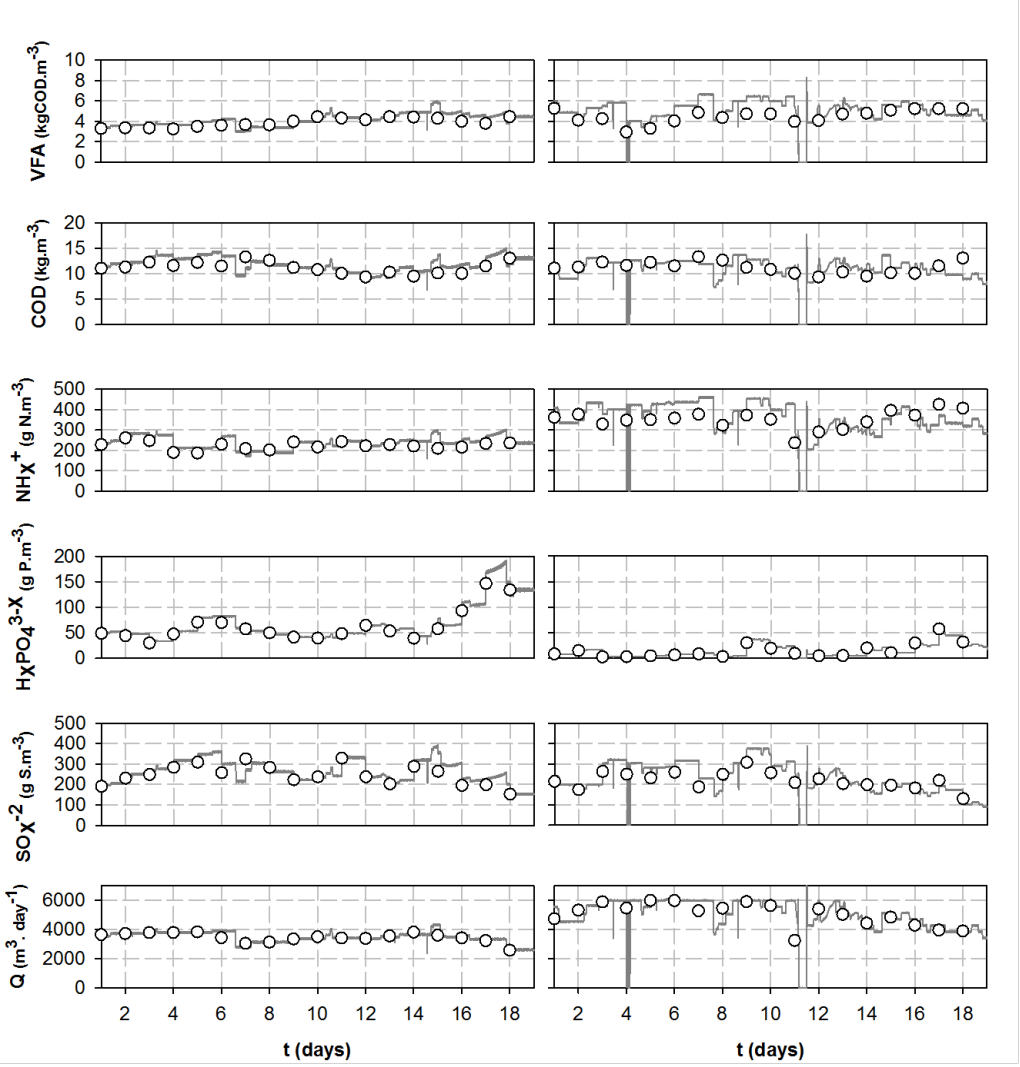

Figure 2.7. Simulation results (lines) and measured influent data (markers) for data set 1 (#D1) (left column) and 2 (#D2) (right column) (Feldman et al., 2017).

and #D2) have shown that the loading of organics, nutrients and sulfur compounds has increased in #D2 as compared to #D1. The amount of particulate matter in the second dataset has furthermore increased. This is in part due to the addition of the reject water stream. Regardless, both datasets contain high concentrations of biodegradable COD, which is characteristic for industrial wastwaters (Akarsubasi et al., 2006; Parawira et al., 2005; Ahn et al., 2001a). The COD conversion rate was 74 % and 60 % respectively for #D1 and #D2. These values lie within the range of other full-scale industrial wastewater treatment plants. Parawira et al. (2005) reported a 57 % COD conversion rate for a 500 m^3 anaerobic digester treating brewery waste. Ahn et al. (2001a) also studied anaerobic digestion of brewery waste, and found a conversion rate of above 75 % at an HRT of 6.7 hours. This is a relatively low HRT, but the total COD in the wastewater was only 2500 mg/L (>10000 mg/L in this study and in Parawira et al. (2005)). Nevertheless, the conversion range is similar to that of #D1, while #D2 has a significantly lower value. This can be partly explained by the biodegradability of #D1 and #D2. In #D1 the COD_{sol}/COD_{part} ratio is 5.23, which is similar to the value found by Ahn et al. (2001a), namely 6.0. The ratio obtained for #D2 is 2.48, a result of the high inert concentration in the reject water stream that was added during this time period.

It should be noted that stoichiometric parameters for the influent fractionation are based on the model calibration performed in Chapter 3 (Model I). In Chapter 5 Model II is presented, in which most stoichiometric parameters are kept at default values. Therefore, the influent fractionation is slightly different when it comes to X_{pr} and X_{li}.

2.7 Conclusions

Two datasets of three weeks were collected over two separate time periods. Influent fractions were estimated using rigorous COD, N, P and S balances in order to characterize: 1) influent biodegradability (defined as the COD conversion to biogas); and, 2) the ratio between soluble and particulate compounds. An important difference between the two datasets was the addition of reject water in Dataset #2. This increased the loading rate of COD, phosphorus, nitrogen and sulfur compounds, but also increased the amount of non-biodegradable material. The generated high frequency influent will be used to calibrate two different models: Model I in Chapter 3 and Model II in Chapter 5.

3 Model I - Flow and reactor model

The datasets described in the previous chapter are used for the calibration of a model of the previously described anaerobic digester. The International Water Association (IWA) Anaerobic Digestion Model No. 1 extended with phosphorus (P), sulphur (S) and ethanol (Et-OH) is used to describe the main biological and physico-chemical processes. The high-rate conditions within the reactor are simulated using a flow + reactor model comprised of a series of continuous stirred tank reactors (CSTRs) followed by an ideal total suspended solids (TSS) separation unit. This chapter is based on the following article:

Feldman, H., Flores-Alsina, X., Kjellberg, K., Jeppsson, U., Batstone, D.J. and Gernaey K.V. (2018). Model-based optimization of a full-scale industrial high rate anaerobic bioreactor. *Biotechnology and Bioengineering*, **115**(11), 2726-2739.

3.1 Introduction

The implementation of a model to describe the reactor performance of an anaerobic digester helps to understand the process reactions. Due to the complex nature of an anaerobic digester (many different micro-organisms that together convert a wide spectrum of nutrients and organics) it is not simple to prove the separate biochemical reactions taking place in an experimental setting. With the aid of a model, important process parameters, dominant reactions and effects of inhibitors can be elucidated. This knowledge can later be used for the model-based optimization of the reactor.

As described in Chapter 2, the studied system contains an expanded granular sludge bed. Important factors to account for when representing sludge bed systems are flow and reactor models (Saravanan and Sreekrishnan, 2006). With respect to flow patterns there are numerous studies in the literature proposing several hydraulic

schemes (Batstone et al., 2005; Bolle et al., 1986; Chen et al., 2009). Indeed, the flow model should be able to describe the dynamics of particulates, for example in the sludge bed, the sludge blanket and the polishing section as well as the effect of multiple splitters/combiners (Ren et al., 2009). Regarding reactor models, it is important to reproduce high-rate conditions representing biomass accumulation. In these situations, granular type models could be implemented since they account for mass transfer limitations and microbial competition/affinity within the biofilm (Wanner et al., 2006). The works of Batstone et al. (2004b), Odriozola et al. (2016) and Feldman et al. (2017) show the benefits of using multi-scale models (biofilm, granule, reactor) when predicting process performance, microbial community structure and how these interact, and are affected by loading conditions.

High rate conditions can also be empirically represented by artificially separating the hydraulic and the sludge retention time (Batstone et al., 2002b; Vanhooren et al., 2002), without the need of overcomplicated biofilm reactors. Indeed, it is well known that the multi-scale (spatial/temporal) nature of biofilm/granular sludge models (Xavier et al., 2005) makes them very unstable (difficult to reach steady state state), stiff (computationally demanding) and consequently very difficult to calibrate (Boltz et al., 2010; Brockmann et al., 2013). This might pose a major problem, particularly within an industrial context, where the time horizon for results is relatively short and many simulations are required to determine optimal operational conditions (Rieger et al., 2012).

The objective of this chapter is to present the model-based implementation of a full-scale anaerobic granular IC reactor treating industrial wastewater from the fermentation industry, producing various pharmaceutical and enzymatic products (depending on the production schedule). A flow + reactor model is used to describe high-rate conditions typically found in industrial settings. Biological and physico-chemical processes are based on the ADM1 upgraded with the fate of P and S compounds, the role of ethanol as well as an improved physico-chemical description in order to correctly deal with wastewater produced in industry.

3.2 (Bio) chemical model

The Anaerobic Digestion Model No 1. (ADM1) (Batstone et al., 2002a) is used to describe the reaction rates and kinetics under mesophilic conditions (35°C). The default implementation is upgraded to include phosphorus (P), sulfur (S) and ethanol (Et-OH) related conversion processes as reported in Batstone et al. (2006), Soda

et al. (2011) and Flores-Alsina et al. (2016). Figure 3.1 gives an overview of all biochemical processes taking place.

Phosphorus is modelled using a source-sink approach assuming a predefined elemental (C, H, N, P, O) composition of biomass and inert material (de Gracia et al., 2006). It is assumed that there are no phosphate accumulating organisms (PAO) present, and therefore no production of polyhydroxyalkanoates (PHA) is modelled. Biological production of sulfides ($[S_{IS}$) is described by means of sulfate reducing bacteria (X_{SRB}) utilising hydrogen (autolithotrophically) as electron source (Batstone et al., 2006), thereby competing with methanogens. Potential hydrogen sulfide (Z_{H2S}) inhibition and stripping to the gas phase (G_{H2S}) is also considered (Fedorovich et al., 2003). Finally, ethanol (S_{eth}) degradation is modelled assuming a specific group of microorganisms (X_{EtOH}), which ends up producing hydrogen (S_{H2}) and acetate (S_{ac}). Furthermore, sulfate reducing bacteria utilizing ethanol were taken into account. Since the ΔG values and stoichiometry of hydrogen production are similar for ethanol and butyrate degraders, the default kinetic parameters and hydrogen inhibition parameters for butyrate degraders were used as starting values to describe ethanol degradation (Batstone et al., 2004b). The model also includes physico-chemical equations that simulate the acid-base system and therefore pH can be modelled dynamically (Solon et al., 2015b). The model corrects for ionic strength via the Davies approach to consider chemical activities instead of molar concentration running all the calculations under non-ideal conditions (Flores-Alsina et al., 2015). The equations of the model can be found in the references given accordingly.

3.3 Flow and reactor model

Figure 3.2 gives an overview of the proposed hydraulic configuration to simulate the industrial reactor shown in Figure 2.1 (Chapter 2). R1 (expanded sludge bed) and R2 (polishing section) are modelled as a series of continuous stirred tank reactors (CSTR). High-rate conditions in the reactor are achieved by adding an ideal total suspended solids (TSS) separation unit (Jeppsson et al., 2007). As a result, it is possible to separate hydraulic residence time (HRT) and residence time of biomass (SRT). The latter is arbitrarily set to 100 days by calibrating the thickener percentage and TSS removal percentage in Equations 3.1, 3.2 and 3.3.

$$Thickener factor = \frac{Thickener percentage * 10000}{TSS_{in}} \tag{3.1}$$

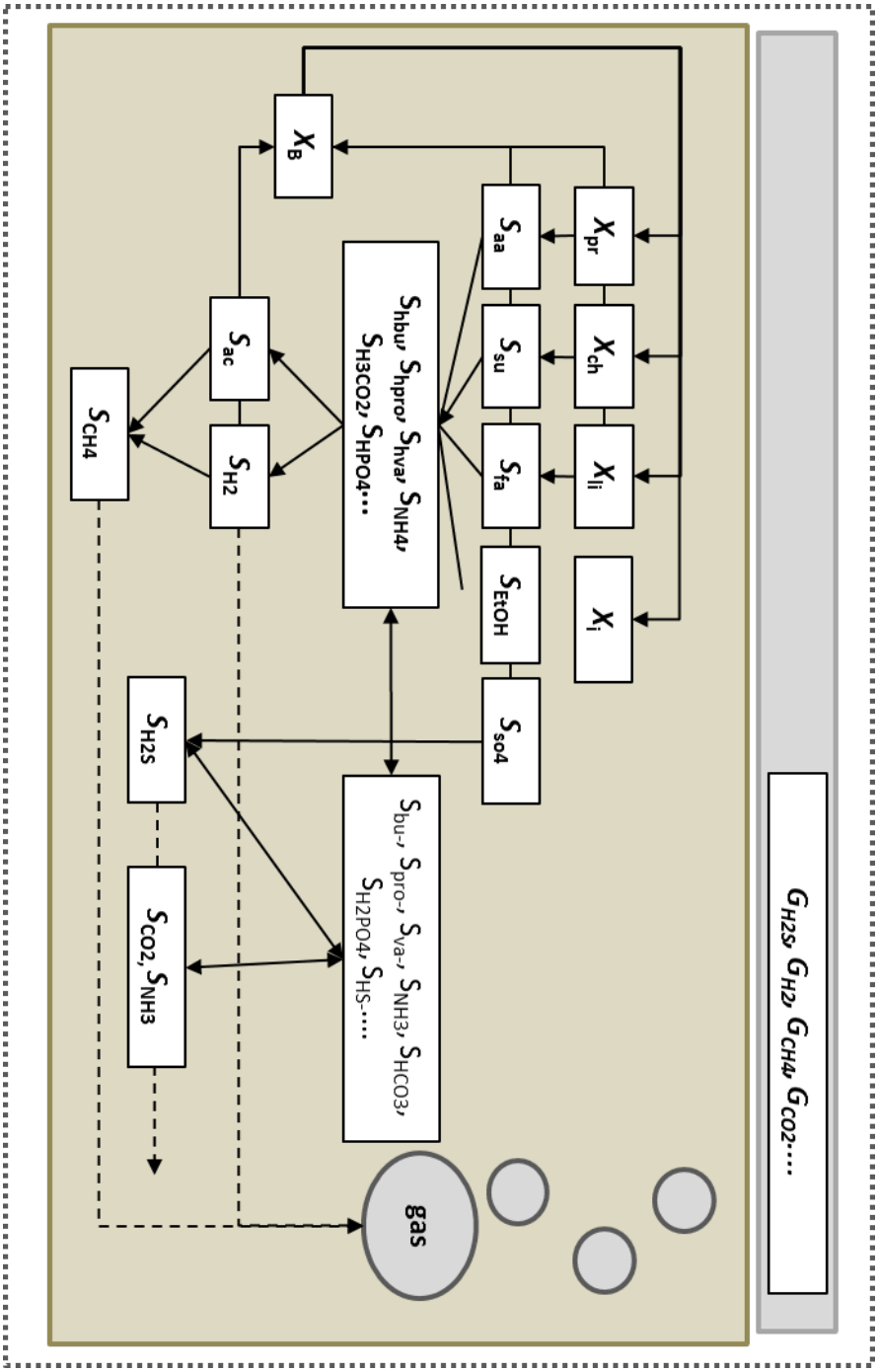

Figure 3.1. Schematic representation of the main processes/states considered by the biochemical model.

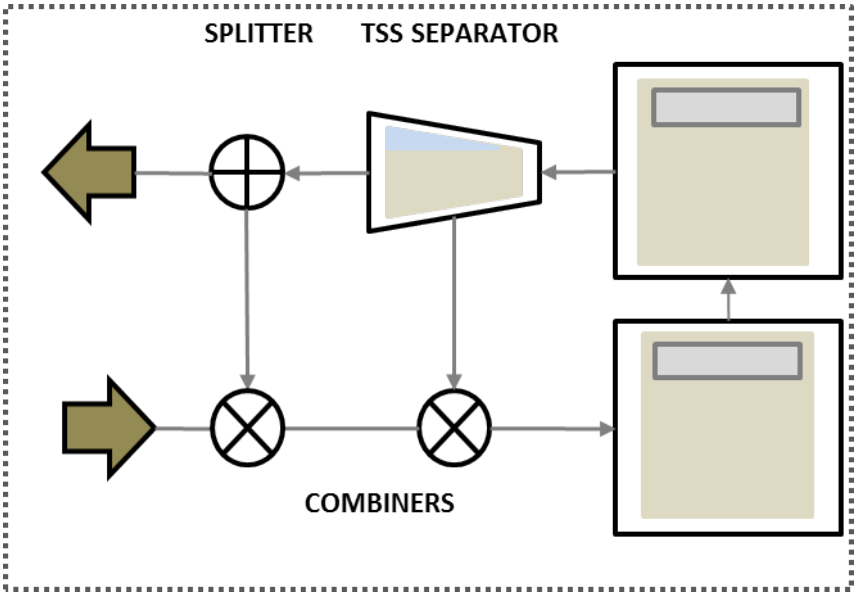

Figure 3.2. Schematic representation of the flow and reactor model describing the IC reactor.

$$Q_u factor = \frac{TSSremoval percentage}{100 * Thickener factor} \tag{3.2}$$

$$Thinning factor = 1 - \frac{TSSremoval percentage}{100} * \frac{1}{1 - Q_u factor} \tag{3.3}$$

In the separation unit, the thickener factor is multiplied with the particulate components to calculate the concentration in the solids stream. In the reject stream, the particulate components are mulitplied with the thinning factor. The Q_u factor is used to re-calculate the flow rates of both streams. Underflow is recirculated and combined back to R1, while the overflow with mainly soluble compounds leaves the reactor through the effluent. Finally, an additional external recirculation is included as a combiner and a splitter system, in which the influent flow rate is set to desired operational conditions. All model blocks have been implemented in the Matlab-Simulink software package (Mathworks, Natick, MA, USA).

3.4 Parameter estimation

3.4.1 Methods

Optimum values of kinetic coefficients for selected model parameters (Table 3.1) are estimated by separately fitting the dataset from each experiment, using a non-

linear local optimization technique, lsqcurvefit, in MATLAB with the default 'trust-region-reflective' algorithm (Optimization Toolbox User's Guide Release 2014b, The MathWorks, Inc., Natick, Massachusetts, United States). Biogas production values (CH_4, CO_2, H_2S) and process state variables (VFA, COD_{sol}, COD_{part}, COD_t, NH_x, $H_XPO_4^{3-x}$) are used as the fitted output being optimized. The optimization is performed for one parameter and one output at a time (Table 3.1). The residual sum of squares (RSS) is used as objective function. The selection of the parameters is based on the Global Sensitivity Analysis results reported in Solon et al. (2015a). Further information about the method can be found elsewhere (Lobry et al., 1991).

3.4.2 Results

The dynamic profiles of selected operational variables for the first evaluation period (#D1) are illustrated on the left side in Figures 3.3 and 3.4 (dotted lines). Simulation results (solid lines) show that the proposed approach is capable to reasonably reproduce the process performance in terms of biogas production, COD conversion and nutrients transformations (N, P) (average deviations 13 % and 15 % for #D1 and #D2, respectively, see Tables A.2 and A.3 in the appendices for the specifics).

The SO_4^{2-}, CH_4, CO_2 and H_2S profiles reveal the correct description of the mass transfer (liquid-gas) methanogenesis, sulfidogenesis and competition between methanogens (MET) and sulfate reducing bacteria (SRB). The model also predicts N (see NH_X profiles) and P (see $H_XPO_4^{3-X}$ profiles) release during the anaerobic digestion process from the hydrolysis of proteins and lipids. In the case of phosphorus release, the P content of bacteria (P_{bac}) and lipids (P_{li}) is modified to close the mass balances and correctly describe the kinetics. It should be noted that the influent fractionation presented in Chapter 2 takes the modified parameters into account. These modifications can be due to the previously mentioned model simplification where no PAO activity is assumed, or because precipitation kinetics are not taken into account. Furthermore, the nitrogen content of inert soluble material (N_{SI}) is modified, as well as the content of C in S_I (C_{SI}) (Table 3.1).

Uptake rates for hydrogen degraders (X_{H2}, $X_{SRB,H2}$) had to be adjusted in order to give a competitive advantage to SRB (Batstone et al., 2006; Barrera et al., 2015) (see Table 3.1). The slight accumulation of VFAs in the system is achieved by modifying two parameters. Firstly, K_s for acetate is increased in order to reduce the growth of specific biomass. Secondly, an additional inhibition factor is added to the VFA degraders, methanogens, SRB and ethanol degraders. This inhibition factor is directly multiplied with the corresponding K_s. The most probable reason for this

Table 3.1. Parameter estimation results for Dataset #1 and Dataset #2. The modified stoichiometric parameters are also used for the influent fractionation in Chapter 2 (Feldman et al., 2018a).

Parameter	Default	#D1	#D2	95 % confidence interval	Output
$K_{s,ac}$ ($kmol.m^{-3}$)	0.15	0.65	0.15 (default)	0.020	VFA
$K_{m,hSRB}$ ($kgCOD\,kgCOD^{-1}\,d^{-1}$)	52.5	34.8	34.8	1.92	S_{SO4}
Inhibition factor	-	7.62	7.62	0.50	VFA
N_{pr} ($kmolN\,kgCOD^{-1}$)	0.0079	0.0079	0.047	-	S_{IN}
N_{SI} ($kmolN\,kgCOD^{-1}$)	0.0043	0.14	0.14	-	S_{IN}
C_{XI} ($kmolC\,kgCOD^{-1}$)	0.030	0.0028	0.0028	-	CO_2
P_{bac} ($kmolP\,kgCOD^{-1}$)	0.00069	0.0025	0.005	0.0007	S_{IP}
P_{li} ($kmolP\,kgCOD^{-1}$)	0.00034	0.0025	0.0034	-	S_{IP}

addition is the potential inhibition on acetogens (X_{c4}, X_{pro} and X_{ac}) by an inorganic/organic compound neither measured nor described by the model. All other parameters are left at their default values (Batstone et al., 2002a; Flores-Alsina et al., 2016).

Regarding the second dataset, it is important to highlight that the addition of reject water during the second period (#D2) substantially changes influent biodegradability (see Figure 2.6 in Chapter 2). As a result it was necessary to adjust the P content of bacteria and lipids, as well as the N content of proteins. Furthermore, the K_s for acetate has to be reset to the default value (probably because the inhibition component was not there anymore, changing the inhibition kinetics). The other parameter values are either default or the adjusted values found in #D1. This results in a good fit between model simulations and measured data (right side of Figures 3.3 and 3.4).

3.5 Discussion

This chapter has shown the implementation of a modified and extended ADM1 to a full-scale industrial anaerobic granular sludge reactor. After the estimation of

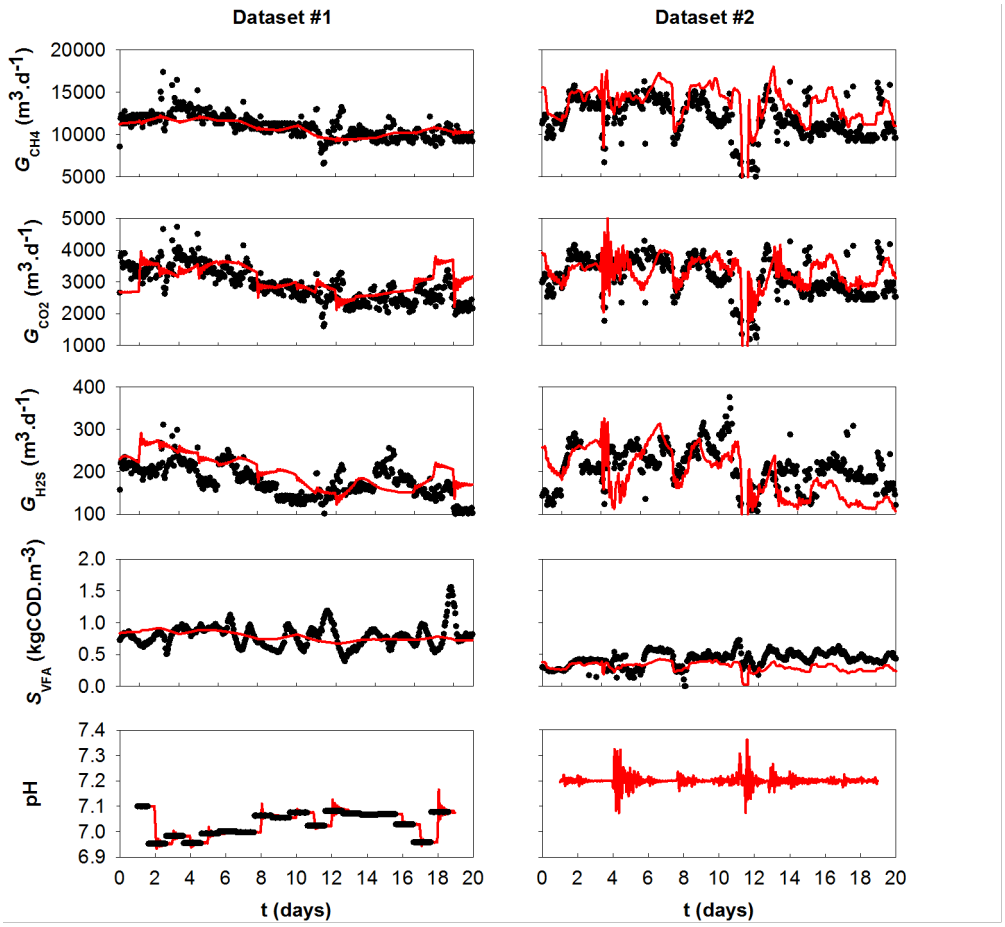

Figure 3.3. Simulated/on-line measurements for biogas (rows 1,2,3), VFA (row 4) and pH (row 5) (Feldman et al., 2018a).

both kinetic and stoichiometric parameters, the model showed a 13 % and 15 % deviation with the measurements for #D1 and #D2, respectively.

3.5.1 Model hydraulics

A detailed flow + reactor model was constructed in order to reproduce high-rate conditions. The advantage of using two reactors as opposed to more is simulation speed. The more reactors that are used, the slower the simulation will become. On the other hand, more CSTRs will give a more stratified reactor (as in reality, where there is a gradient in biomass concentration from the bottom to the top). The simulation in two reactors was based on the IC reactor configuration, in which two

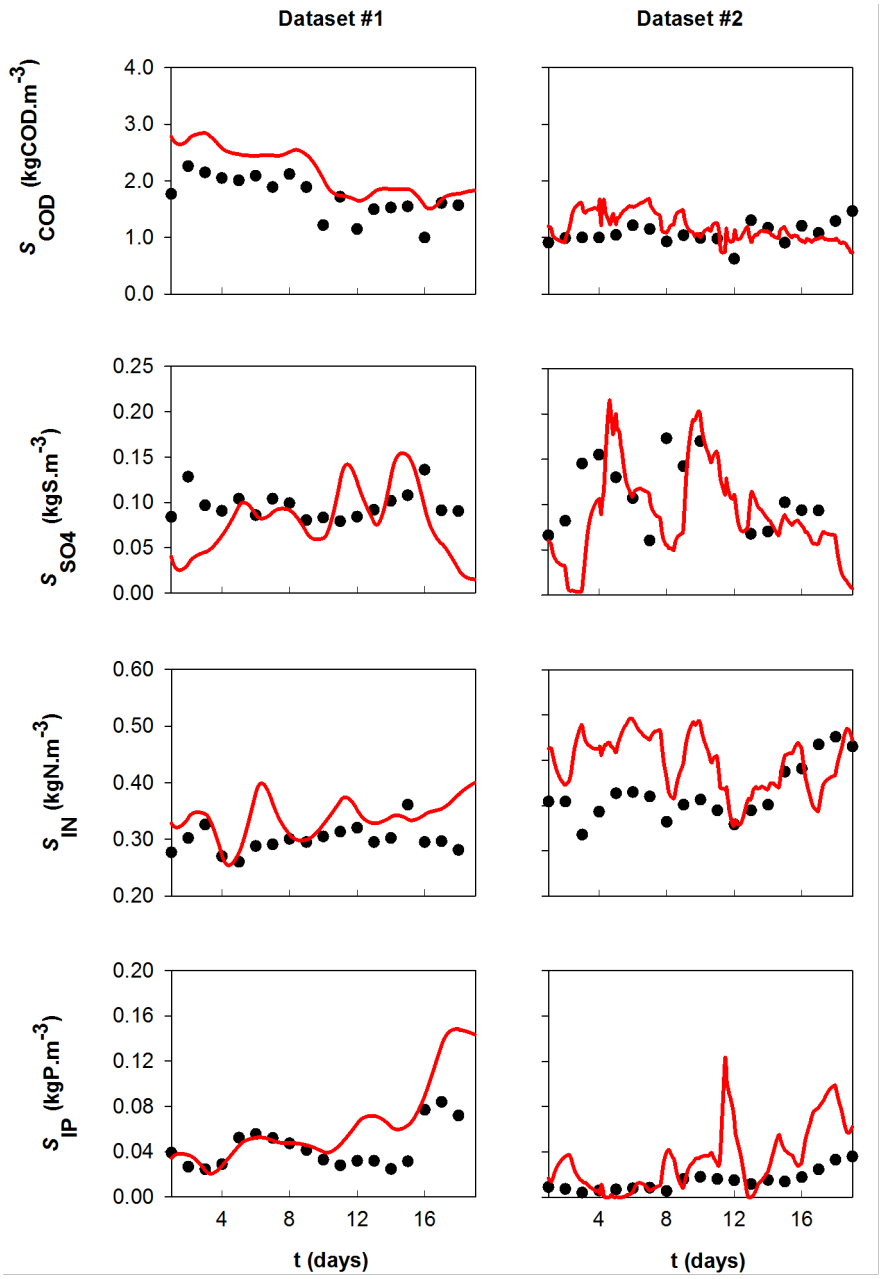

Figure 3.4. Simulated/off-line measurements for COD (row 1), SO_4 (row 2), NH_X (row 3) and $H_XPO_4^{3-X}$ (row 4). (Feldman et al., 2018a).

main parts can be distinguished (Figure 2.1, chapter 2). A hydraulic computational fluid dynamics (CFD) model will be needed to determine how big the biomass gradient in fact is, and how important it is to model this as close to reality as possible.

3.5.2 Parameter estimation

While the implementation of anaerobic models has been done on industrial wastewaters before, the datasets are often collected from lab- or pilot-scale experiments where industrial wastewater is used as feed. Nevertheless, comparable results are achieved between the studies found in literature, as well as this study. A major difference is that in this study it was decided to only change the $K_{s,ac}$, and not its correlated pair ($K_{m,ac}$). The estimation of correlated pairs of parameters is troublesome, as there are many different combinations that give similar results. Furthermore, the specific parameters cannot be validated in full-scale. The studies in literature have also often estimated several K_s and K_m pairs as well as different types of inhibitors. In the study of Dereli et al. (2010) the K_m values of acetate, amino acids, fatty acids, hydrogen and sugars are estimated based on the COD, CH_4 and biogas flow rate, and pH. Practically, it is impossible to know the correct values for all these parameters solely based on the outputs given. In the study of Antonopoulou et al. (2012) it was possible to estimate different K_m parameters, as the respective compounds were measured individually in lab-scale experiments. In the current study it was chosen to add a general inhibition parameter to the K_s values of methanogens, acidogens, SRB and ethanol degraders, as individual measurements were not available. This method is close to the method used by Boubaker and Ridha (2008), where an inhibition factor based on the total VFA concentration was added. A recent study of Elaiuy et al. (2018) only estimated a lumped hydrolysis rate (K_{hyd}) and an added COD degradation parameter against the biogas flow rate. While good results were obtained for biogas production, the COD conversion and the pH in the system did not follow the measured data. Furthermore, Elaiuy et al. (2018) study show no data on nutrient conversion. This indicates that it is indeed necessary either to estimate separate hydrolysis rates or the stoichiometric fractionations of compounds to correctly simulate the COD and nutrient transformations. In the current study, it was chosen to calibrate the stoichiometric parameters, as these were also used to close the mass balances of the influent fractionation presented in Chapter 2.

3.5.3 Limitations

The model presented in this chapter shows a good compromise between model complexity and prediction capabilities. While the average deviations are satisfactory, the model is not able to capture the dynamics of several components, as can be observed from the R^2 values in Tables A.2 and A.3 in the appendices. This deficiency is most pronounced in #D2 and most likely due to processes not considered in the model, such as inhibition by VFAs (Ahn et al., 2001b) or compounds that were not measured. Furthermore, the proposed approach cannot describe the effect that (influent) inorganic material will have on process performance. Hence, high mineral content can lead to precipitation within the reactor. Precipitates will compete with bacteria for space in the reactor, again affecting the granular structure and the reactor performance (van Langerak et al., 2000). These effects cannot be modelled with the current model, where an artificial loop is introduced to mimic the hydraulics of the reactor and the high biomass concentrations. This can, however, be done using a model based on a biofilm structure (Batstone et al., 2004b; Feldman et al., 2017; Wanner et al., 2006). Chapter 5 will present a biofilm model, that has been developed for the same system and yields similar results for the datasets available, but includes the precipitation model, in order to take into account the probable precipitation taking place in the reactor, due to the high mineral content of the influent.

3.6 Conclusions and outlook

A mathematical model (ADM1 extended with physico-chemical, S and Et-OH reactions) has been developed and succesfully applied to an industrial anaerobic granular sludge internal circulation (IC) reactor. High loading conditions are reproduced using a flow + reactor model, in which an artificial loop retains the biomass inside the reactor.

The model has been adjusted using two datasets corresponding to different operational periods. A good resemblance between the experimental data and the model simulations indicates that the model is capable of describing hydrolysis, acidogenesis, acetogenesis, methanogenesis, sulfidogenesis, liquid-gas mass transfer and weak acid-base chemistry (13 % and 15 % deviation). The relatively few parameters that had to be estimated indicates not only that the ADM1 is applicable to a wide variaty of wastewaters, but also that microbes in anaerobic digestion behave similarly under different process conditions.

The model assumed a well-mixed behaviour inside the compartments, while practically the reactor is a type of expanded granular sludge bed, with plug-flow behaviour. To gain more insight of the hydraulics inside the reactor, and how the internal circulation is affected by biogas production, future research aims to use CFD to study the flow patterns of the IC reactor.

The next chapter will apply the presented model to evaluate different scenarios for the optimization of the energy recovery in the anaerobic digester under study.

4 Optimization of energy recovery in the anaerobic digester

The model previously described in Chapter 3 is applied for process optimization. Different scenarios are analyzed to evaluate strategies for increasing energy recovery and lowering operational costs through chemical dosage (together the reactor performance index; RPI). The chapter is based on the following article:

Feldman, H., Flores-Alsina, X., Kjellberg, K., Jeppsson, U., Batstone, D.J. and Gernaey K.V. (2018). Model-based optimization of a full-scale industrial high rate anaerobic bioreactor. *Biotechnology and Bioengineering*, **115**(11), 2726-2739.

4.1 Introduction

Mathematical models can be used not only for process understanding and evaluation, but also optimization. Model-based optimization of the reactor performance in wastewater treatment plants is an effective way to evaluate different scenarios before implementing them on industrial scale. The complexity of the ADM1 allows for a wide variety of process parameters to be optimized, depending on the desired output. Wett et al. (2007) used the ADM1 to optimize the reactor hydraulics in a multiple chamber reactor, and simulated different retention times and recycle flows between chambers to find the best configuration for robustness and load flexibility. Pokorna-Krayzelova et al. (2017) were interested in removing H_2S from the biogas due to the toxic and corrosive behaviour of this chemical. Model-based optimization of the micro-aeration inside an anaerobic digester was performed. Finally, Zaher et al. (2009) aimed to maximize the biogas production rate, by optimizing the feedstock ratio and retention time. These three case studies have shown some of the diversity of optimization problems that can be encountered in practice.

The aim of this study is to simulate different scenarios and create response surfaces to identify the best strategy to maximize energy (electricity/heat) recovery and minimize operational costs (chemical dosage for pH control). Not only is the biogas production for energy recovery important for industry, but also the operational costs must remain as low as possible. The optimization in this chapter is done by applying the flow + reactor model as described in Chapter 3.

4.2 Methods

4.2.1 Optimization scenarios

The flow + reactor model as described in Chapter 3 is used to generate response surfaces (RSs) indicating optimal operational conditions. These RSs show the potential energy recovery from the IC reactor when operational conditions are modified. The operational settings tested are chosen based on the applicability, as only those that can practically be implemented in full-scale systems are taken into account. The optimization study is based on #D2. The following settings are tested: 1) influent S versus operational pH, and 2) influent pH and dissolved CO_2.

4.2.1.1 Influent S (SO_4 and dissolved H_2S) versus operational pH

The pH in the plant is adjusted by chemical dosage. Due to the acidifying behaviour of the reactor, it is assumed a lower pH setpoint will decrease the dosage of sodium hydroxide (NaOH). On the other hand, free sulfide has an inhibitory effect, which becomes more pronounced at a lower pH. This is due to the pKa of H_2S, which lies at 6.9. Therefore, this study aims to look at the effect pH has on the S concentration in the influent. The S components in the influent are SO_4 and dissolved H_2S. Besides the direct inhibitory effect of H_2S, the reduction of SO_4 by sulfate reducing bacteria (SRB) produces more H_2S. Furthermore, SRB compete with methanogens for substrate.

The S content of the influent can be modified by removing SO_4 and H_2S prior to the anaerobic digester. There are currently ongoing studies running to determine the best course of action for this process. One of the most economical ways to remove sulfate is through crystallization using calcium, producing gypsum (Tait et al., 2009). This method is most viable for waste streams containing more than 1 $gS\,L^{-1}$, as sulfate and gypsum are in equilibrium at around 500 $mg\,L^{-1}$ (Silva et al., 2012). As the sulfate concentrations in this study are below 1 g $gS\,L^{-1}$, a more viable option would be adsorption on limestone (Silva et al., 2012). In WWTP, removal of

dissolved H_2S in the AD can be achieved by dosing iron salts in a tank prior to the AD reactor (Ge et al., 2013; Solon et al., 2017). Nevertheless, the COD in H_2S is still lost from energy recovery.

4.2.1.2 Influent pH and dissolved CO_2 (influent alkalinity)

As the reactor effluent is recycled back into the reactor (Chapter 2) with a ratio of 3.7:1 (effluent to influent ratio), a large amount of alkalinity in the form of CO_2 stays in the reactor. The dissolved CO_2 has an acidic effect.

The content of inorganic carbon in the influent can be reduced by recycling part of the effluent stream into a smaller tank prior to the main anaerobic digester. The latter will promote CO_2 stripping to the gas phase causing an increase in pH. This is common practice in P recovery systems, where stripping units are added to raise pH, which causes an increase of the concentation of PO_4^{3-} ions, which subsequently will lead to increased struvite crystallization (Jaffer et al., 2002).

4.2.2 Estimation of energy recovery and reactor performance index

The estimation of the energy recovery is based on the amount of methane produced. It is assumed all methane goes through a gas motor with 40 % efficiency for electricity and 50 % efficiency for heat. Electricity and heat prices are set to 0.15 €/kWh and 0.045 €/kWh, respectively (AgroTech, 2014). The reactor performance index (RPI) (Gernaey et al., 2014) is used to evaluate the effects of the previously defined changes on the overall process performance. Specifically, the RPI accounts for: 1) the periodic purchase of chemicals for pH control; and, 2) methane production (and potential energy recovery) (Equation 4.1). The cost of chemicals is based on the market price of NaOH (367 €/ton NaOH (INTRATEC, 2017)).

$$\text{RPI} = \text{Profit}_{\text{energy}} - \text{Costs}_{\text{chemicals}} \tag{4.1}$$

4.3 Results

4.3.1 Default operational conditions

For the current mode of operation (at a pH of 7.2), 135 MWh/d of electricity and heat is produced and 14 tons NaOH/d consumed, based on the model analysis. At an expected 320 production days per year and considering the economic numbers of the previous section, this leads to an RPI of 1.96 M€/year. Hence, for the current

mode of operation and expected 320 production days per year, the estimated RPI is 1.96 M€/year.

4.3.2 pH vs S

At the default operational pH, a lower influent S marginally increases methane production, and thus energy recovery (+ 5.7 %), reduces the use of chemicals (- 17.4 %) and finally increases the RPI (+ 24.6 %) (see Figure 4.1). This higher methane production is attributed to two factors: 1) competitive advantage to MET over SRB due to low influent S (Hao et al., 2014); and, 2) enhanced acidogenesis/acetogenesis due to less H_2S inhibition (Kalyuzhnyi and Fedorovich, 1998). There is also a lower dosing of NaOH for pH control. Indeed, the reduction of S in the influent decreases the production of H_2S, which acidifies the reactor in its dissolved form. At the end of the year, this would lead to a RPI difference of 0.48 M€/year.

When the S load is not modified and the operational pH is decreased to 6.6, there is a slight reduction of methane production and energy recovery (- 1.3 %). On the other hand, there is a lower use of chemicals for pH control (less base addition required). In addition, it reduces the potential precipitation problems in the digester (not currently accounted for in this version of the model, but commented upon in the discussion section) (van Langerak et al., 2000; Latif et al., 2015). All in all, this would suggest an improvement of 1.24 M€/year with respect to the default situation (+ 63.5 %), resulting in a RPI of 3.20 M€/year. However, a pH of 6.6 is considered to be in the low range for anaerobic digestion, as the buffer capacity decreases at lower pH levels. From an operational point of view, a pH of 6.8 would therefore be more stable (Kroeker et al., 1979). This pH increases the RPI with 0.88 M€/year (+ 45.2 %). Combining these two strategies (removing the S from the influent and reducing the pH to 6.8), leads to a RPI of 3.31 M€/year (+69.2 %), an increase of 1.35 M€/year.

The results generated in this section clearly indicate that S does not impose any substantial reduction in process efficiency to warrant the potential cost for removal, which is approximately 3.58 M€/year. In the most optimistic case, S removal would lead to a 1.67 M€/year increase in RPI. Calculation of S removal is based on the amount of limestone needed (23.7 mg SO_4/g limestone) (Silva et al., 2012) for the quantity of S in this case study (131 kg SO_4/h), as well as an assumed market price of 0.085 €/kg limestone (Cree and Rutter, 2015).

Interestingly, the additional simulation results depicted in Figure 4.2 reveal that

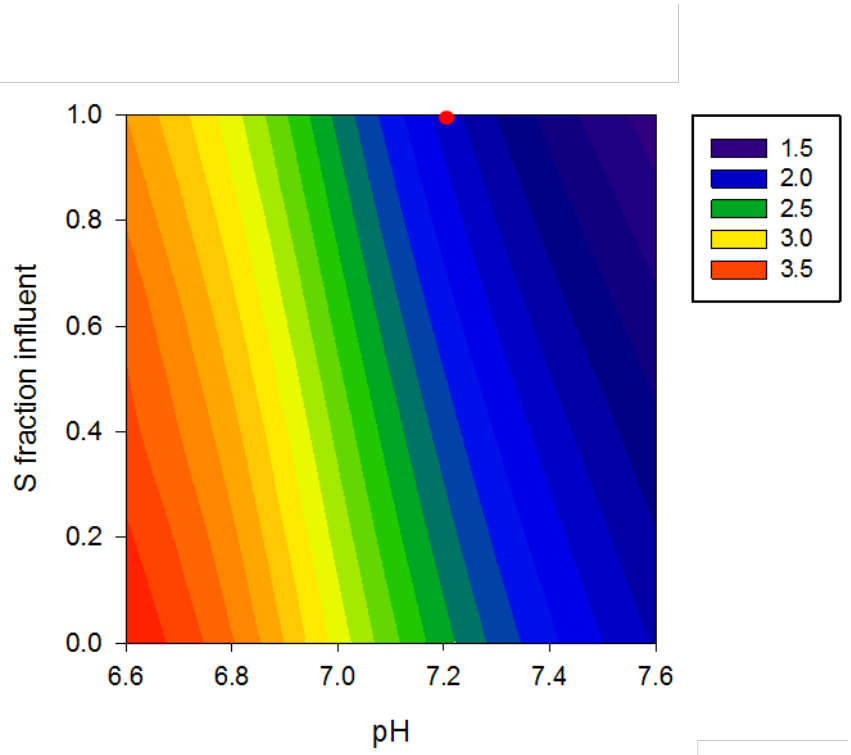

Figure 4.1. Response surfaces generated by changing: pH (x-axis) and the concentration of sulfate and sulfide (y-axis). The simulations are based on #D2. The red dot represents current parameter settings. Results represent the RPI in M€/year. (Feldman et al., 2018a).

the process could ensure similar methane production even at higher S loads as long as the operational pH is maintained above 6.8 (left plot in Figure 4.2). This is caused by the higher presence of H_2S (and decreased HS^-) increasing the S inhibition power at lower pH values (pKa of H_2S = 6.9). However, the cost for pH control would increase drastically in the event of a higher S load in the influent (middle plot in Figure 4.2). In this case a lower pH is more beneficial, as the dissolved H_2S is acidic and NaOH is needed to increase the pH. The S loading can increase up to 2.5 times with a pH below 7.0 without exceeding the current need for NaOH. Combining these two effects into the RPI, the right hand side in Figure 4.2 reveals that for a twofold increase of S, a decreased degree of performance compared to the current operational conditions can be expected starting at a pH of 7.0 and upwards.

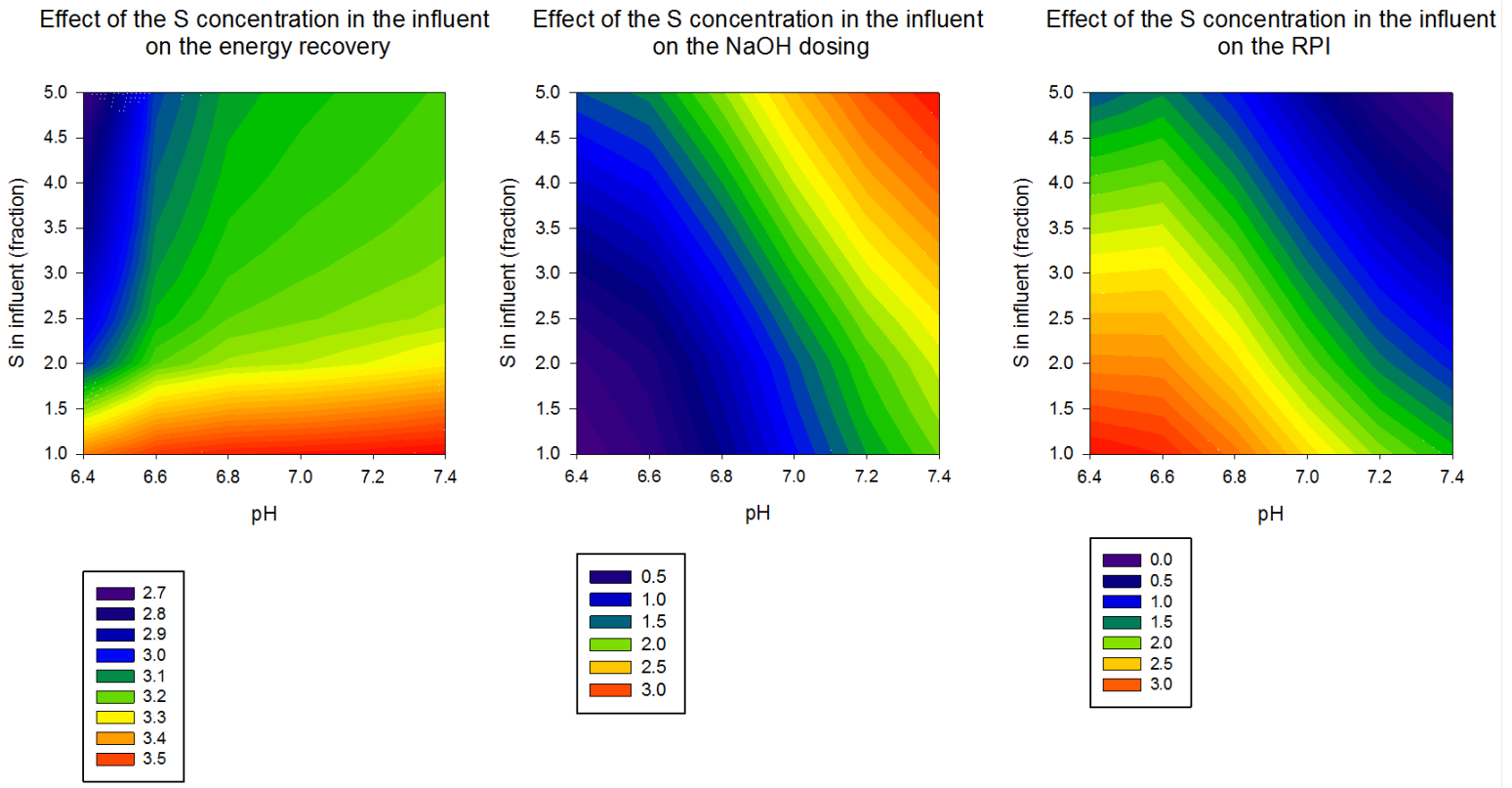

Figure 4.2. Response surface generated by increasing by changing the pH (x-axis) and sulfur compounds (y-axis) up to 5 times the current value in #D2. Left plot: RPI when only taking into account the energy recovery (M€/year); Middle plot: The cost of NaOH (M€/year); Right plot: The RPI when taking both the energy recovery and need of NaOH into account (M€/year (Feldman et al., 2018a).

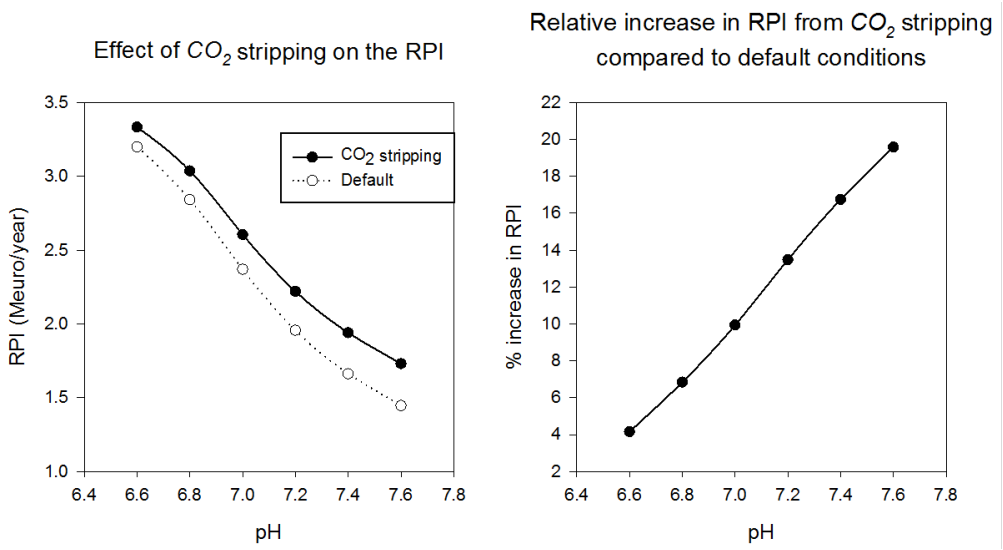

Figure 4.3. Effect of CO_2 stripping and the pH on the RPI (left) and the increase in RPI (%) compared to the case when CO_2 stripping is not applied (right) (Feldman et al., 2018a).

4.3.3 CO_2 stripping

CO_2 stripping has mainly an effect on the NaOH dosing (effect on energy recovery no more than 0.1 % for all pH values simulated). The higher the pH, the more impact CO_2 stripping has on the RPI (linear impact; right hand side in Figure 4.3). This is because the stripping of acidic CO_2 results in a loss of buffer capacity (Lisitsin et al., 2008), and it takes less caustic to reach a pH set point than in default conditions (no CO_2 stripping). At a pH of 7.2, which is the current operational pH, the RPI increases by 13.5 % (+ 0.62 M€/year) when CO_2 stripping is applied. However, it was recommended to operate at a pH of 6.8. At this pH an additional 6.8 % increase (+ 0.19 M€/year) can be achieved on top of the previously determined 45.2 %.

4.4 Discussion

The model presented in Chapter 3 was applied for reactor optimization, to explore different strategies to increase the energy recovery from the organics produced within the Novozymes and Novo Nordisk factories. It was found that decreasing the pH showed the highest potential in overall process performance. Hence, similar process performance could be achieved at lower pH and consequently increasing

the RPI. It should be noted that the S loading to the reactor must not exceed a twofold increase compared to the current conditions when lowering the pH below 6.8 due to the formation of H_2S, which inhibits the methanogenic activity. On the other hand, the cost for NaOH addition increases substantially when the S loading is increased twofold and the pH set point is kept above 7.0. Under the current conditions the S loading does not limit the energy recovery such that it warrants removal. Furthermore, while stripping of CO_2 had no immediate impact on energy recovery, the loss of buffer capacity led to a decrease in NaOH addition, and thus an increase in RPI.

4.4.1 Economics

It is important to highlight that the RPI used in this case study provides an approximate idea of the potential running expenses for the reactor under study, but the entire picture is far from being complete. A proper energy balance should be carried out in order to have a more informed idea about potential recovery potential (Fernández-Arévalo et al., 2017). The costs derived from S are based on rough estimates found in literature (Cano et al., 2015; Cree and Rutter, 2015). The implementation of a new potential technology should be properly evaluated using rigorous metrics, such as net present value (NPV) and internal rate of return (IRR) (Gebrezgabher et al., 2010). These calculations should also capture uncertainty factors, such as the price of chemicals and operation, as well as unforeseen costs (Gargalo et al., 2016). Finally, the price of electricity and heat mentioned in Section 3.3 is assumed to be constant. However, energy prices can fluctuate on a daily basis and are location dependent (Weron, 2014). Aymerich et al. (2015) have shown that changing the energy consumption/production does not necessarily mean the energy costs or profits change. Still the results are valuable and can guide the process engineers in charge of running the plant to achieve better performance.

4.4.2 Opportunities

The presented methodology was applied for the optimization of energy recovery, by increasing the efficiency of the reactor performance. It was found that the largest increase in RPI (+ 45 %) could be obtained by decreasing the pH to 6.8. Another way to use the model is to find where the process is limited or where the limits of the process are, and thus determine its robustness. This study found that the evaluated bioreactor is robust to pH changes, which can be beneficial for control of the process, as well as to save costs on the addition of sodium hydroxide. It was also found that the presence of sulfur compounds does limit the methanogenic activity,

but the highest impact was found for the NaOH dosing. When the concentration was increased up to twofold, the process had a higher dependency on NaOH, thus decreasing the RPI significantly (> 25 %).

4.5 Conclusions and outlook

This chapter presented the optimization of the reactor performance to increase the energy recovery of the anaerobic digester under study. Surface response plots were generated to demonstrate the potential of process optimization and increasing the energy recovery from the anaerobic digester. The optimization study shows that potential savings of 0.88 M€/year can be obtained simply by controlling the pH. This strategy was succesfully implemented on full-scale.

Removing S from the influent does not yield enough energy to warrant the costs for its removal. However, at a twofold increase the drastic increase of NaOH addition reduces the RPI significantly at a pH of 7.0 and above. Furthermore, no significant effect could be obtained by stripping the CO_2 in a recycle loop for energy recovery, but it does lead to chemical cost savings (due to lower buffer capacity).

The scenarios evaluated in this study were chosen after careful consideration with the industrial partner. However, there are many more optimization strategies that could be evalulated in the future:

- The external circulation increases the flow rate in the reactor without increasing the loading. An optimization study can evaluate what the optimal recirculation rate should be to maximize energy production
- Prior to the anaerobic digester is a pre-acidification tank. Future studies could include this reactor to optimize the degree of pre-acidification prior to anaerobic digestion. Scenarios could include variations in pH and retention time.

5 Model II - Biofilm model

While Chapter 3 succesfully implemented a flow + reactor model to the anaerobic digester under study, the presented model is not capable of describing what happens inside the granules regarding microbial composition and phenomena involving inorganic compounds. This chapter describes a granular sludge model, which includes not only the transformations taking place in the liquid phase, but also precipitation kinetics and granular composition. The chapter has been published before as the following journal paper:

Feldman, H., Flores-Alsina, X., Kjellberg, K., Jeppsson, U., Batstone, D.J. and Gernaey K.V. (2017). Modelling an industrial anaerobic granular reactor using a multi-scale approach. *Water Research*, **126**, 488-500.

5.1 Introduction

In multi-scale systems, such as upflow anaerobic sludge blanket reactors (UASB), expanded granular sludge bed (EGSB) reactors or anaerobic fluidized bed reactors (AFBR) (Saravanan and Sreekrishnan, 2006), processes occur at very different spatial (from mm to m) and temporal scales (from seconds to days) (Wanner et al., 2006; Xavier et al., 2005). For example, acid-base reactions are very fast, while microbial growth is rather slow. Such slow and fast variations causes well-known numerical stiffness problems in mathematical models and hence special solvers are necessary (Flores-Alsina et al., 2015). This can be critical when the modelling is to be used for control using rigorous sensor and actuator models (Rosen et al., 2008). At reactor scale, the effects of the hydrodynamics on the overall process performance should be included (Batstone et al., 2005). In systems where microorganisms are anchored into granules, their structure, size and distribution within the reactor must be taken into account since these have strong effects on the overall process performance (Volcke et al., 2010, 2012). Finally, a third scale to consider

is the microbial metabolism along with transport of soluble (diffusion) and particulate (convection) compounds (van Lier et al., 2015). These processes will govern the spatial location of the particulate compounds, such as the bacteria, inert material and other particulates, e.g. precipitates (Rittmann and McCarty, 1980; Boltz et al., 2011). At present, most of the full-scale modelling studies dealing with high rate anaerobic systems have not taken all these aspects (full-scale, multi-scale, N, P and S, multiple mineral precipitation) into account simultaneously (Batstone and Keller, 2003; Batstone et al., 2004a; Ersahin et al., 2007; Chen et al., 2009; Dereli et al., 2010; Hinken et al., 2014; Aymerich et al., 2015; Barrera et al., 2015). As a consequence, it is not possible to properly describe liquid, gas and granule transport processes, including liquid to granule and liquid to gas transfer or inter-granule mass transfer limitations and intergranule heterogeneity (Wanner et al., 2006).

Chapter 3 presented a model of a granular sludge reactor, where the high biomass concentration was simulated by artificial recirculation loops, keeping the biomass inside the reactor. One of the limitations of this method is that one cannot simulate the granular behaviour, where microbes compete for space with inorganic material, which is deposited as a consequence of local supersaturation and the resulting precipitation. Another option is to model the system with a biofilm model, where movement of solubles and particulates is simulated inside granules, where the chemical and biochemical conversion processes take place. The main difference between the two modelling approaches is therefore the location of the reactions. In Model I (Chapter 3) the reactions take place in the bulk and it is assumed there is always enough biomass available. In the biofilm model, the reactions take place in the biofilm, where the available biomass can be a limiting factor for reactor activity.

In order to circumvent the limitations mentioned above, the objective of this chapter is to develop a multi-scale (reactor, granule, biofilm) approach for mechanistic description of the main biological and physico-chemical processes taking place in industrial anaerobic granular sludge reactors. At the biofilm level, special emphasis is placed on describing the competition between sulfate reducing bacteria and methanogens, the addition of ethanol as a separate model component, the effect of ionic strength/activity corrections and the formation of multiple mineral precipitates. Flow patterns, granular distribution and size are addressed at reactor and granular level, respectively. The proposed approach is experimentally tested using two different data sets corresponding to different operational modes (Chapter 2).

5.2 Methods

5.2.1 Multi-scale reactor model

A multi-scale, fully-coupled modelling approach is adopted to describe the system under study (see Figure 2.1 in Chapter 2). The model is based on the Anaerobic Digestion Model No. 1 (ADM) (Batstone et al., 2002a). See Chapter 3 for details on the (bio) chemical processes taking place. The granular sludge model presented in this chapter contains a precipitation module, where multiple mineral precipitation is based on Saturation Index (SI) calculations as stated in Kazadi Mbamba et al. (2015a,b).

5.2.1.1 Reactor scale

At *reactor scale*, R1 and R2 are modelled as a series of continuous stirred tank reactors (CSTR). Each CSTR contains a liquid (V_{Liq}) and a gas phase (V_{Gas}) volume in order to take into account mass transfer phenomena. The total liquid (V_{Liq}) and gas phase (V_{Gas}) volumes are 1 963 and 213 m^3, respectively. Different splitters and combiners (Jeppsson et al., 2007) are used to reproduce the effect of the mixing section (M) and external circulation.

5.2.1.2 Granular scale

At the granular scale, the number of granules (n_g)/total contact area (A_b) are calculated from VSS measurements (Vangsgaard et al., 2012). These values change as a function of reactor height, as does the assumed maximum granule diameter ($L_{max,granule}$). It is assumed that the granular size decreases as the reactor height increases (see Figure 5.1). In this way, the model describes a differential granular size distribution as a function of R1 and R2, in which the granular size is assumed to be constant in each discretized reactor. For simplicity purposes, granules are assumed to be spherical and have constant density ($\rho_{biofilm} = 252$ ($kgTSS\,m^{-3}$) (Batstone et al., 2004b).

5.2.1.3 Biofilm scale

Finally, at the biofilm scale, a one-dimensional model is constructed according to Wanner et al. (2006). The model contains both soluble (S) and particulate (X) state variables. The mass balance assumes that the transport of soluble compounds is governed solely by (homogenous) diffusion whereas movement of particulate compounds takes place by convection (Saravanan and Sreekrishnan, 2006) (see Figure 5.2 for details). Biofilm thickness (L) is given as the radial distance (z)

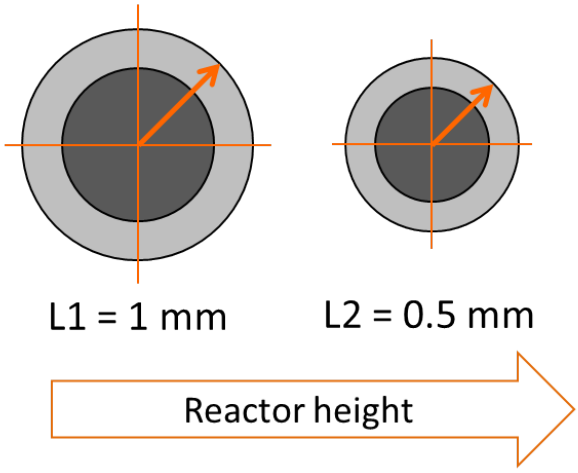

Figure 5.1. Granule size distribution dependent on reactor height.

from the centre to the surface of the granule and varies due to two phenomena (Equation 5.1): i) the net growth (u_F) of the particulate species (Equation 5.2), and ii) detachment (u_D) from the biofilm surface (Equation 5.3) (Lackner et al., 2008). It should be noted that the defined maximum granule size for each layer cannot be exceeded (as is apparant from Equation 5.3, where the detachment rate is dependent on the maximum granule size).

$$\frac{dL}{dt} = u_F + u_D \tag{5.1}$$

$$u_F = \frac{1}{A_k} \cdot \int_0^k A_k \sum_{i=1}^{n_{part}} \frac{r_{organic} + r_{biomass} + r_{precipitation}}{\rho_{biofilm}} \cdot dz \tag{5.2}$$

$$u_D = u_F \left(\frac{L}{L_{max}} \right)^2 \tag{5.3}$$

The resulting system of partial differential equations (PDEs) is solved using the method of lines (Press et al., 2007). In this case, discretization of space (z = the radial distance) is chosen to obtain a system of ordinary differential equations (ODEs). The second-order space derivative describing diffusion (solubles only) is approximated by the finite central difference method in spherical coordinates. The first-order derivative for convective movement of particulates is solved using a backward difference approximation of the first-order concentration space derivative (unless it is the first node, where it is a forward difference). The integral in the

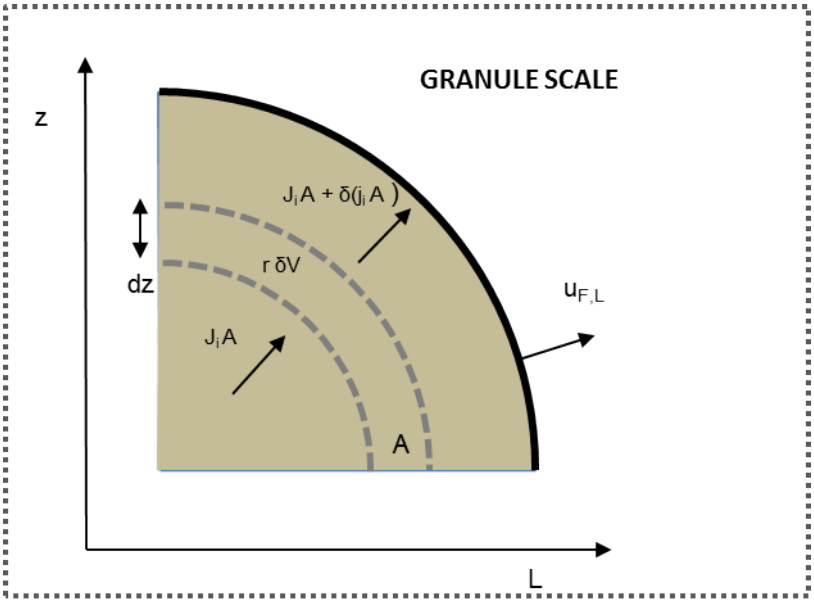

Figure 5.2. Schematic representation of the one-dimensional movement of solubles (diffusion) and particulates (convection).

Table 5.1. Model assumptions and simulation details.

Parameter	Description	Value	Unit
$\rho_{biofilm}$	Biofilm density (constant)	252	$kgTSS\,m^{-3}$
$L_{max,granule}$	Biofilm maximum thickness (R1)	0.001	m
$L_{max,granule}$	Biofilm maximum thickness (R2)	0.0005	m
$L_{boundary}$	Boundary layer	1e-5	m
$N_{biofilm}$	Number of layers within the biofilm	25	-
N_{bulk}	Bulk layer	1	-
t_f	Assumed steady state time	1000	days

equation describing the biofilm growth velocity is approximated by the trapezoidal rule. Further information about biofilm/bulk mass balancing, boundary conditions and numerical resolution can be found in Vangsgaard et al. (2012). The model has been implemented from these first principles in Matlab-Simulink (Mathworks, Natick, MA, USA). All dynamic simulations are preceded by steady state simulations to ensure correct model initialization (Gernaey et al., 2014). An overview of simulation details can be found in Table 5.1.

5.2.2 Parameter estimation

The parameter estimation is done in a similar way as to the method used in Chapter 3. Key parameters affecting biogas (CH_4, CO_2, H_2S), organics profiles (COD_{part}, COD_{sol}, VFA), nutrients (NH_x, $H_xPO_4^{3-X}$) and several cations/anions (SO_x^{2-}, Ca^{2+}, Mg^{2+}) are estimated. The selection of these parameters is based on previous global sensitivity analysis studies (Solon et al., 2015a; Barrera et al., 2015).

5.3 Results

5.3.1 Dynamic modelling of effluent data

5.3.1.1 Dataset #1

Simulation results in Figure 5.3 (solid lines) show that the proposed approach is capable of reproducing (dotted lines) hydrolysis (see COD_{part} profiles), acidogenesis (see COD_{sol} profiles) and acetogenesis (see VFA profiles) for #D1 (see Figure 5.3). The pH, SO_x^{2-}, CH_4, CO_2 and H_2S profiles reveal the correct description of the weak acid-base chemistry, mass transfer (liquid-gas) methanogenesis, sulfidogenesis and competition between methanogens (MET) and sulfate reducing bacteria (SRB). The model also predicts N (see NH_x profiles) and P (see $H_xPO_4^{3-X}$ profiles) release with good agreement to the available data. Finally, although the SI values identify potential precipitation of $CaCO_3$ and $Ca_3(PO_4)_2$, the mass balances indicate that this does not occur (or if it does, only to a very low degree) (see Ca^{2+} and Mg^{2+} profiles).

Compared to the default parameter values (not considering X_c as stated in Batstone et al. (2015)), hydrolysis rates (k_{carb}, k_{prot}, k_{lip}) had to be increased considerably (around 10 times). This is mainly due to the extremely biodegradable influent (around 70 % of the total COD is converted to CH_4). The pre-acidification tank (PAT) tank before the AD does contribute to that purpose as the degree of acidification (DA) in the influent and effluent is 40 %. Moreover, uptake rates for hydrogen degraders (X_{H2}, X_{SRB}) had to be slightly adjusted in order to give a competitive advantage to SRB (Batstone et al., 2006; Barrera et al., 2015; Flores-Alsina et al., 2016). This study assumes that S conversion (around 50 % of the incoming S) is done autolithotrophically (Batstone et al., 2006; Flores-Alsina et al., 2016). The inhibition parameter for H_2S had to be decreased substantially ($K_{I,H2S}$) in order to describe VFA dynamics effectively. The most probable reason is the potential inhibition on acetogens (X_{c4}, X_{pro} and X_{ac}) by an inorganic/organic/metal compound that is neither measured nor described by the model, as explained in Chapter 3.

The N and P contents in biomass/inerts had to be re-estimated to match the nutrient dynamics. The other parameters were set to their default values (Batstone et al., 2002a; Flores-Alsina et al., 2016). Further information about parameter values can be found in Table A.4 and Table A.5 in the appendices.

5.3.1.2 Dataset #2

Figure 5.4 shows the dynamic profiles for the second evaluation period (#D2). Again, simulation results reveal that the model successfully predicts the trends of selected operational variables. The good agreement between the measured (dotted lines) and the simulated (solid lines) data supports that the developed multi-reactor scale model properly captures the interactions between the influent wastewater and relevant microorganisms. Only occasional pH measurements were available, averaging at 7.3. Another important difference with respect to #D1 is the role of precipitation. The higher operational pH and Ca^{2+} concentrations and lower $H_xPO_4^{3-X}$ concentrations indicate that $CaCO_3$ is the dominant compound. High SI values and literature data (van Langerak et al., 1998) reinforce the hypothesis. The same rationale was used to select and adjust model parameters.

Specifically for #D2, hydrolysis rate values (k_{carb}, k_{prot}, k_{lip}) are closer to the values reported in Batstone et al. (2015). This is attributed to the lower biodegradability of the substrate. Mass balances in Chapter 2 show a decrease of the COD conversion to CH_4 from 70 to 60 % when comparing #D1 with #D2. The COD_{part} / COD_T ratio is also substantially higher (from 15 to 28 %) for #D2. Uptake rates for hydrogen degraders (X_{H2}, X_{SRB}) are slightly modified. Despite the higher S load, a similar reduction (50 %) to sulfides is achieved. The value of the inhibition parameter for H_2S ($K_{I,H2S}$) is set back to the default values, which reenforces the previous hypothesis of the presence of an unidentified inhibiting compound for #D1 (the DA in the effluent is lower in #D2). With respect to the precipitation kinetics, k_{CaCO3} is close to the values reported by Kazadi Mbamba et al. (2015b). It is important to highlight that this section only considers precipitation in the bulk. The effect of inter-granular precipitation is studied in the following chapter. As in the previous case, the other parameters are set to their default values (Batstone et al., 2002a; Flores-Alsina et al., 2016).

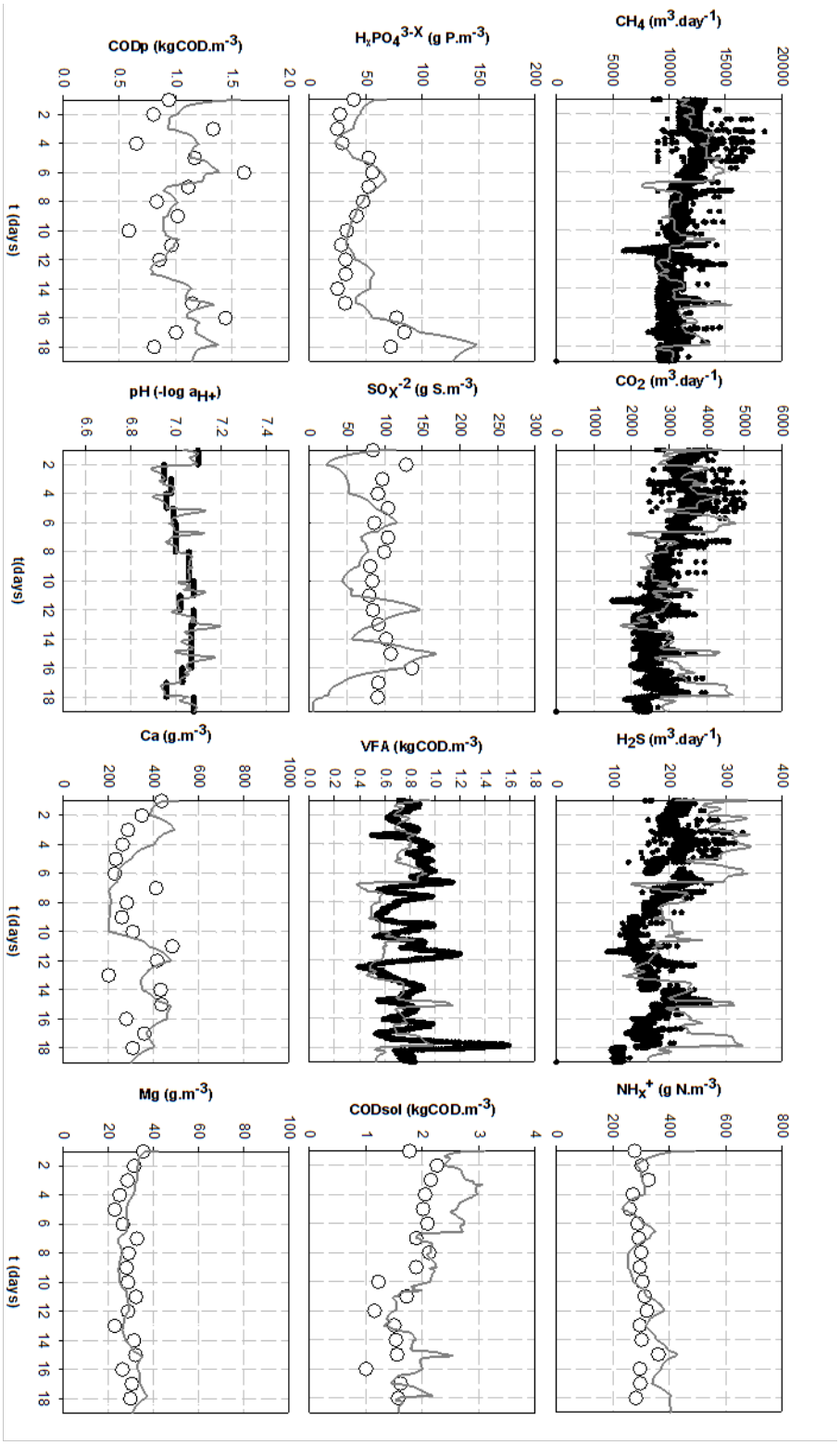

Figure 5.3. Simulation results (lines) and measured effluent data (markers) for dataset #1 (#D1) (Feldman et al., 2017).

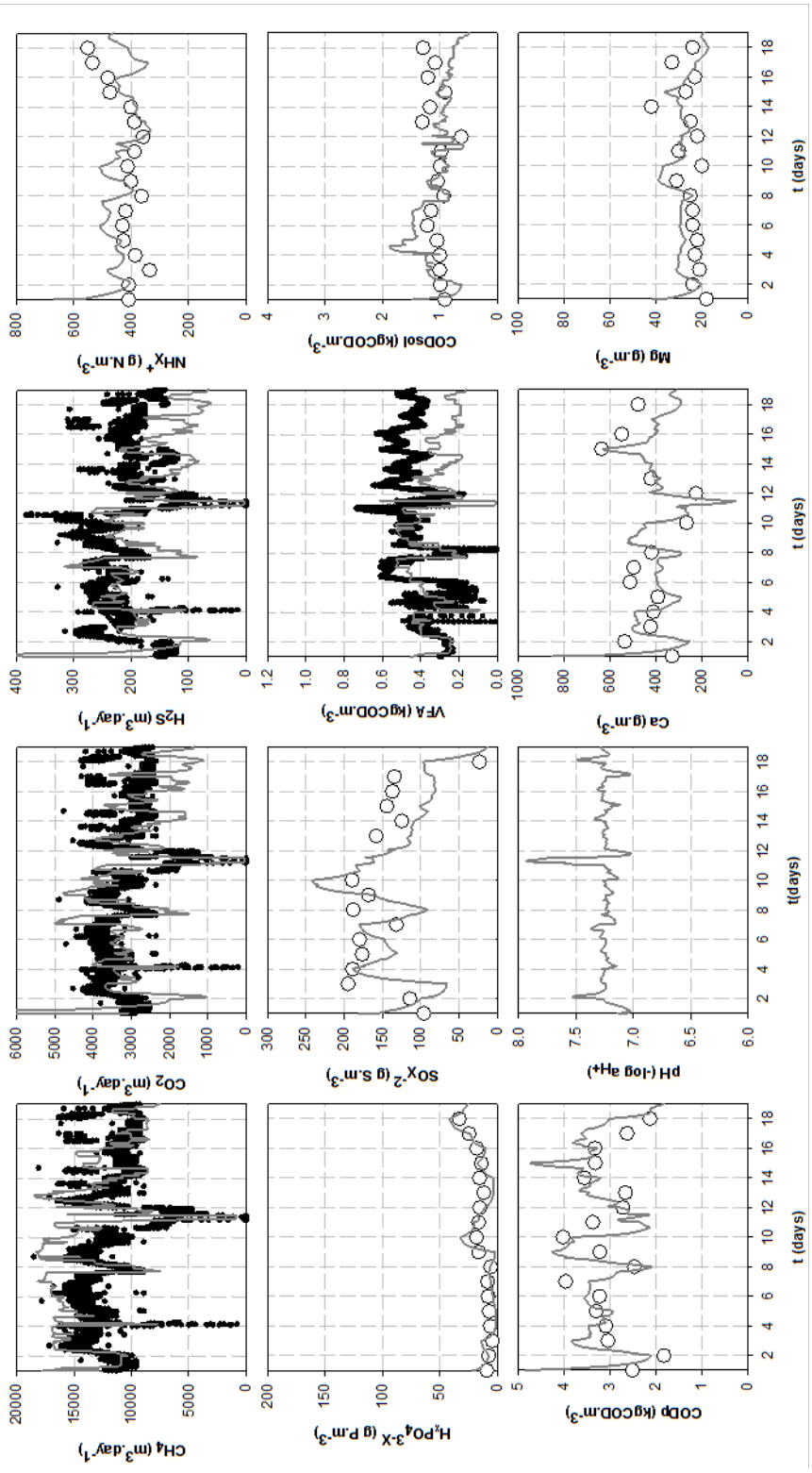

Figure 5.4. Simulation results (lines) and measured effluent data (markers) for dataset #2 (#D2) (Feldman et al., 2017).

5.4 Prediction of granular structure

This section looks in more detail at the granular structure. Both the diffusion of substrates into the granule, as well as the biomass distribution are taken into account.

5.4.1 Relative substrate/biomass distribution within the granule

The simulation results depicted in Figure 5.5 show the concentration profiles of fermentables (S_{su}, S_{aa}, S_{fa}, S_{eth}), organic acids (S_{va}, S_{bu}, S_{pro}, S_{ac}) and hydrogen (S_{H2}) as a function of granule depth for both R1 and R2. These substrates were predicted to degrade to a concentration level of approximately 10 % of the affinity constant K_S (Batstone et al., 2002a) within the outer 100 μm of the biofilm. Methane (S_{CH4}) and pH, on the other hand, show the opposite behaviour: higher values in the centre of the granule and a significant decrease towards the surface. Regarding R1 and R2 one can observe the same trends, but organic soluble substrates (S) and pH are higher in the lower reactor compartment due to the higher loading conditions. The model also indicates that the centre of the granule is inactive due to the high concentration of inert material (X_I) resulting from biomass death. The biomass (X_{bio}) and organics (X_{org}) concentrations increase for an increasing radial distance (z), i.e. the closer to the surface, the higher the biomass concentration. Similar experimental observations were reported by de Beer et al. (1992), Flora et al. (1995), Batstone et al. (2004b) and Saravanan and Sreekrishnan (2006). Regarding the distribution of specific groups of microorganisms, a high portion of methanogens (X_{ac}) is placed in the inner zone, and this fraction decreases as the radius of the granule increases. The presence of acidogens (X_{su}, X_{aa}, X_{fa}) and acetogens (X_{c4}, X_{pro}) is comparatively higher in the outer layers of the biofilm (see Figures 5.5 and 5.6, first column), though it should be noted no clear borders exist outlining specific activity zones in the granules. The role of X_{SRB} is quite marginal due to limited turnover. This distribution responds to: 1) applied loading rates; 2) mass transfer limitations; 3) the specific (bacterial) affinity for substrates; and, 4) relative kinetic uptake rate of the substrates, as well as substrate placement within the overall process. Again, similar trends can be observed between the upper and lower reactors but there is a lower quantity of X_I in R2 due to loading conditions. Both uni/multi-dimensional models presented in Batstone et al. (2004b, 2006) and Odriozola et al. (2016) have presented comparable predictions.

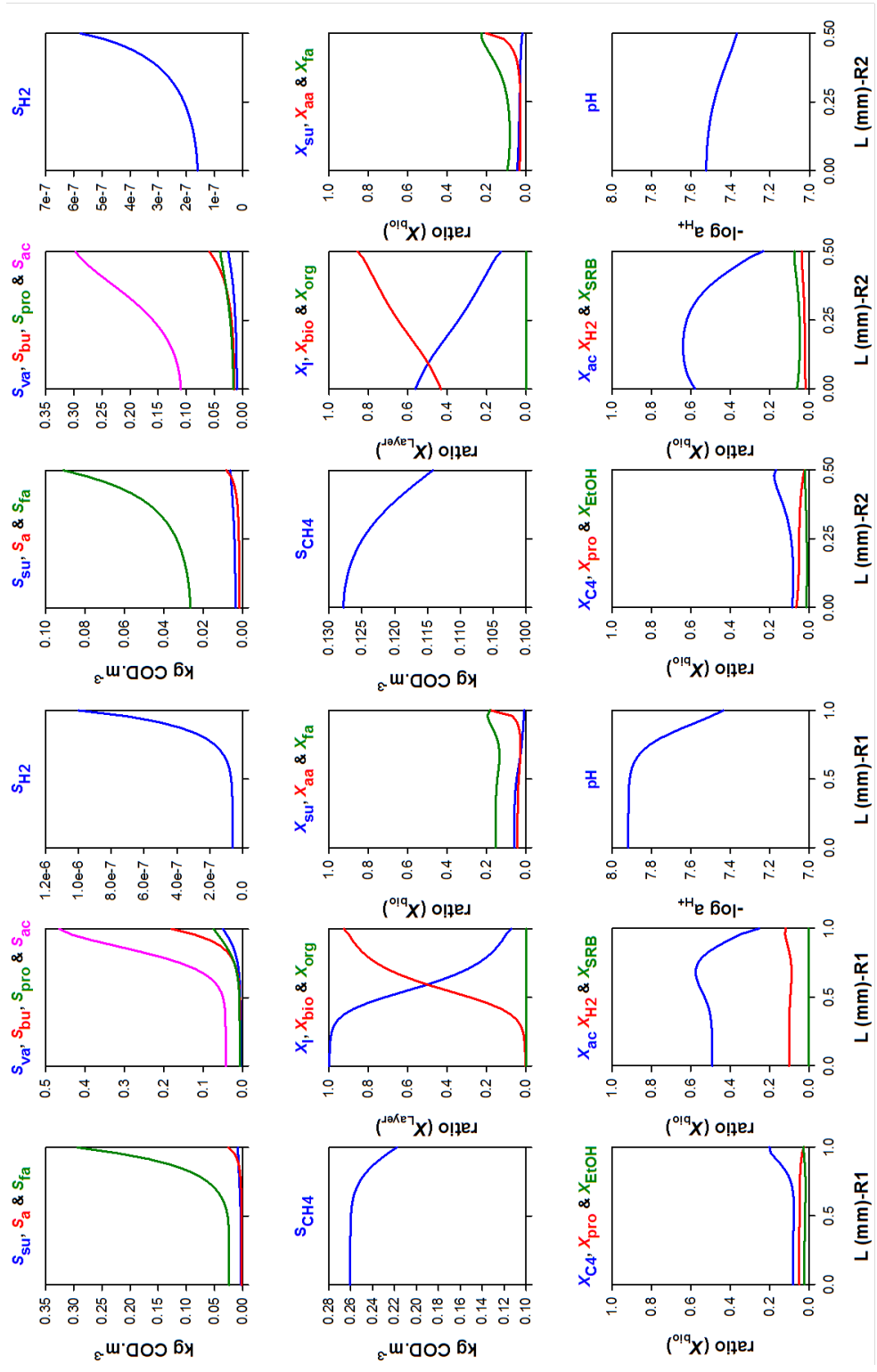

Figure 5.5. Predicted biomass/organics/pH distributions within the biofilm in the lower (R1) (columns 1,2,3) and upper (R2) (columns 4,5,6) parts of the bioreactor for dataset #1 (#D1). 0.000 = centre. X_I and X_{bio} are total particulates and biomass per each discretized layer. The presence of organics, inerts and biomass is displayed in relative terms (Feldman et al., 2017).

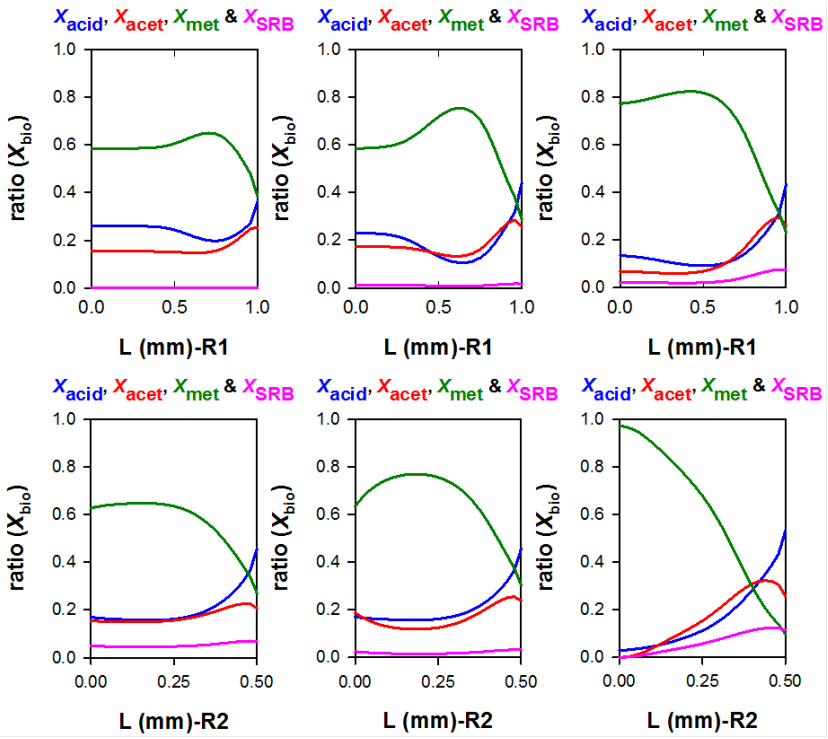

Figure 5.6. Predicted biomass distributions in the granules under three different conditions: default operational conditions (column 1), pH decrease (column 2) and higher S loads (column 3). #D1 is used to run the simulations. $X_{\text{acid}} = X_{\text{su}} + X_{\text{aa}} + X_{\text{fa}}$; $X_{\text{acet}} = X_{\text{C4}} + X_{\text{pro}} + X_{\text{EtOH}}$; $X_{\text{met}} = X_{\text{H2}} + X_{\text{ac}}$. The presence of biomass is displayed in relative terms (Feldman et al., 2017).

5.4.2 Impact of operational/loading conditions

While the previous chapter focussed on process optimization, the impact on the granular structure in terms of microbial community was not taken into account. This section aims to look at the stability of the microbial community within the granule. The scenarios are not defined as extensively as in Chapter 4, as here the objective is only to show how the microbial community might change as the operational conditions change. In the first scenario the pH was lowered from 7.0 to 6.0 (middle column Figure 5.6), and in the second scenario the S load was increased three times (right column Figure 5.6). Simulation results reveal that while the impact on process performance is significant (a decrease in methane production by 15 % and 30 %, respectively, for scenario 1 and scenario 2), the microbial community itself remains stable. This indicates that changes in process conditions mainly have an impact on the activity of the microbes, at least on the short-term.

5.5 Discussion

The results summarized in this study bring a substantial advance in the field of wastewater treatment modelling by introducing a multi-scale representation of the anaerobic digestion process. At the reactor level the model describes general hydrodynamics accounting for high (R1) and low (R2) loading conditions, gas-liquid (G - L) transfer as well as multiple instances of flow combining (M) and flow splitting (R1). At the granule level, size is a function of biomass growth and decay. The maximum diameter is assumed to change with reactor height. Finally at the biofilm level, species competition/inhibition for substrates/space is described following well-established biochemical/physico-chemical models, like the ADM1. While these approaches are applied piecemeal in the literature, this chapter demonstrates the strength of an integrated approach, using a comprehensive data set (#D1, #D2). Development of such models, including their validation with full-scale data, is critical to enable future development of better operational strategies or optimization studies (Jeppsson et al., 2013), with particular opportunity in industrial systems. In the following sections, the suitability of the number of considered processes and some practical implications for the plant-wide modelling of resource recovery strategies are discussed.

5.5.1 Parameter estimation

The parameters that needed to be estimated for Model II were similar as the ones estimated for Model I (Chapter 3). However, the resulting parameter values were not equal. The disparity can be explained as follows:

- The kinetic parameters for Model I contain mass transfer limitation. Model II has mass transfer as part of diffusion and convection of substrates and products in and out of the biofilm. Therefore, the mass transfer phenomena are not a part of the kinetic parameters.
- The ADM1 contains a large number of correlated parameters. Thus, in Model I parameter A can be re-estimated, while in Model II the estimation of parameter B yields the same result. This is mainly of significance in the case of the re-estimation of the H_2S inhibition parameters in Model II. In Model I, it was chosen to add an extra inhibition parameter multiplied with the existing inhibition parameters, while in this chapter these parameters themselves were re-estimated. In the end, the result is the same.
- In Model II the hydrolysis rates of proteins, lipids and carbohydrates are re-estimated, while these parameters remain at their default values in Model

I. This can be a leading cause to the difference between the stochiometric parameters in Model I and Model II.

5.5.2 Opportunities and limitations

The approach presented in this chapter offers a moderately parsimonious, yet mechanistic representation of the digestion process under study given the high complexity of the problem. The reader should be aware that the system under investigation is an industrial plant and the composition of the feed together with the way to operate the reactor changes substantially according to yearly production schemes, in comparison with the relatively high predictability of domestic wastewaters (see also Introduction when describing some of the challenges related to industrial wastewater treatment). As discussed in this chapter, it could explain the changes in the influent biodegradability (k_{carb}, k_{prot}, k_{lip}) and the unusually low ($K_{I,H2S}$) values, which forced the re-estimation of a few parameters when switching from #D1 to #D2. Yet, the study has shown that the model provides very reasonable predictions with minimal parameter value modifications. Indeed, almost all parameters are kept at their default values (see Tables A.4 and A.5 in the appendices).

Additional experimental results are necessary to validate the predicted profiles within the biofilm. In that sense micro-sensors are promising tools (Garcia-Robledo et al., 2016). The same applies to the prediction of the microbial distribution in the granules, which is far more readily evaluated using molecular techniques. This type of research is currently being done using fluorescence in-situ hybridisation (Batstone et al., 2004b; Winkler et al., 2013), but also extraction and bulk methods are used (Lu et al., 2013). Molecular techniques will provide additional insights on how microorganisms are distributed within the granule, and if this distribution changes as a function of: 1) reactor height; 2) ash content (quantity of precipitation); and, 3) granular sizes. A proper assessment of the last factor has not been performed in this study, and literature data was used instead. However, all this information will help to construct better mechanistic models and increase the overall knowledge about anaerobic (industrial) biofilms.

Model upgrades could substantially improve the model prediction capabilities. There are numerous studies that demonstrate the effect of granular size (Volcke et al., 2010, 2012). This can be critical in systems with a clear competition between MET and SRB (Sun et al., 2016). In this paper, the assumption that precipitation was only taking place in the bulk worked out because the evaluation period was rather short. When considering a longer evaluation period, intra-granular precipitation must be

included since it has a major importance in industrial reactors (van Langerak et al., 1998, 2000). It is also a request from the process managers running the plant that future model development should include this type of phenomena. The next chapter looks further into this.

Finally, it should be noted that no systematic procedure has been used for model calibration (Brockmann et al., 2008, 2013). The results of the global sensitivity analyses by Solon et al. (2015a) and Barrera et al. (2015) serve as a good indication and provide a good way to start. The methods might not be applicable in other systems, but in this case, the number of parameters to be adjusted was rather small in order to produce reasonable values.

5.5.3 Model-based optimization of reactor performance

The model implementation presented in this chapter will allow the development of benchmarking procedures for optimizing resource recovery (e.g. biogas recovery) in an industrial context (Copp, 2002; Gernaey et al., 2014). Implementation of special routines has been necessary, to allow the use of non-stiff solvers (Flores-Alsina et al., 2015). As a consequence, it is now also possible to use sophisticated sensor and actuator models accounting for different step responses, delay and noise levels (Rieger et al., 2003; Rosen et al., 2008). This will allow to develop, test, implement and evaluate realistic control strategies. This is a clear advantage with respect to state of the art biofilm software (Reichert, 1994) allowing a whole new set of possibilities. Control strategies, such as the ones presented in Steyer et al. (1999), Irizar et al. (2015) and Strömberg et al. (2012), could be tested as well in (anaerobic) granular sludge systems.

The model has the potential to evaluate more traditional process options, such as the financial benefits resulting from an improved biogas production balanced against the addition of selected chemicals (Flores-Alsina et al., 2016), calcium control (van Langerak et al., 1997), or the addition of substrates for co-digestion (Arnell et al., 2016). Appropriate performance evaluation indices should be developed for that purpose (Solon et al., 2017). In the previous chapter, the reactor performance index was defined as a combined calculation of the profit (or savings in case of re-use within the factory) from energy recovery as well as the cost of chemical dosage for pH control. This allowed for the evaluation of different optimization strategies to increase the energy recovery and decrease chemical dosage to the anaerobic digester. The model presented in this chapter can further add to the optimization simulations of the previous chapter by simulating the specific

methanogenic activity as a function of available biomass. Due to the format of the artificial recycling of biomass in Chapter 4, the maximum biomass capacity was not a limiting factor.

5.6 Conclusions

A multi-scale mathematical model approach is developed and used to predict the performance of an industrial full-scale anaerobic digester. The model deals with reactor hydrodynamic issues, granule growth, gas stripping, intra-granular convective movement and mass transfer limitations as well as multi-species/multi-substrate competition/inhibition within the biofilm. The datasets presented in Chapter 2 were used for model calibration. The modified version of the BSM2 influent generator provided additional dynamics (diurnal and weekly variation/cleaning of equipment/reactor shut down) and increased data frequency (from days to minutes).

The model is capable to describe hydrolysis, acidogenesis, acetogenesis, methanogenesis, sulfidogenesis, liquid-gas mass transfer, weak acid-base chemistry and multiple mineral precipitation as demonstrated by the good agreement between the (macroscopic) experimental data and the model simulations. The potential biomass distribution within the granule and for each reactor is assessed based on influent loadings, mass transfer limitations and bacterial affinity for substrate. Competition between inorganics (precipitates) and organics (biomass) can be analyzed on the basis of the developed models.

6 Assessing the efffects of intra-granule precipitation in a full-scale industrial anaerobic digester

The model presented in Chapter 5 is used for simulating the long-term impact precipitation has on the energy recovery of the anaerobic digester under study. This chapter is based on the following article:

Feldman, H., Flores-Alsina, X., Ramin, P., Kjellberg, K., Jeppsson, U., Batstone, D.J. and Gernaey, K.V. (2018). Assessing the effects of intra-granule precipitation in a full-scale industrial anaerobic digester. Submitted to *Chemical Engineering Journal*.

Part of the experimental results have been presented in the following paper:

Prevedello, M., Feldman, H., Nesme, J., Mortensen, M., Flores-Alsina, X., Sørensen, S.J., and Gernaey, K.V. (2018). The effect of high precipitate concentration on the microbial community structure in an industrial anaerobic granular sludge reactor. IWA Biofilms: Granular Sludge conference 2018, Delft, The Netherlands, 18-21 March, 2018. Poster/Flash presentation.

6.1 Introduction

The water in the treatment plant at Novozymes A/S originates from fermentation processes for the production of pharmaceuticals and enzymatic products. In biotechnology industries producing wastewater streams with high content of salts, the formation of multiple mineral precipitates might cause the accumulation of inorganic particulates at different locations in the reactor (granules, pipes), which might lead to detrimental (loss of methanogenic activity) or even catastrophic (ce-

mentation) effects on reactor performance (van Langerak et al., 1998, 2000). The formation of precipitates in either bulk or biofilm, for example in anaerobic granular systems, may depend on many factors, such as cationic/anionic load, degree of influent acidification and/or granule size. The potential assessment (a priori) of the conditions promoting the formation of multiple mineral precipitates is of paramount importance for process engineers deciding amongst competing operational procedures when optimizing plant performance.

The industrial partner in the project observed precipitation inside the anaerobic digester after the addition of a reject water stream. This stream originates from sludge dewatering, which prior to the dewatering process is stabilized with quick lime (CaO). The stream is high in COD as well as alkalinity, which was expected to be beneficial for the reactor performance in terms of energy recovery and chemical dosage for pH control. On the other hand, the stream also contains a high mineral content, which could lead to precipitation.

The multi-scale model based approach presented in Chapter 5 describes the reactor performance in terms of influent and effluent conditions, such as COD, VFA, nutrients and minerals, biogas production as well as the microbial content of the granules. The model was able to reproduce the effluent concentrations and biogas production from two separate datasets (Chapter 5). The current chapter extends this work to evaluate the impact of elevated calcium levels, and further explore the impact of precipitation on granule structure and activity at longer time frames, specifically through displacement of active microbial biomass via precipitates when ionic inputs increase through use of saline reject water.

The main objective of this study is to use a model-based approach, using the biofilm model presented in Chapter 5:

- To assess of the potential formation of intra-granule mineral precipitation in industrial anaerobic reactors.
- To describe the spatial competition between biomass inorganic particulates within granules.
- To evaluate the effect of mineral precipitation on COD conversion and potential energy recovery. The multi-scale modelling approach is used for describing how growth/decay of microorganisms and formation of inorganic precipitates compete for space.

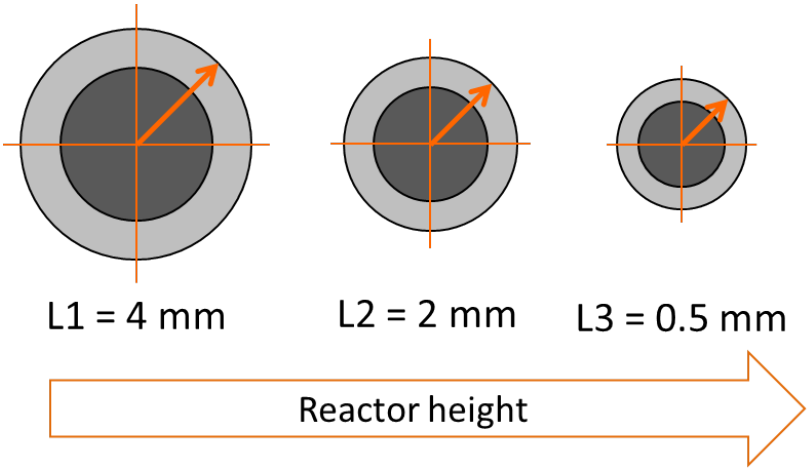

Figure 6.1. Granule size distribution dependent on reactor height.

Furthermore, an experimental procedure is presented to validate the simulation results. Obtained results are used to give an indication on the quality of the model results regarding granular behaviour in terms of precipiation and activity.

6.2 Methods

6.2.1 Plant configuration and data measuring campaign

Refer to Chapter 2 for the description of the plant configuration and the characterization of the measured datasets. Dataset#1 is without reject water, while dataset #2 is with the addition of reject water, in which the calcium loading is increased from 47 $\mathrm{kg\,h^{-1}}$ to 124 $\mathrm{kg\,h^{-1}}$.

6.2.2 Multi-scale reactor model

Chapter 5 details the development of the multi-scale reactor model used for this study. However, a few changes were made before the study of this chapter was conducted. First of all, in Chapter 5 only 2 CSTRs in series are considered, while this has increased to 3 reactors in this chapter. This is followed by further discretization of the maximum biofilm size (Figure 6.1). Furthermore, precipitation inside the granules is taken into account for the current study, while this was only the case for the bulk liquid in the simulations of the previous chapter.

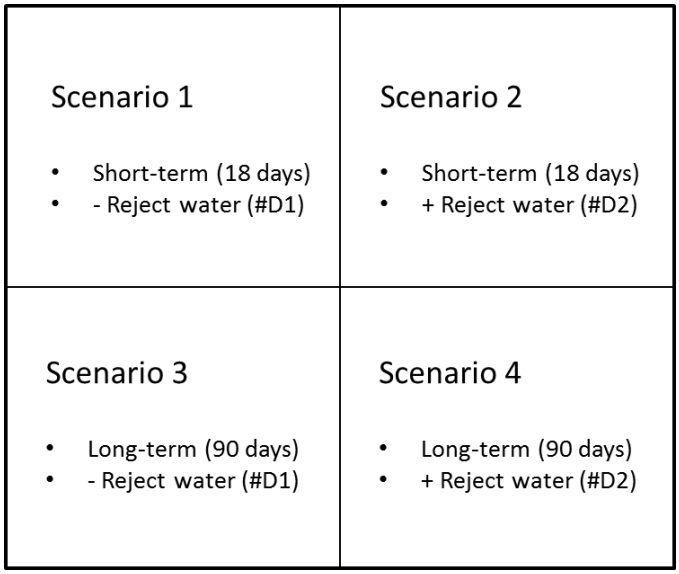

Figure 6.2. Scenarios analyzed in the case study.

6.2.3 Scenario analysis and long term evaluation

Four scenarios are evaluated (Figure 6.2). The short-term analysis consists of 18 days of simulation time, while in the long-term evaluation these 18 days are repeated five times (to a total of 90 days). #D1 and #D2 are used as model inputs to simulate no reject water and addition of reject water, respectively.

6.2.4 Experimental methods

Samples from the IC reactor were taken on 9-3-2017 to analyze the methanogenic activity in L1 (bottom of the reactor) and L2 (top of the sludge bed). Shake flasks were prepared with 100 mL IC effluent and 1 mL of a 275 g/L acetate solution. The pH was set to be between 7.0 and 8.0. 5 g of biomass with a known VSS content was added per shake flask, after which the flasks were sparged with nitrogen gas for 20 seconds. The flasks were closed subsequently with an oxitop. The shake flasks were incubated at 35 °C and 60 RPM. After one hour the pressure inside the flasks was released and the oxitop meter was started. The analysis was run for 3 days, after which the shake flasks were fed with 1 mL of acetate solution and another run was started. Pressure data from the second run was used for calculating the methanogenic activity according to Equation 6.1, in which SMA is the specific methanogenic activity, ΔP the pressure difference, V the volume of the

headspace (mL), VSS the concentration of VSS in the shake flask (g), R the gas constant (L atm/mol K) and T the temperature (K).

$$SMA(gCOD/gVSS/d) = \frac{\Delta PV}{VSS \cdot 24} \cdot \frac{64}{RT} \tag{6.1}$$

6.3 Results

6.3.1 Effects of adding reject water on influent/effluent characteristics and operational conditions

Chapter 5 has shown that the multi-scale biofilm model is capable of describing the transformation of organics, nutrients and minerals, the production of methane, carbon dioxide, sulfide and the formation of precipitates within the bulk phase for both datasets (#D1 and #D2) satisfactorily. Both full-scale measurements and model simulations show that the immediate effect of adding reject water is an increase of pH (Figures 6.3 a, b) and a reduction of the quantity of chemicals (NaOH) used for pH control within the reactor (even though the reactor pH is fixed to a higher set-point compared to the scenario without reject water addition) (Figures 6.3 c, d, g, h). This effect is mainly due to the addition of reject water, which creates an increase of the buffer capacity due to the presence of calcium ions (related to quick lime CaO use in sludge stabilization prior to dewatering). The results also show that the physico-chemical framework (PCF) is capable of predicting influent/effluent pH + buffer capacity from the influent/effluent cationic/anionic composition. Finally, the addition of COD coming from the reject water increases biogas production and consequently energy recovery by an average of 9.5 %. It should be noted that for Figure 6.3d, the measured pH is only measured occasionally (as mentioned in Chapter 5). In this case, a filter has been applied to the datapoints to generate a high-frequency input.

6.3.2 Location dependency of precipitation

The proposed approach indicates a stratified structure within the granule, which is the result of: 1) applied loading rates; 2) mass transfer limitations; 3) specific (bacterial) affinity for substrate; and, 4) relative kinetic uptake rate of the substrates, as well as substrate placement within the overall process. For exemplary purposes, the top part of Figure 6.4 shows the changes in the granule composition as a function of reactor height for dataset #D2 when reaching steady state (M, R1 and R2). In this figure each circle shows the percentage of the different particulate compounds at each layer of the biofilm. It should be noted that this image does not represent

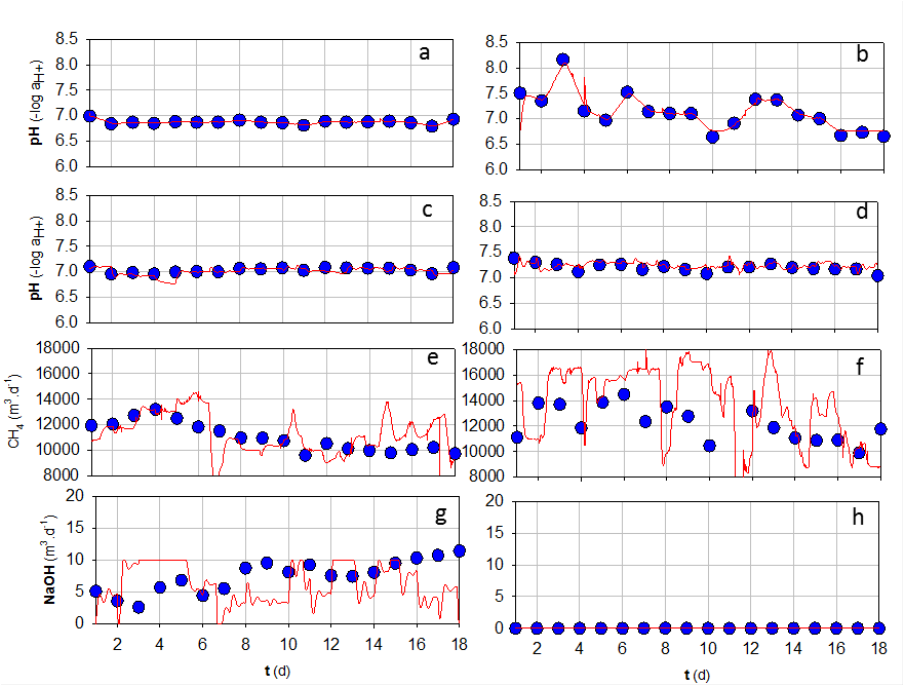

Figure 6.3. Simulation results (red lines) compared to measurements (blue dots) for the impact of dosing no reject water (left column) and with dosage of reject water (right column) on pH influent (a,b) and effluent (c,d), methane production (e,f) and NaOH addition for pH control (g,h).

the exact location of the different fractions in 2D. Precipitation within the granule is assumed to be inactive at the beginning, and only takes place in the bulk phase to avoid running into numerical problems when reaching steady state. These initial (good) conditions are then used to run dynamic simulations. At t = 0 d in M, the center of the granule is inactive due to the high concentration of inert material (X_I) resulting from biomass decay. The biomass (X_{bio}) and organics (X_{org}) concentrations increase with an increasing radial distance (z), i.e. the closer to the surface of the granule, the higher the biomass concentration. The fraction of inerts (X_I) decreases at the top of the reactor, where the granule composition essentially consists of biomass. In this particular case SI for all precipitates are negative, and therefore most of the inorganics ($X_{inorganic}$) are associated with biomass products, such as polyphosphates (Ekama and Wentzel, 2004). Similar experimental observations were reported by de Beer et al. (1992), Flora et al. (1995), Batstone et al. (2004b) and Saravanan and Sreekrishnan (2006).

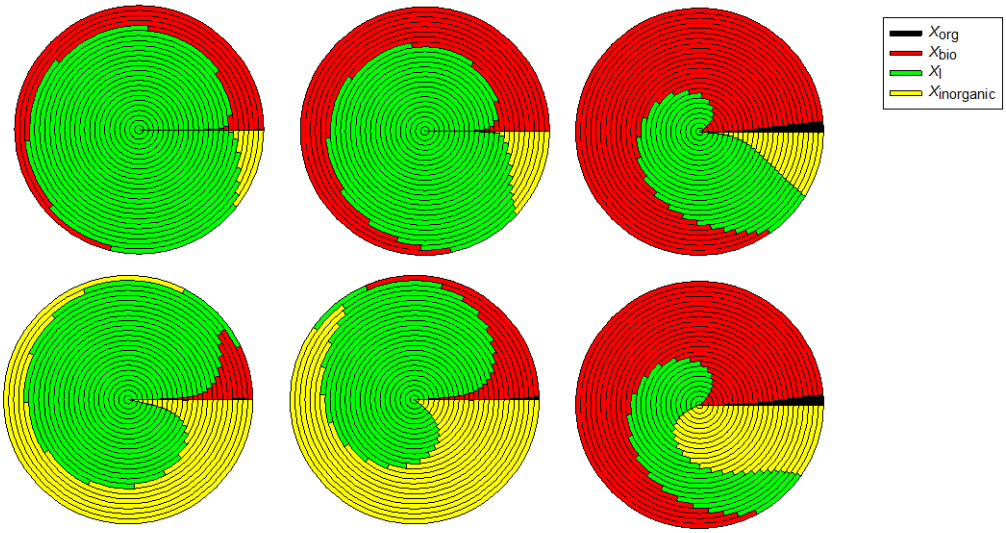

Figure 6.4. Granule composition – organics (X_{org}), inorganics ($X_{inorganic}$), biomass (X_{bio}) and inerts (X_{inerts}) at different reactor heights: left (mixing section, M), centre (expanded sludge bed, R1), right (polishing section, R2). Top: steady state, bottom: after 100 days of dynamic simulations. This figure illustrates the relative abundance of the different biomass fractions as a function of granule radius for three types of granules (three different biofilm thicknesses, one for each reactor compartment). The figure does not show the exact location of the different biomass fractions. (Feldman et al., 2018b).

Additional simulation results show higher pH values in the center of the granule and a significant decrease towards the surface (see Figure 6.5 top). This is mainly due to VFAs, which are converted into the weaker carbonic acid leading to elevated pH conditions. This corresponds with the experimental observations reported by de Beer et al. (1992) and Flora et al. (1995). Higher influent Ca concentration and increasing intra-granular pH gradients also favours saturation conditions (SI) for $CaCO_3$ when reject water is added (see Figure 6.5 top). Assuming both biological activity and formation of inorganic solids, simulation results indicate a vertical gradient: high concentration of precipitates in M and R1 and lower in R2 (see Figure 6.5), i.e. precipitates tend to accumulate in the bottom part of the reactor. The latter corresponds with experimental observations where the content of ash in TSS (ISS/VSS ratio) decreases when moving from the bottom to the top of the bioreactor (see experimental results in Section 6.3.4). The location of precipitates depends on the granule size. In large granules (L_{max} > 2 mm), the conversion of organic

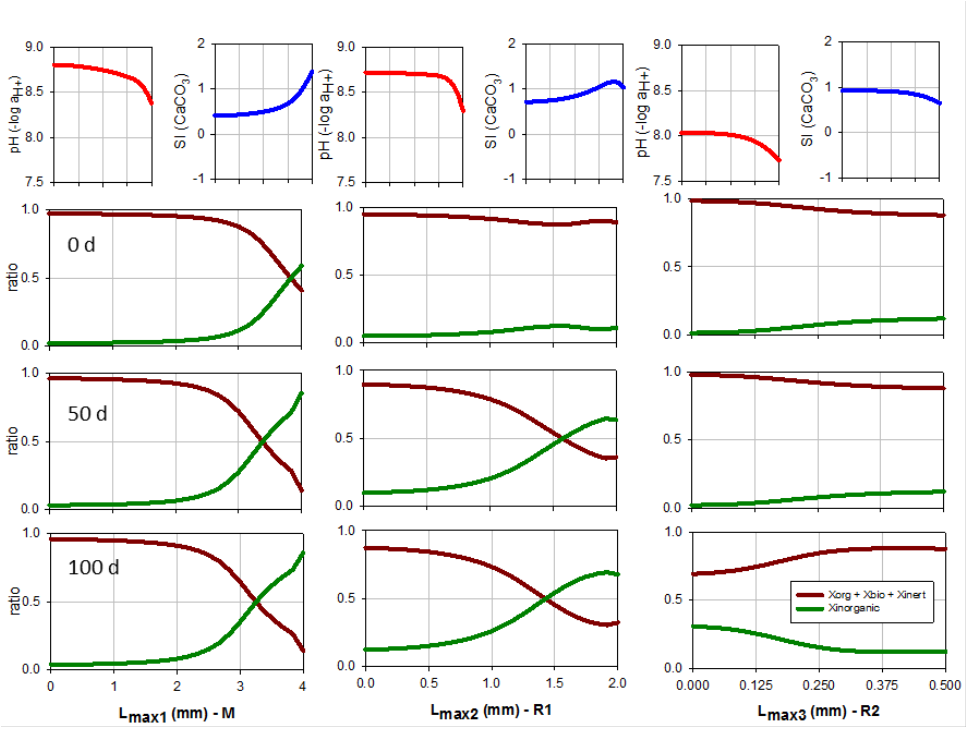

Figure 6.5. Top: pH and SI within the granule at different reactor heights (M, R1, R2). Bottom: Predicted organic (X_{org} + X_{inert} + X_{bio}) versus inorganic ($X_{inorganic}$) contents within the granule at different reactor heights (M, R1, R2: columns 1-3) and simulation times (t = 0, t = 50, t = 100 days: rows 1-3) (Feldman et al., 2018b).

acids to inorganic carbon takes place in the first 0.1 mm of the biofilm due to diffusion limitations. As a consequence, $CaCO_3$ precipitation tends to occur close to the surface of the granule. In smaller granules (L_{max} < 1 mm) substrates diffuse to the centre of the granule, and therefore, deposition of precipitates will take place in the core. This corresponds with the experimental observations described by Alphenaar et al. (1993). Due to the precipitation in the granule, $X_{inorganic}$ increases, and subsequently decreases the fraction of X_{bio} in all granule sizes (Figure 6.5).

6.3.3 Undesirable effects of long-term use of reject water

Figure 6.6 shows the potential long-term effects of adding reject water. Even though on the short term the effects of adding reject water are beneficial (lower use of chemicals, higher buffer capacity), in the long run, the accumulation of precip-

Table 6.1. Results of the VSS and methanogenic activity measurements at different reactor heights.

Reactor level	VSS (% of TSS)	Specific methanogenic activity ($gCOD\,gVSS^{-1}\,d^{-1}$)
L1 (bottom)	15	0.050
L2 (top of the sludge bed)	69	0.24

itates in the granules decreases methanogenic activity and consequently energy recovery. This is mainly due to the space occupation within the granule by inorganic (see Figure 6.5) precipitates that compete for space with acidogenic/acetogenic/methanogenic bacteria. As a consequence, the VFA concentration increases (197 %) and CH_4 production decreases by 20 % from the first 18 days to the last 18 days in a 100-day simulation period (see Figure 5). This corresponds to the experimental observations reported by Keenan et al. (1993), El-Mamouni et al. (1995) and van Langerak et al. (1998) when comparing anaerobic systems with different levels of precipitation.

6.3.4 Experimental results

The VSS fractions indicated a high presence of inorganic precipitates in L1 compared to L2 (Table 6.1), with only 15 % of the dry weight in the form of VSS for L1 (as opposed to 69 % for L2). Furthermore, the specific methanogenic activity (SMA; gCOD/gVSS/d) was almost 5 times lower for L1 (see Table 6.1 for details). This could indicate that there are few methanogens remaining in L1, which could be a result of the competition for space between precipitates and biomass (in this case mainly methanogenic biomass). Another reason for the decreased SMA could be due to diffusion limitations as a result of precipitation around the granule. If the precipitation takes place on the outside of the granule, as simulation results have shown is the case for bigger granules in the bottom of the reactor, the substrates diffusing into the granules will need to pass the layer of precipitates, which can lead to mass transfer limitations (van Langerak et al., 1998) and thus a decreased methanogenic activity. Further research on microbial analysis will be needed to elucidate the detailed mechanisms and the effects that precipitates have on the microbial content of granules (Prevedello et al., 2018).

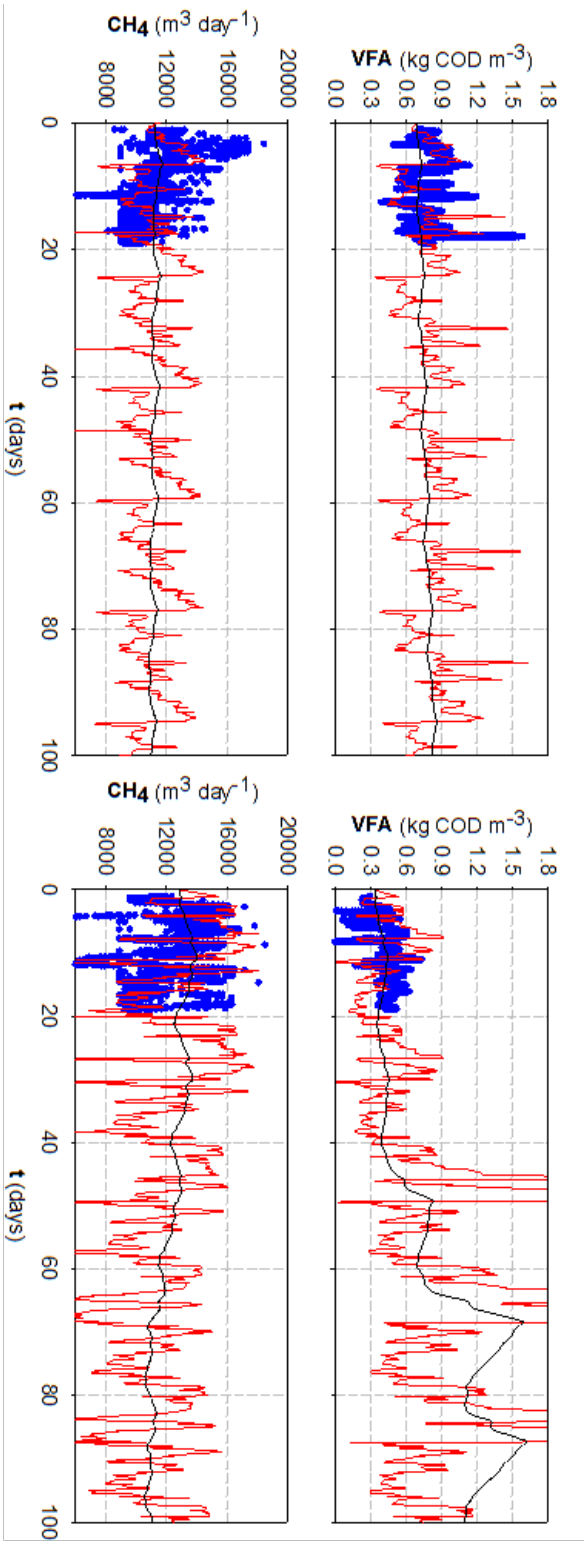

Figure 6.6. Scenario analysis results assuming a long-term (LT) period for both data sets, which corresponds to the different operational modes (addition/no addition of reject water). Markers indicate measurements and red lines are simulated results. A 20 day exponential moving average filter (black line) is included to better visualize the trends (Feldman et al., 2018b).

6.4 Discussion

6.4.1 Main achievements and limitations

Inactivation of mineral precipitates in industrial high-rate anaerobic reactors is one of the main challenges in application of this technology to wastewaters that are rich in calcium and/or magnesium. These are widely distributed, and include paper mills (van Langerak et al., 1998; Batstone and Keller, 2003), beet sugar factories as well as the potato and wheat starch industry (Austermann-Haun et al., 1999). The issues are well known, and mitigation strategies include the use of calcium carbonate pre-precipitation (van Langerak et al., 1998), or the periodic reseeding of reactors. Model-based analysis has been previously used to optimize these systems (Batstone et al., 2002a), but the ability to predict the trajectory of granule inactivation substantially enhances the ability to optimize mitigation processes. The ability to predict in-biofilm processes has further application to among others, the recovery of metals through sulfide precipitation in a system with sulfate reducing bacteria (Fu and Wang, 2011), and microbial electrolysis cells for hydrogen production (Picioreanu et al., 2008). Predicting both the growth/decay of microorganisms simultaneously with the potential formation of inorganic precipitates within the granule, resulting in space competition in the biofilm, does involve a complex implementation with a number of underlying biochemical (Batstone et al., 2002b; Flores-Alsina et al., 2016), physico-chemical (Kazadi Mbamba et al., 2015a,b) and speciation model components (Flores-Alsina et al., 2015) in the bulk phase and each discretized layer of the biofilm (Wanner et al., 2006), but allows for full mechanistic description of these critical phenomena.

Even with the good description achieved with the presented model, there is still room for improvement. There are important processes, which play a role in anaerobic systems with intra-granule precipitation, which are not described by the present approach, for example, this study does not account for changes in biofilm density and diffusivity (Winkler et al., 2013). The latter has an important effect on the transport of soluble compounds (Chomiak et al., 2014). The impact of precipitation on diffusion limitations has also not been taken into account (Zhang et al., 2015). It could be expected that a precipitation layer around the granules will impede diffusion (Keenan et al., 1993; El-Mamouni et al., 1995). Other important aspects not properly handled are related to the physical properties of the granules and how precipitates could affect them. For example, the formation of new granules (Doloman et al., 2017) or the effect of mechanical interactions (Storck et al., 2014). Additionally, the impact of existing seeding material is known to

favour nucleation/growth (Kazadi Mbamba et al., 2015b), which could accelerate localised precipitation. Nucleation could be addressed in the existing 1-D model, or expanded into a multi-dimensional model.

Finally, to avoid an over-complicated implementation, the granule size distribution is assumed to change vertically (decreasing with increased reactor height), where each discretized CSTR has one specific granule type (M = L_{max1}, R1 = L_{max2}, R2 = L_{max3}). A better description of the real system would include a granule size distribution at each reactor level, where growth and detachment rates determine the maximum granule size. All these aspects could help to further improve model predictions and provide valuable additional information in model-based studies.

6.4.2 Decision support tool within the company

The company involved in the study has experienced an increased use of salts in the production, and these salts could potentially disturb the proper operation of the anaerobic digestion processes at the wastewater treatment plant. There is therefore an interest to investigate the effects of high salt concentrations (e.g. sulfate, calcium, phosphate) on the performance of anaerobic digestion processes in more detail. The mathematical model developed in this study can be used as a decision support tool for implementing strategies to control precipitation kinetics within granules. Methods to reduce the impact of salts on anaerobic digestion processes (e.g. precipitation) are also being investigated.

6.4.3 Future research directions

Current research efforts are put into studying the effects of multiple mineral precipitation on the methanogenic activity and microbial community structure. Granular sludge is sampled from an industrial scale anaerobic digester, using state of the art biomass activity tests and 16S rRNA amplicon sequencing. The preliminary results obtained in Section 6.3.4 reveal that the higher concentration of mineral precipitates at the bottom of the reactor has detrimental effects on the reactor performance. A decrease of the methanogenic activity, together with a reduced abundance of methanogenic archaea and lower biomass concentration were observed. This study, besides increasing the current knowledge in industrial microbial ecology, has the potential to elucidate the micro-scale effect of precipitate formation within anaerobic granules in a full-scale system and lead to improved operation of anaerobic digesters (Prevedello et al., 2018).

Another potential option explored is model-based evaluation of the addition of other salts instead of NaOH (for example MgO and CaO) (Jeison et al., 2008). Such scenario analysis can be helpful for predicting the impact of increased use of a specific salt in the production process. The addition of chemicals for pH control has a significant impact on the overall reactor performance. Chapter 4 showed that a saving in operating costs of about 0.88 M€/year can be obtained by decreasing the pH in the reactor by up to half a pH unit compared to the default operational values that were used at full-scale (ensuring the same methane yield). Thus, on top of energy recovery, the potential formation of precipitates can be included in order to have a more informed assessment. An excessive formation of precipitates may force the company to purchase new (granular) biomass, which is a considerable financial expenditure.

6.5 Conclusions and outlook

This chapter has evaluated the effect which the addition of a reject water stream has on the reactor performance and granular structure. The high alkalinity of the reject water stream increases influent pH and reduces the quantity of NaOH used for pH control within the reactor. In addition, the extra COD load initially increases biogas production and consequently energy recovery by 9.5 %.

Formation of precipitates results in accumulation of inorganic material at the bottom of the reactor and changes depending on the granule size. In larger granules, $CaCO_3$ is expected to form in the outer layers of the granule due to diffusion limitations. In smaller granules precipitates will tend to spread all the way to the centre of the granules.

The scenario analysis shows the potential effects of continuous intra-granule precipitation within the reactor and how acidogenic/acetogenic/methanogenic activities can be affected. The study demonstrates how an initially good operational option can become less desirable when evaluated over a long time period (20 % decrease in energy recovery over a 100 day time period). In full-scale a decrease in energy recovery was also observed over time, and the reject water stream is no longer added.

Experimental results showed that the bottom of the reactor contained a lower amount of biomass than the top of the sludge bed, and that the available biomass had a lower specific methanogenic activity. This indicates that the precipitation inside granules has a detrimental effect on energy recovery.

Future analysis of the granular content and specific methanogenic activity should be done over a longer time period, to follow the precipitation kinetics over time at several reactor heights. This will help in validating the precipitation kinetics of the model and together with a microbial analysis elucidate the mechanisms behind a lower methanogenic activity when the content of precipitates is high.

Part II

Autotrophic nitrogen removal

7 Evaluating the potential of the anammox process for nitrogen removal as post-treatment to anaerobic digestion

7.1 Introduction

In the previous chapters the focus was on increasing the performance of anaerobic digestion in order to optimize energy recovery and reduce operational costs. One way to increase the energy recovery of the wastewater treatment plant is by increasing the loading to the reactor. This has not been evaluated so far, as the loading rate to the anaerobic digester is limited by the nitrogen removal requirement. Currently, nitrogen is removed through the activated sludge process, which needs COD for complete nitrification and denitrification (see Chapter 1). This COD requirement is not needed for the anammox process, which means an increased amount of COD could be converted to energy if this process is implemented (van Lier et al., 2001). Another important fact to point out is that it is expected that the capacity of the wastewater treatment plant under study will need to be extended in the future, as the nitrogen load to the plant will increase. Installing an anammox reactor and another anaerobic digester could be an attractive opportunity, as opposed to the installation of a new activated sludge reactor. Alternatively, if the current anaerobic digesters can be optimized to increase the capacity further, it may not be necessary to install another anaerobic digester. However, the rest of this section does not take into account further optimization of the anaerobic digesters.

The succesful post-treatment of AD effluent in a one-stage granular sludge anammox reactor on industrial scale has previously been published by Abma et al. (2010). UASB effluent from potato wastewater as well as reject water are treated in this installation. Laboratory- and pilot-scale studies have also proven that anammox is

a viable option to treat AD effluent (Van Hulle et al., 2010; Vázquez-Padín et al., 2014; Zhao et al., 2015). An important aspect to take into account when treating AD effluent in an anammox reactor is the impact inhibitory compounds will have on the process. Residual COD can have a negative impact on the reactor performance (van de Graaf et al., 1996), as anammox is outcompeted by dentrifying bacteria at high COD concentrations (Ni et al., 2012). Ni et al. (2012) found that the ammonium removal efficiency dropped below 80 % at a COD:N ratio of 3.1, indicating that at higher ratios anammox cannot compete with denitrifying bacteria. Another important compound typical for industrial AD effluents is sulfide, as sulfate in the influent will be converted to sulfides in the anaerobic digester (Chen et al., 2008). Sulfide has been found to be inhibitory to the anammox process, although the literature is not clear on the exact inhibitory concentrations (Jin et al., 2012). One final point to highlight is the impact a high mineral content will have on the anammox process. Like the anaerobic digester studied in the previous chapters, the anammox configuration chosen for this study is a granular sludge reactor. Chapter 6 discussed the impact of precipitation on an anaerobic granular sludge reactor. The expected impact on a granular anammox reactor is similar in that way, that it is expected that too much precipitation in granules will reduce the nitrogen removal efficiency (Fernández et al., 2008). A method to overcome precipitation inside the anammox reactor is by removing the minerals prior to the process. This can be done through an aerobic pre-treatment reactor, where; 1) minerals are precipitated, and; 2) stripping of H_2S, CO_2 and CH_4 occurs.

The next sections will investigate under what circumstances it would be economically attractive to install an anammox reactor, what is needed for achieving stable performance without inhibition of the previously mentioned compounds (such as pre-treatment), and under what conditions an anammox evaluation for full-scale implementation is considered succesful. The first section will look at an economic evaluation taking into account literature values. Based on this evaluation further experimental and modelling work is recommended and explored further.

7.2 Economic evaluation

For the economic evaluation two scenarios are taken into account (Figure 7.1):

- Scenario 1: Redirect 2 tons N per day from the activated sludge reactors to an anammox reactor, thereby enabling the redirection of 10 tons of COD per day to anaerobic digestion. This assumes a COD:N demand of 5 for denitrification

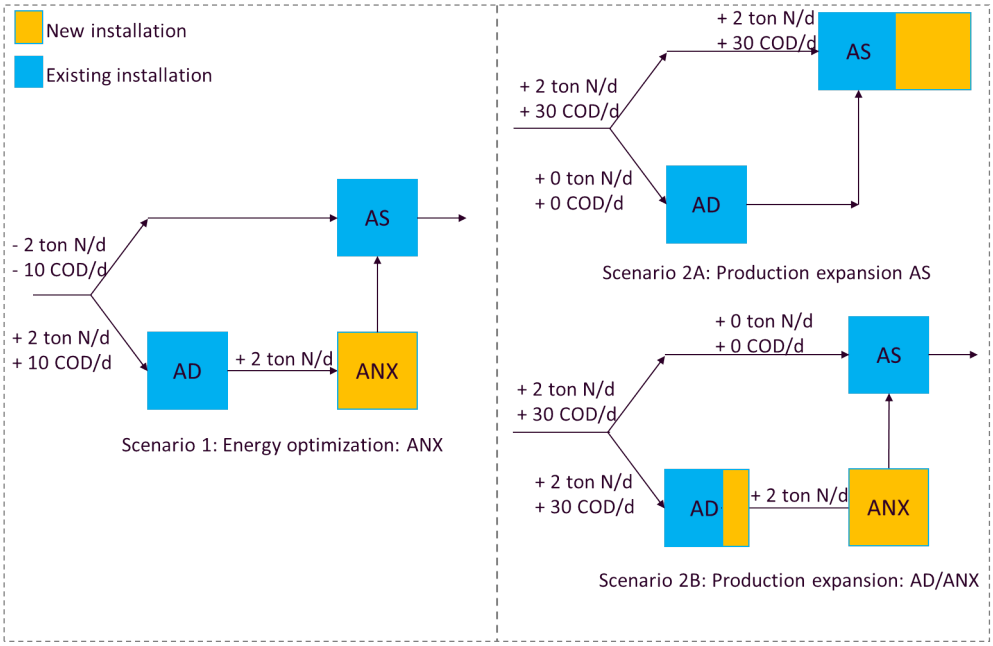

Figure 7.1. Graphical representation of the scenarios for the economic evaluation. Left: scenario 1; right: scenario 2 with the option of installing an activated sludge reactor (top), and the option of installing an anaerobic digester and anammox reactor (bottom).

(Sobieszuk and Szewczyk, 2006). As there is a 10 ton COD capacity available in the existing anaerobic digesters, no new reactor has to be installed.

- Scenario 2: Increased loading rate into the wastewater treatment plant (2 tons N/day). This is removed by installing an anammox reactor as well as an anaerobic digester to remove the extra COD contained in the wastewater (30 tons COD/day) (Scenario 2A). This scenario is a benchmark against the installation of a new activated sludge plant treating 2 tons N/day (Scenario 2B).

In both scenarios, the installation of an anammox reactor is combined with a pre-treatment reactor, which is needed to remove, 1) calcium to prevent precipitation in the anammox reactor, 2) sulfide, as it inhibits the anammox process, and 3) biological COD that remains after the anaerobic digester, to give anammox a competitive advantage over heterotrophic bacteria. The anammox reaction takes place in a one-stage process, where partial nitritation and anammox occur in one reactor.

The costs taken into account for both scenarios are aeration, sludge handling, energy production and capital cost. Below a cost estimate is broken down into each cost parameter, while a summary can be found in Table 7.1.

7.2.1 Aeration energy

A large part of the energy demand for an anammox and activated sludge reactor is the aeration energy. The energy demand in the full-scale granular sludge reactor in Olburgen, The Netherlands is 1.86 kWh/kgN (Lackner et al., 2014), which is relatively high compared to anammox systems (Lackner et al., 2014). Nevertheless, for the economic analysis performed here, this number was chosen so the reality might be better but likely not worse. Removing 2 tons N/day, assuming an electricity price of 0.15 €/kWh (AgroTech, 2014) and 320 operational days per year, this results in an energy cost of 0.18 M€/year. Anammox processes have a reported 60 % lower energy requirement than activated sludge processes (Hu et al., 2013), resulting in an energy cost of 0.45 M€/year for an activated sludge reactor.

7.2.2 Sludge disposal

The excess sludge produced during wastewater treatment must be disposed of. de Bruin et al. (2004) reported a sludge disposal cost of 320 €/ton dry solids. Assuming a sludge production of 4.27 gVSS/gN and 0.14 gVSS/gN for activated sludge and anammox, respectively (Vangsgaard, 2013), it costs 0.87 M€/year to get rid of excess sludge in the activated sludge process and 0.029 M€/year for the anammox process.

7.2.3 Energy production

In the first scenario, 10 tons of COD per day can be redirected to anaerobic digestion to be converted to energy. Each ton of COD produces on average 282 m^3 CH_4 (Dataset #1, Chapter 4). Using the same calculations as in Chapter 4 for methane to energy, these 10 ton will yield 0.74 M€/year. Similarly, for the second scenario an extra IC reactor is built with a capacity to convert 30 tons COD/day. This yields 2.23 M€/year from energy production.

7.2.4 Reactor volume

The capital cost will depend greatly on the reactor volume needed to treat 2 tons N/day. The desired anammox activity is to remove 2 kg N/m^3 reactor volume. This leads to a total reactor volume of 4000 m^3 (2000 m^3 for anammox and 2000 m^3 for

pre-treatment). Comparatively, to reach the same nitrogen removal in an activated sludge reactor, a total volume of 8000 m^3 is needed (based on the current activity of 0.25 kg N/m^3 reactor volume). In case of Scenario 2, an additional anaerobic digester of 2000 m^3 will need to be installed, as well as a gas motor.

7.2.5 Economic outlook

As can be observed in Table 7.1, Scenario 1 saves aeration and sludge disposal costs by diverting part of the nitrogen from the activated sludge reactors. On top of that, the energy production resulting from an increased loading to the anaerobic digester leads to negative operational costs, i.e. money can be saved by selecting this route. On the other hand, the capital costs have not yet been taken into account, as no commercial numbers are freely available. To keep the payback time below 5 years a maximum capital cost of 9.3 M€ is allowed.

For Scenario 2, a comparison is made between the installation of an activated sludge reactor and the installation of a combined anammox reactor and anaerobic digester. In this case the operational costs of the anammox reactor and the anaerobic digester are lower than the profit resulting from energy production, leading to yearly savings of 2.0 M€/year. This means that the installation costs can be earned back over time (depending on how high the installation costs are). This is not the case when an activated sludge reactor is installed. To keep the payback time of the anammox + AD system below 5 years, a maximum additional capital cost of 10.1 M€ is advised.

The economic analysis indicates that the additional energy production that results from directing the nitrogen to the anammox process instead of the activated sludge process, and thus increase the COD loading to the anaerobic digestion, has a large impact on the yearly savings. This is especially true when comparing the two systems as in Scenario 2. In Scenario 1, the largest impact was gained from operational cost savings from the activated sludge, due to the reduced load that is to be treated there. Indeed, the total operational cost of an anammox reactor in terms of aeration energy and sludge disposal for the removal of 2 ton N/day equals 0.21 M€/day. For an activated sludge process this is 1.32 M€/day, nearly 6.5 times more.

It should be noted that the economic evaluation performed in this section is simplified and based on literature values. Assumptions have been made on oxygen consumption and sludge production, while dosage of chemicals has been neglected. To perform a more accurate evaluation of the operational parameters of an anammox process, a pilot-plant study will need to be performed to determine the nitrogen

Table 7.1. Economic evaluation of operational parameters and profit from energy production.

	Anammox	Activated sludge
Scenario 1		
Aeration energy (M€/year)	0.18	
Sludge disposal (M€/year)	0.0028	
Energy production from AD (M€/year)	0.74	
Operational cost savings from activated sludge (M€/year)	1.32	
Operational cost/yearly savings (M€/year)	-1.86	
Scenario 2		
Aeration energy (M€/year)	0.18	0.45
Sludge disposal (M€/year)	0.028	0.87
Energy production from AD (M€/year)	2.23	0
Operational cost/yearly savings (M€/year)	-2.0	1.32

removal efficiency, oxygen consumption, sludge production, as well as chemical dosage. A mathematical model can be applied to the pilot-plant data to scale up the system, and compare the anammox process to the activated sludge process.

7.3 Anammox pilot-plant

The previous section highlighed the importance of running a pilot-plant. Currently, a pilot-plant study is being performed on-site in Kalundborg, Denmark. The pilot-plant was started in March 2018, but due to technical issues a full dataset could not be collected before this thesis was written. The work is followed up by a new PhD student. A final dataset consisting of 5 weeks will be collected. The dataset will consist of online measurements of DO, temperature, pH, ammonium, nitrite, nitrate, flow rate and chemical dosage. Offline measurements of ammonium, nitrite, nitrate, total nitrogen, soluble COD, paticulate COD and sulfide are collected on a daily basis. Samples are collected from the anaerobic digester effluent (in this case influent to the pilot-plant), after the separator following pre-treatment (influent to the anammox reactor) and finally from the anammox effluent. From these measurements the reactor performance and process conditions of both the pre-treatment and anammox reactor can be obtained. This data can then be used as inputs for the model to evaluate full-scale performance.

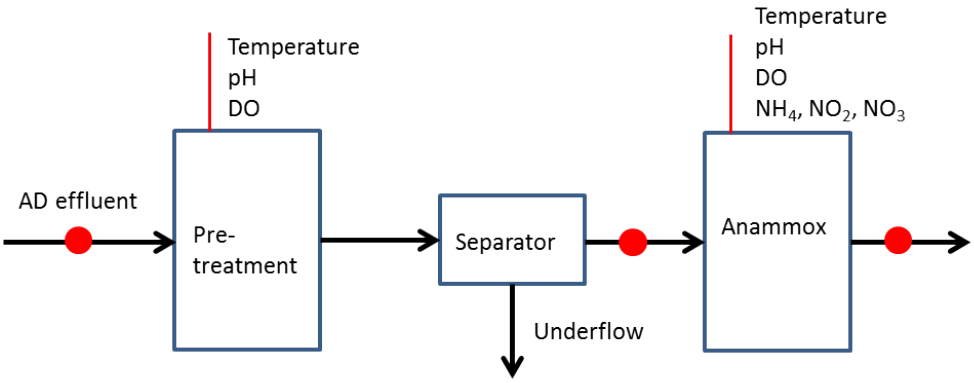

Figure 7.2. Schematics of the anammox pilot-plant. The red dots indicate where samples are taken for offline analysis. The red lines show which online measurements are available.

7.3.1 Anammox model

The model that is being developed is based on the model published by Vangsgaard et al. (2012). The model can be run as either two-stage, where pre-treatment is included, or one-stage where the AD effluent is fed directly to the anammox reactor. In this way the effect of pre-treatment on the anammox process can be studied. The anammox part is a granular sludge model, and extended with sulfide and methane oxidation reactions (see Figure 7.3 for an overview of all model reactions taking place). The impact of these reactions is probably negligible in case there is pre-treatment prior to the anammox reactor, which removes sulfide and methane from the wastewater. However, if the pre-treatment is not available, these compounds could impact the nitrogen removal efficiency by competing for oxygen, nitrite or space in the granules.

7.4 Outlook

The application of the anammox process as an alternative method for nitrogen removal in the Novozymes wastewater treatment plant (Kalundborg, Denmark) will depend on the pilot-plant results, as well as the economic outlook as predicted by the mathematical model. Only if it is proven that this method is more cost-effective than activated sludge, will it be taken into serious consideration by the industrial partner. Academically speaking, the study of the impact of pre-treatment on the anammox process will be of interest, considering the high concentrations of sulfide,

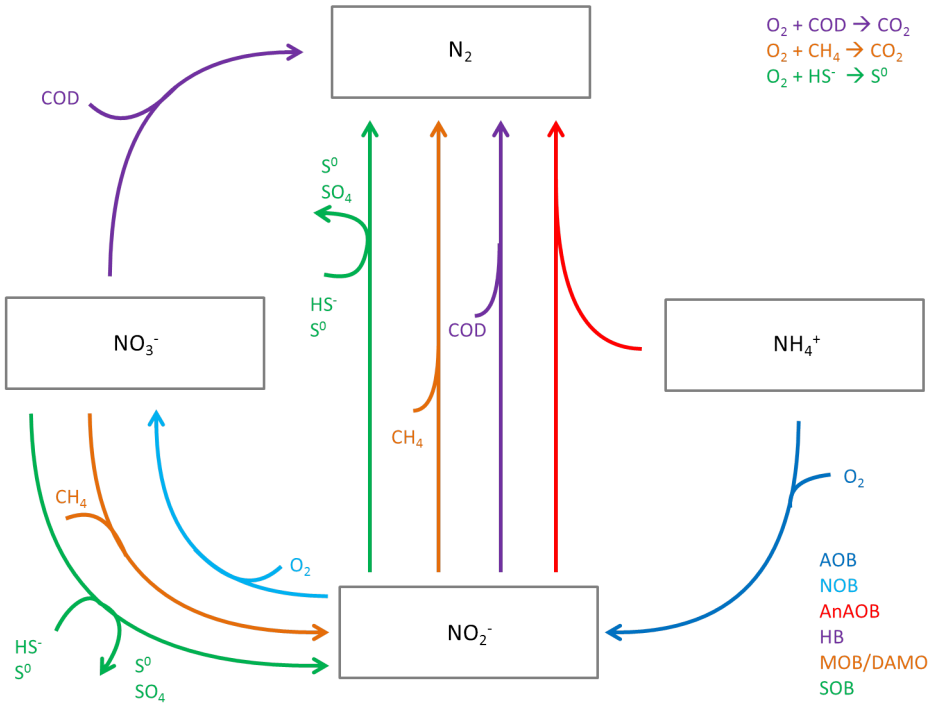

Figure 7.3. Overview of the reactions taken into consideration in the anammox model. AOB: aerobic ammonium oxidizing bacteria; NOB: nitrite oxidizing bacteria; AnAOB: anaerobic ammonium oxidizing bacteria (anammox); HB: heterotrophic bacteria; MOB: methane oxidizing bacteria; DAMO: denitrifying anaerobic methane oxidizing bacteria; SOB: sulfide oxidizing bacteria.

COD and methane in the wastewater. The potential highly competitive conditions in the granules of the anammox reactor might be able to shed more light on the reaction and inhibition kinetics of the different micro-organisms present than is currently known.

8 Conclusions and perspective

The main objective of this project was to study different methods to increase the energy recovery in an industrial wastewater treatment plant treating fermentation wastewater. The project was divided into two main parts. In the first section, two model-based methods were applied to an industrial anaerobic digester, aiming to optimize the biogas production, and thus the energy recovery. In the second section the aim was to study the applicability of the anammox process as an alternative method for achieving nitrogen removal, to increase the COD loading to anaerobic digestion (and thus increase biogas production and the energy recovery).

Mathematical modelling of anaerobic digestion

Prior to the mathematical modelling, two datasets of three weeks were collected (Chapter 2). The datasets were approximately half a year apart. This was on the one hand positive, as it was possible to model two separate conditions, which led to the development of the granular sludge model due to precipitation. On the other hand the large differences between the two datasets, with large differences in loading conditions, made it impossible to perform a traditional calibration and validation procedure of the models. Instead, several parameters had to be modified to fit the second dataset. Nevertheless, the minimal number of parameters that had to be re-estimated for both models and a good fit between simulation and data, indicate that the chosen methods were sufficient for the model applications of the study.

The first model that was presented (Chapter 3) was a flow + reactor model, where an artificial loop was implemented to retain the biomass inside the reactor. This model was applied for optimization of the reactor conditions (Chapter 4). Both energy production and chemical dosage for pH control were taken into account for the economic sustainability of the optimization scenarios. The main finding of this optimization study was that the pH can be decreased to 6.8 without compromising

on energy production, thereby decreasing the amount of chemicals needed for pH control, leading to an overall increase in reactor performance index (profit of energy recovery - cost of chemicals). This strategy was in fact applied on the full-scale reactor, where similar results were obtained. While the other optimization strategies (removal of sulfate/sulfide in the influent and CO_2 from the recycle stream) have shown to increase the reactor performance index, the cost of doing this outweighed the profit. This has clearly demonstrated that an important part in process optimization is to take into account all costs involved.

Chapter 5 presented the granular sludge model. This model takes into account that the biomass in the anaerobic digester is present as granular biomass. This modelling approach increases the complexity of the model, and increases simulation time. However, when modelling of the granular structure and competition between different organisms and between biomass and precipitates is important, this is the model that should be implemented. The long-term simulations performed in Chapter 6 illustrate the impact a high mineral content of the incoming wastewater has on the process performance. Due to precipitation, biomass is outcompeted from the granules and the energy recovery decreases over time. This is an issue which was also observed by the industrial partner, who decided to stop the addition of the reject water stream to the anaerobic digester. While this stream initially increased the energy recovery due to the high COD content, the long-term impact of precipitation have both been simulated and shown in practice to have detrimental effects on reactor performance.

The two models simulate the same system, and each model has its own application. For each case study, it is important that one has a clear objective of what the aim of the simulations is. If the model output should be the impact influent conditions have on the effluent/biogas conditions, the flow + reactor model can be used, as the biomass can be seen as a black box. However, if the biomass itself affects the output, due to for example precipitation kinetics or mass transfer limitations, the granular sludge model should be used.

Anammox implementation

The economic calculations presented in Chapter 7 show that the anammox process has potential as post-treatment to anaerobic digestion for nitrogen removal. A pilot-plant and mathematical model should yield sufficient data to fine-tune these calculations.

Impact and future perspectives

The modelling work presented in this study can aid in the decision making process of full-scale plants when it comes to process optimization and the introduction of new waste streams. As mentioned earlier, the optimization results obtained in this study regarding pH have been implemented at full-scale, proving that simulation results can be implemented on industrial level. Besides implementing simulation results directly on full-scale, they can also be used as a screening method to design laboratory- or pilot-scale studies. As experimental work costs time, energy and money, screening the relevant experiments beforehand with a mathematical model will potentially save costs.

As it was found that precipitation kinetics has a detrimental effect on the energy recovery due to the competition between precipitates and biomass, a study was started to look into the microbial structure of the granules in the industrial anaerobic digester. This study looks further into which microbes are present at different reactor heights and how this affects the methanogenic activity. Results can be used to further improve the granular sludge model.

Another important application of the mathematical models on industrial wastewaters is to simulate the impact a sudden change of the wastewater composition will have on the reactor performance. As mentioned in the introduction, industrial treatment plants have fluctuating wastewater characteristics, which depend on the production scheme of the factory upstream. The model can be used not only for evaluation of the impact, but also control of process parameters such as pH, loading rate and retention time to maintain a high efficiency of energy recovery.

Finally, a developed model should not be reinvented again and again. By sharing the models with other research institutions, they can hopefully be developed and improved further. New case studies can potentially strengthen the applicability of the models to different systems. The future of wastewater lies in the recovery of resources, such as energy, and mathematical models can help increase the potential gains to be achieved from water resource recovery facilities.

List of publications

Journal articles

Feldman, H., Flores-Alsina, X., Kjellberg, K., Jeppsson, U., Batstone, D.J. and Gernaey K.V. (2017). Modelling an industrial anaerobic granular reactor using a multi-scale approach. *Water Research*, **126**: 488-500.

Feldman, H., Flores-Alsina, X., Kjellberg, K., Jeppsson, U., Batstone, D.J. and Gernaey K.V. (2018). Model-based optimization of a full-scale industrial high rate anaerobic bioreactor. *Biotechnology and Bioengineering*, **115**(11), 2726-2739.

Feldman, H., Flores-Alsina, X., Ramin, P., Kjellberg, K., Jeppsson, U. and Batstone, D.J., Gernaey, K.V. (2018). Assessing the effects of intra-granule precipitation in a full-scale industrial anaerobic digester. Submitted to *Chemical Engineering Journal*.

Mears, L., Feldman, H., Falco, F.C., Bach, C., Wu, M., Nørregaard, A. and Gernaey, K.V. (2017) Continuous Fermentation for Biopharmaceuticals?, in Continuous Manufacturing of Pharmaceuticals (eds. P. Kleinebudde, J. Khinast, J. Rantanen), John Wiley & Sons, Ltd, Chichester, UK. doi: 10.1002/9781119001348.ch6

Udugama, A.I.A., Feldman, H., de las Heras, S.C, Kizhedath, A., Bryde-Jacobsen, J., van den Berg, F., Mansouri, S.S. and Gernaey, K.V. (2018). BIOPRO World Talent Campus: A weeek of real world challenge for biotechnology post-graduate students. *Education for Chemical Engineers*, **25**: 1-8.

Udugama, A.I.A., Feldman, H., Bryde-Jacobsen, J., and Gernaey, K.V. (2018). 5 år og fuld fart frem. *Dansk Kemi*, **99**(1): 10-11.

Conference contributions

Feldman, H., FaraghiPrapari, N., Bendix Larsen, S., Kjellberg, K., Flores-Alsina, X., Sin, G., Jeppsson, U. and Gernaey, K.V. (2016). Model-based optimization of an industrial wastewater treatment plant combining a full-scale granular sludge reactor and autotrophic nitrogen removal. IWA World Water Congress & Exhibition, Brisbane, Australia, 9-14 October 2016. Poster presentation.

Feldman, H., Flores-Alsina, X., Kjellberg, K., Jeppsson, U., Batstone, D.J. and Gernaey, K.V. (2017). Modelling methane, sulphide and multiple mineral precipitation in a full-scale industrial granular anaerobic digester. 10th International Conference on Biofilm Reactors, 9-12 May 2017, University College Dublin, Ireland. Poster presentation.

Feldman, H., Flores-Alsina, X., Kjellberg, K., Blum, J.M., Valverde-Pérez, B., Sin, G., Smets, B.F. and Gernaey, K.V. (2017). Feasibility-test of a complete autotrophic nitrogen removal process treating the effluent of an industrial anaerobic digester. 10th International conference on biofilm reactors, 9-12 May 2017, University College Dublin, Ireland. Accepted for poster presentation.

Feldman, H., Flores-Alsina, X., Ramin, P., Kjellberg, K., Jeppsson, U., Batstone, D.J. and Gernaey, K.V. (2017). Optimizing the operational/control conditions of a full-scale industrial granular anaerobic digester. 12th IWA Specialized Conference on Instrumentation, Control and Automation, Quebec, Canada, 11-16 June 2017. Oral presentation.

Feldman, H., Flores-Alsina, X., Ramin, P., Kjellberg, K., Jeppsson, U., Batstone, D.J. and Gernaey, K.V. (2017). Calibration and validation of an anaerobic digestion model for process optimization of an industrial granular sludge reactor. The 15th IWA World Conference on Anaerobic Digestion, 17-20 October 2017, Beijing, China. Oral presentation.

Feldman, H., Flores-Alsina, X., Ramin, P., Kjellberg, K., Jeppsson, U., Batstone, D.J. and Gernaey, K.V. (2017). Model-based optimization of a full-scale industrial anaerobic reactor producing biogas. 8th International Young Water Professionals Conference, 10-13 December 2017, Cape Town, Republic of South Africa. Oral presentation.

Feldman, H., Flores-Alsina, X., Ramin, P., Kjellberg, K., Jeppsson, U., Batstone, D.J. and Gernaey, K.V. (2018). Predicting the effects of intra-granule $CaCO_3$ precipitation in a full-scale industrial anaerobic biofilm reactor. IWA Biofilms: Granular sludge conference 2018, Delft, the Netherlands, 18-21 March 2018. Accepted for oral presentation.

Prevedello, M., Feldman, H., Nesme, J., Mortensen, M., Flores-Alsina, X., Sørensen, S.J., and Gernaey, K.V. (2018). The effect of high precipitate concentration on the microbial community structure in an industrial anaerobic granular sludge reactor. IWA Biofilms: Granular Sludge conference 2018, Delft, The Netherlands, 18-21 March, 2018. Poster/Flash presentation.

Bibliography

Abbasi, T., Tauseef, S., and Abbasi, S. (2012). A brief history of anaerobic digestion and "biogas". In *Biogas Energy*, pages 11–23. Springer, New York, NY, USA.

Abma, W. R., Driessen, W., Haarhuis, R., and Van Loosdrecht, M. C. M. (2010). Upgrading of sewage treatment plant by sustainable and cost-effective separate treatment of industrial wastewater. *Water Science and Technology*, 61(7):1715–1722.

AgroTech (2014). Methane emission from Danish biogas plants - Economic impact of identified methane leakages. Technical Report March, AgroTech, Aarhus, Denmark.

Ahn, Y. H., Min, K. S., and Speece, R. E. (2001a). Full scale UASB reactor performance in the brewery industry. *Environmental Technology*, 22(4):463–476.

Ahn, Y. H., Min, K. S., and Speece, R. E. (2001b). Pre-acidification in anaerobic sludge bed process treating brewery wastewater. *Water Research*, 35(18):4267–4276.

Akarsubasi, A. T., Ince, O., Oz, N. A., Kirdar, B., and Ince, B. K. (2006). Evaluation of performance, acetoclastic methanogenic activity and archaeal composition of full-scale UASB reactors treating alcohol distillery wastewaters. *Process Biochemistry*, 41(1):28–35.

Alphenaar, P., Pérez, M., and Lettinga, G. (1993). The influence of substrate transport limitation on porosity and methanogenic activity of anaerobic sludge granules. *Applied Microbiology and Biotechnology*, 39(2).

Antonopoulou, G., Gavala, H. N., Skiadas, I. V., and Lyberatos, G. (2012). Modeling of fermentative hydrogen production from sweet sorghum extract based on modified ADM1. *International Journal of Hydrogen Energy*, 37(1):191–208.

Arnell, M., Astals, S., Åmand, L., Batstone, D. J., Jensen, P. D., and Jeppsson, U. (2016). Modelling anaerobic co-digestion in benchmark simulation model no.

2: Parameter estimation, substrate characterisation and plant-wide integration. *Water Research*, 98:138–146.

Astals, S., Esteban-Gutiérrez, M., Fernández-Arévalo, T., Aymerich, E., García-Heras, J. L., and Mata-Alvarez, J. (2013). Anaerobic digestion of seven different sewage sludges: A biodegradability and modelling study. *Water Research*, 47(16):6033–6043.

Austermann-Haun, U., Meyer, H., Seyfried, C., and Rosenwinkel, K. (1999). Full scale experiences with anaerobic/aerobic treatment plants in the food and beverage industry. *Water Science and Technology*, 40(1):305–312.

Aymerich, I., Rieger, L., Sobhani, R., Rosso, D., and Corominas, L. (2015). The difference between energy consumption and energy cost: Modelling energy tariff structures for water resource recovery facilities. *Water Research*, 81:113–123.

Barrera, E. L., Spanjers, H., Solon, K., Amerlinck, Y., Nopens, I., and Dewulf, J. (2015). Modeling the anaerobic digestion of cane-molasses vinasse: Extension of the Anaerobic Digestion Model No. 1 (ADM1) with sulfate reduction for a very high strength and sulfate rich wastewater. *Water Research*, 71:42–54.

Batstone, D., Torrijos, M., Ruiz, C., and Schmidt, J. (2004a). Use of an anaerobic sequencing batch reactor for parameter estimation in modelling of anaerobic digestion. *Water Science & Technology*, 50(10):295–303.

Batstone, D. J. (2006). Mathematical modelling of anaerobic reactors treating domestic wastewater: Rational criteria for model use. *Reviews in Environmental Science and Bio/Technology*, 5(1):57–71.

Batstone, D. J., Hernandez, J. L. A., and Schmidt, J. E. (2005). Hydraulics of laboratory and full-scale upflow anaerobic sludge blanket (UASB) reactors. *Biotechnology and Bioengineering*, 91(3):387–391.

Batstone, D. J. and Keller, J. (2003). Industrial applications of the IWA anaerobic digestion model No.1 (ADM1). *Water Science and Technology*, 47(12):199–206.

Batstone, D. J., Keller, J., Angelidaki, I., Kalyuzhnyi, S. V., Pavlostathis, S. G., Rozzi, A., Sanders, W. T. M., Siegrist, H., and Vavilin, V. A. (2002a). The IWA Anaerobic Digestion Model No 1. *Water Science and Technology*, 45(10):65–73.

Batstone, D. J., Keller, J., and Blackall, L. L. (2004b). The influence of substrate kinetics on the microbial community structure in granular anaerobic biomass. *Water Research*, 38(6):1390–1404.

Batstone, D. J., Keller, J., and Steyer, J. P. (2006). A review of ADM1 extensions, applications, and analysis: 2002 – 2005. *Water Science & Technology*, 54(4):1–10.

Batstone, D. J., Puyol, D., Flores-Alsina, X., and Rodríguez, J. (2015). Mathematical modelling of anaerobic digestion processes: Applications and future needs. *Reviews in Environmental Science and Biotechnology*, 14(4):595–613.

Batstone, D. J., Torrijos, M., Ruiz, C., and Schmidt, J. E. (2002b). Use of an anaerobic sequencing batch reactor for parameter optimisation in modelling of anaerobic digestion. *Water Science and Technology*, 50(10):295–304.

Bolle, W. L., Van Breugel, J., van Eybergen, G. C., Kossen, N. W. F., and van Gils, W. (1986). An integral dynamic model for the UASB reactor. *Biotechnology and Bioengineering*, 28(11):1621–1636.

Boltz, J. P., Morgenroth, E., Brockmann, D., Bott, C., Gellner, W. J., and Vanrolleghem, P. A. (2011). Systematic evaluation of biofilm models for engineering practice: Components and critical assumptions. *Water Science & Technology*, 64(4):930–944.

Boltz, J. P., Morgenroth, E., and Sen, D. (2010). Mathematical modelling of biofilms and biofilm reactors for engineering design. *Water Science and Technology*, 62(8):1821–1836.

Bond, T. and Templeton, M. R. (2011). History and future of domestic biogas plants in the developing world. *Energy for Sustainable Development*, 15(4):347–354.

Boubaker, F. and Ridha, B. C. (2008). Modelling of the mesophilic anaerobic codigestion of olive mill wastewater with olive mill solid waste using anaerobic digestion model No. 1 (ADM1). *Bioresource Technology*, 99(14):6565–6577.

Brockmann, D., Caylet, A., Escudié, R., Steyer, J. P., and Bernet, N. (2013). Biofilm model calibration and microbial diversity study using Monte Carlo simulations. *Biotechnology and Bioengineering*, 110(5):1323–32.

Brockmann, D., Rosenwinkel, K. H., and Morgenroth, E. (2008). Practical identifiability of biokinetic parameters of a model describing two-step nitrification in biofilms. *Biotechnology and Bioengineering*, 101(3):497–514.

Cano, R., Pérez-Elvira, S. I., and Fdz-Polanco, F. (2015). Energy feasibility study of sludge pretreatments: A review. *Applied Energy*, 149:176–185.

Cao, Y., van Loosdrecht, M. C. M., and Daigger, G. T. (2017). Mainstream partial nitritation–anammox in municipal wastewater treatment: Status, bottlenecks, and further studies. *Applied Microbiology and Biotechnology*, 101(4):1365–1383.

Chen, Y., Cheng, J. J., and Creamer, K. S. (2008). Inhibition of anaerobic digestion process: A review. *Bioresource Technology*, 99(10):4044–4064.

Chen, Z., Hu, D., Zhang, Z., Ren, N., and Zhu, H. (2009). Modeling of two-phase anaerobic process treating traditional Chinese medicine wastewater with the IWA Anaerobic Digestion Model No. 1. *Bioresource Technology*, 100(20):4623–4631.

Chomiak, A., Sinnet, B., Derlon, N., and Morgenroth, E. (2014). Inorganic particles increase biofilm heterogeneity and enhance permeate flux. *Water Research*, 64:177–186.

Christensson, M., Ekström, S., Chan, A. A., Le Vaillant, E., and Lemaire, R. (2013). Experience from start-ups of the first ANITA Mox Plants. *Water Science and Technology*, 67(12):2677–2684.

Copp, J., editor (2002). *The Cost Simulation Benchmark: Description and Simulator Manual*. Office for Official Publications of the European Community, Luxembourg.

Corbalá-Robles, L., Picioreanu, C., van Loosdrecht, M. C. M., and Pérez, J. (2016). Analysing the effects of the aeration pattern and residual ammonium concentration in a partial nitritation-anammox process. *Environmental Technology*, 37(6):694–702.

Cree, D. and Rutter, A. (2015). Sustainable bio-inspired limestone eggshell powder for potential industrialized applications. *ACS Sustainable Chemistry and Engineering*, 3(5):941–949.

Dalgaard, T., Halberg, N., and Porter, J. (2001). A model for fossil energy use in Danish agriculture used to compare organic a model for fossil energy use in Danish agriculture used to compare organic and conventional farming. *Agriculture, Ecosystems & Environment*, 87:51–65.

de Beer, D., Huisman, J., Van den Heuvel, J., and Ottengraf, S. (1992). The effect of pH profiles in methanogenic aggregates on the kinetics of acetate conversion. *Water Research*, 26(10):1329–1336.

de Bruin, L. M., de Kreuk, M. K., van der Roest, H. F., Uijterlinde, C., and van Loosdrecht, M. C. M. (2004). Aerobic granular sludge technology: An alternative to activated sludge? *Water Science and Technology*, 49(11-12):1–7.

de Gracia, M., Sancho, L., García-Heras, J. L., Vanrolleghem, P. A., and Ayesa, E. (2006). Mass and charge conservation check in dynamic models: Application to the new ADM1 model. *Water Science and Technology*, 53(1):225–240.

Dereli, R. K., Ersahin, M. E., Ozgun, H., Ozturk, I., and Aydin, A. F. (2010). Applicability of Anaerobic Digestion Model No. 1 (ADM1) for a specific industrial

wastewater: Opium alkaloid effluents. *Chemical Engineering Journal*, 165(1):89–94.

Doloman, A., Varghese, H., Miller, C. D., and Flann, N. S. (2017). Modeling de novo granulation of anaerobic sludge. *BMC Systems Biology*, 11(1):69.

Ekama, G. A. and Wentzel, M. C. (2004). A predictive model for the reactor inorganic suspended solids concentration in activated sludge systems. *Water Research*, 38(19):4093–4106.

El-Mamouni, R., Guiot, S. R., Mercier, P., Safi, B., and Samson, R. (1995). Liming impact on granules activity of the multiplate anaerobic reactor (MPAR) treating whey permeate. *Bioprocess Engineering*, 12(1):47.

Elaiuy, M. L. C., Borrion, A. L., Poggio, D., Stegemann, J. A., and Nour, E. A. A. (2018). ADM1 modelling of large-scale covered in-ground anaerobic reactor treating sugarcane vinasse. *Water Science and Technology*, 77(5):1397–1409.

Ersahin, M. E., Insel, G., Dereli, R. K., Ozturk, I., and Kinaci, C. (2007). Model based evaluation for the anaerobic treatment of corn processing wastewaters. *CLEAN – Soil, Air, Water*, 35(6):576–581.

Fang, H. H. P. and Liu, H. (2002). Effect of pH on hydrogen production from glucose by a mixed culture. *Bioresource Technology*, 82(1):87–93.

Fedorovich, V., Lens, P., and Kalyuzhnyi, S. (2003). Extension of Anaerobic Digestion Model No. 1 with processes of sulfate reduction. *Applied Biochemistry and Biotechnology*, 109:33–45.

Feldman, H., Flores-Alsina, X., Kjellberg, K., Jeppsson, U., Batstone, D. J., and Gernaey, K. V. (2018a). Model-based optimization of a full-scale industrial high rate anaerobic bioreactor. *Accepted for publication in Biotechnology and Bioengineering*.

Feldman, H., Flores-Alsina, X., Ramin, P., Kjellberg, K., Jeppsson, U., Batstone, D. J., and Gernaey, K. V. (2017). Modelling an industrial anaerobic granular reactor using a multi-scale approach. *Water Research*, 126:488–500.

Feldman, H., Flores-Alsina, X., Ramin, P., Kjellberg, K., Jeppsson, U., Batstone, D. J., and Gernaey, K. V. (2018b). Assessing the effects of intra-granule precipitation in a full-scale industrial anaerobic digester. *Submitted to Chemical Engineering Journal*.

Fernández, I., Vázquez-Padín, J. R., Mosquera-Corral, A., Campos, J. L., and Méndez, R. (2008). Biofilm and granular systems to improve Anammox biomass retention. *Biochemical Engineering Journal*, 42(3):308–313.

Fernández-Arévalo, T., Lizarralde, I., Fdz-Polanco, F., Pérez-Elvira, S. I., Garrido, J. M., Puig, S., Poch, M., Grau, P., and Ayesa, E. (2017). Quantitative assessment of energy and resource recovery in wastewater treatment plants based on plant-wide simulations. *Water Research*, 118:272–288.

Flora, J. R. V., Suidan, M. T., Biswas, P., and Sayles, G. D. (1995). A modeling study of anaerobic biofilm systems: I. detailed biofilm modeling. *Biotechnology and Bioengineering*, 46(1):43–53.

Flores-Alsina, X., Kazadi Mbamba, C., Solon, K., Vrecko, D., Tait, S., Batstone, D. J., Jeppsson, U., and Gernaey, K. V. (2015). A plant-wide aqueous phase chemistry module describing pH variations and ion speciation/pairing in wastewater treatment process models. *Water Research*, 85:255–265.

Flores-Alsina, X., Saagi, R., Lindblom, E., Thirsing, C., Thornberg, D., Gernaey, K. V., and Jeppsson, U. (2014). Calibration and validation of a phenomenological influent pollutant disturbance scenario generator using full-scale data. *Water Research*, 51:172–185.

Flores-Alsina, X., Solon, K., Kazadi Mbamba, C., Tait, S., Gernaey, K. V., Jeppsson, U., and Batstone, D. J. (2016). Modelling phosphorus (P), sulfur (S) and iron (Fe) interactions for dynamic simulations of anaerobic digestion processes. *Water Research*, 95:370–382.

Fu, F. and Wang, Q. (2011). Removal of heavy metal ions from wastewaters: A review. *Journal of Environmental Management*, 92(3):407–418.

Garcia-Robledo, E., Ottosen, L. D. M., Voigt, N. V., Kofoed, M. W., and Revsbech, N. P. (2016). Micro-scale h2-co2 dynamics in a hydrogenotrophic methanogenic membrane reactor. *Frontiers in Microbiology*, 7:1276.

Gargalo, C. L., Cheali, P., Posada, J. A., Gernaey, K. V., and Sin, G. (2016). Economic risk assessment of early stage designs for glycerol valorization in biorefinery concepts. *Industrial & Engineering Chemistry Research*, 55(24):6801–6814.

Ge, H., Zhang, L., Batstone, D. J., Keller, J., and Yuan, Z. (2013). Impact of iron salt dosage to sewers on downstream anaerobic sludge digesters: Sulfide control and methane production. *Journal of Environmental Engineering*, 139:594–601.

Gebrezgabher, S. A., Meuwissen, M. P. M., Prins, B. A. M., and Oude Lansink, A. G. J. M. (2010). Economic analysis of anaerobic digestion-A case of Green power biogas plant in the Netherlands. *NJAS - Wageningen Journal of Life Sciences*, 57(2):109–115.

Gernaey, K. V., Flores-Alsina, X., Rosen, C., Benedetti, L., and Jeppsson, U. (2011). Dynamic influent pollutant disturbance scenario generation using a phenomenological modelling approach. *Environmental Modelling and Software*, 26(11):1255–1267.

Gernaey, K. V., Jeppsson, U., Vanrolleghem, P. A., and Copp, J. B. (2014). *Benchmarking of control strategies for wastewater treatment plants*. IWA Publishing, London, UK.

Girault, R., Rousseau, P., Steyer, J. P., Bernet, N., and Béline, F. (2011). Combination of batch experiments with continuous reactor data for ADM1 calibration: Application to anaerobic digestion of pig slurry. *Water Science and Technology*, 63(11):2575–2582.

Gujer, W. and Zehnder, A. J. B. (1983). Conversion processes in anaerobic digestion. *Water Science and Technology*, 15(8-9):127–167.

Hao, T. W., Xiang, P. Y., Mackey, H. R., Chi, K., Lu, H., Chui, H. K., van Loosdrecht, M. C., and Chen, G. H. (2014). A review of biological sulfate conversions in wastewater treatment. *Water Research*, 65:1–21.

Hao, X., Heijnen, J. J., and van Loosdrecht, M. C. M. (2002). Sensitivity analysis of a biofilm model describing a one-stage completely autotrophic nitrogen removal (canon) process. *Biotechnology and Bioengineering*, 77(3):266–277.

Healy, N. and Barry, J. (2017). Politicizing energy justice and energy system transitions: Fossil fuel divestment and a "just transition". *Energy Policy*, 108(November 2016):451–459.

Hinken, L., Huber, M., Weichgrebe, D., and Rosenwinkel, K. H. (2014). Modified ADM1 for modelling an UASB reactor laboratory plant treating starch wastewater and synthetic substrate load tests. *Water Research*, 64:82–93.

Howarth, R. W. and Marino, R. (2006). Nitrogen as the limiting nutrient for eutrophication in coastal marine ecosystems: Evolving views over three decades. *Limnology and Oceanography*, 51:364–376.

Hu, Z., Lotti, T., de Kreuk, M., Kleerebezem, R., van Loosdrecht, M. C. M., Kruit, J., Jetten, M. S. M., and Kartal, B. (2013). Nitrogen removal by a nitritation-anammox bioreactor at low temperature. *Applied and Environmental Microbiology*, 79(8):2807–2812.

INTRATEC (2017). Caustic Soda Price History. `https://www.intratec.us/chemical-markets/caustic-soda-prices`. [Page accessed: 2017-08-02].

IPCC, editor (1996). *Climate change 1995 - economic and social dimensions of climate change*. IPCC, Cambridge University Press, Cambridge, UK.

Irizar, I., Zambrano, J., Carlsson, B., Morrás, M., and Aymerich, E. (2015). Robust tuning of bending-points detection algorithms in batch-operated processes: Application to autothermal thermophilic aerobic digesters. *Environmental Modelling & Software*, 71:148–158.

Jaffer, Y., Clark, T., Pearce, P., and Parsons, S. (2002). Potential phosphorus recovery by struvite formation. *Water Research*, 36(7):1834–1842.

Jeison, D., Del Rio, A., and van Lier, J. B. (2008). Impact of high saline wastewaters on anaerobic granular sludge functionalities. *Water science and technology*, 57(6):815–819.

Jeppsson, U., Alex, J., Batstone, D. J., Benedetti, L., Comas, J., Copp, J. B., Corominas, L., Flores-Alsina, X., Gernaey, K. V., Nopens, I., Pons, M. N., Rodríguez-Roda, I., Rosen, C., Steyer, J. P., Vanrolleghem, P. A., Volcke, E. I. P., and Vrecko, D. (2013). Benchmark simulation models, quo vadis? *Water Science & Technology*, 68(1):1–15.

Jeppsson, U., Pons, M. N., Nopens, I., Alex, J., Copp, J., Gernaey, K., Rosen, C., Steyer, J. P., and Vanrolleghem, P. A. (2007). Benchmark Simulation Model no 2: General protocol and exploratory case studies. *Water Science & Technology*, 56(8):67.

Jin, R. C., Yang, G. F., Yu, J. J., and Zheng, P. (2012). The inhibition of the Anammox process: A review. *Chemical Engineering Journal*, 197:67–79.

Kalyuzhnyi, S. and Fedorovich, V. (1998). Mathematical Modelling of Competition between Sulphate Reduction and Methanogenesis in Anaerobic Reactors. *Bioresource Technology*, 65:227–242.

Kalyuzhnyi, S. V. (1997). Batch anaerobic digestion of glucose and its mathematical modeling. ii. description, verification and application of model. *Bioresource Technology*, 59:249–258.

Kazadi Mbamba, C., Batstone, D. J., Flores-Alsina, X., and Tait, S. (2015a). A generalised chemical precipitation modelling approach in wastewater treatment applied to calcite. *Water Research*, 68:342–353.

Kazadi Mbamba, C., Tait, S., Flores-Alsina, X., and Batstone, D. J. (2015b). A systematic study of multiple minerals precipitation modelling in wastewater treatment. *Water Research*, 85:359–370.

Keenan, P. J., Iza, J., and Switzenbaum, M. S. (1993). Inorganic solids development in a pilot-scale anaerobic reactor treating municipal solid waste landfill leachate. *Water Environment Research*, 65(2):181–188.

Koch, G., Egli, K., Van der Meer, J. R., and Siegrist, H. (2000). Mathematical modeling of autotrophic denitrification in a nitrifying biofilm of a rotating biological contactor. *Water Science and Technology*, 41(4-5):191–198.

Koch, K., Lübken, M., Gehring, T., Wichern, M., and Horn, H. (2010). Biogas from grass silage - Measurements and modeling with ADM1. *Bioresource Technology*, 101(21):8158–8165.

Kroeker, E. J., Schulte, D. D., Sparling, A. B., and Lapp, H. M. (1979). Anaerobic treatment process stability. *Journal Water Pollution Control Feredation*, 51(4):718–727.

Lackner, S., Gilbert, E. M., Vlaeminck, S. E., Joss, A., Horn, H., and van Loosdrecht, M. C. M. (2014). Full-scale partial nitritation/anammox experiences - An application survey. *Water Research*, 55:292–303.

Lackner, S., Terada, A., and Smets, B. F. (2008). Heterotrophic activity compromises autotrophic nitrogen removal in membrane-aerated biofilms: Results of a modeling study. *Water Research*, 42(4-5):1102–1112.

Latif, M. A., Mehta, C. M., and Batstone, D. J. (2015). Low pH anaerobic digestion of waste activated sludge for enhanced phosphorous release. *Water Research*, 81:288–293.

Lisitsin, D., Hasson, D., and Semiat, R. (2008). The potential of CO2 stripping for pretreating brackish and wastewater desalination feeds. *Desalination*, 222(1-3):50–58.

Lobry, J., Rosso, L., and Flandrois, J. (1991). A FORTRAN subroutine for the determination of parameter confidence limits in non-linear models. *BINARY*, 3:86–93.

Lu, Y., Slater, F., Bello-Mendoza, R., and Batstone, D. J. (2013). Shearing of biofilms enables selective layer based microbial sampling and analysis. *Biotechnology and Bioengineering*, 110(10):2600–2605.

Mozumder, M. S. I., Picioreanu, C., van Loosdrecht, M. C. M., and Volcke, E. I. P. (2013). Effect of heterotrophic growth on autotrophic nitrogen removal in a granular sludge reactor. *Environmental Technology*, 35(8):1027–1037.

Mulder, A., Graaf, A., Robertson, L., and Kuenen, J. (1995). Anaerobic ammonium oxidation discovered in a denitrifying fluidized bed reactor. *FEMS Microbiology Ecology*, 16(3):177–184.

Ni, S. Q., Ni, J. Y., Hu, D. L., and Sung, S. (2012). Effect of organic matter on the performance of granular anammox process. *Bioresource Technology*, 110:701–705.

Nopens, I., Batstone, D. J., Copp, J. B., Jeppsson, U., Volcke, E., Alex, J., and Vanrolleghem, P. a. (2009). An ASM/ADM model interface for dynamic plant-wide simulation. *Water Research*, 43(7):1913–1923.

Odriozola, M., López, I., and Borzacconi, L. (2016). Modeling granule development and reactor performance on anaerobic granular sludge reactors. *Journal of Environmental Chemical Engineering*, 4(2):1615–1628.

Parawira, W., Kudita, I., Nyandoroh, M. G., and Zvauya, R. (2005). A study of industrial anaerobic treatment of opaque beer brewery wastewater in a tropical climate using a full-scale UASB reactor seeded with activated sludge. *Process Biochemistry*, 40(2):593–599.

Parker, W. J. (2005). Application of the ADM1 model to advanced anaerobic digestion. *Bioresource Technology*, 96(16):1832–1842.

Peiris, B. R. H., Rathnasiri, P. G., Johansen, J. E., Kuhn, A., and Bakke, R. (2006). ADM1 simulations of hydrogen production. *Water Science and Technology*, 53(8):129–137.

Picioreanu, C., van Loosdrecht, M. C. M., Katuri, K. P., Scott, K., and Head, I. M. (2008). Mathematical model for microbial fuel cells with anodic biofilms and anaerobic digestion. *Water Science & Technology*, 57(7):965.

Pokorna-Krayzelova, L., Mampaey, K. E., Vannecke, T. P. W., Bartacek, J., Jenicek, P., and Volcke, E. I. P. (2017). Model-based optimization of microaeration for biogas desulfurization in UASB reactors. *Biochemical Engineering Journal*, 125:171–179.

Press, H., Teukolsky, S., Vetterling, W., and Flannery, B. (2007). *Numerical recipes: The art of scientific computing*. Cambridge University Press, New York, NY, USA, third edition edition.

Prevedello, M., Feldman, H., Nesme, J., Mortensen, M. S., Flores-Alsina, X., Sørensen, S. J., and Gernaey, K. V. (2018). The effect of high precipitate concentration on the microbial community structure in an industrial anaerobic granular sludge reactor. In *IWA Biofilms: Granular Sludge conference, Delft, The Netherlands, March 18-21, 2018*.

Punal, A., Trevisan, M., Rozzi, A., and Lema, J. (2000). Technical note influence of C : N ratio on the start-up of up-flow anaerobic filter reactors. *Water Research*, 34(9):2614–2619.

Reichert, P. (1994). Aquasim–a tool for simulation and data analysis of aquatic systems. *Water Science and Technology*, 30(2):21–30.

Ren, T. T., Mu, Y., Ni, B. J., and Yu, H. Q. (2009). Hydrodynamics of upflow anaerobic sludge blanket reactors. *Environmental and Energy Engineering*, 55(1):516–528.

Rieger, L., Alex, J., Winkler, S., Boehler, M., Thomann, M., and Siegrist, H. (2003). Progress in sensor technology - progress in process control? part i: Sensor property investigation and classification. *Water Science and Technology*, 47(2):103–112.

Rieger, L., Takács, I., and Siegrist, H. (2012). Improving nutrient removal while reducing energy use at three swiss WWTPs using advanced control. *Water Environment Research*, 14:637–681.

Rittmann, B. E. and McCarty, P. L. (1980). Model of steady-state-biofilm kinetics. *Biotechnology and Bioengineering*, 22(11):2343–2357.

Rosen, C. and Jeppsson, U. (2006). Aspects on ADM1 implementation within the BSM2 framework. *Technical report*, pages 1–37. Lund University, Lund, Sweden.

Rosen, C., Jeppsson, U., Rieger, L., and Vanrolleghem, P. A. (2008). Adding realism to simulated sensors and actuators. *Water Science & Technology*, 57(3):337.

Saravanan, V. and Sreekrishnan, T. R. (2006). Modelling anaerobic biofilm reactors – A review. *Journal of Environmental Management*, 81(1):1–18.

Seghezzo, L., Zeeman, G., van Lier, J., Hamelers, H., and Lettinga, G. (1998). A review: The anaerobic treatment of sewage in UASB and EGSB reactors. *Bioresource Technology*, 65:175–190.

Shang, Y., Johnson, B. R., and Sieger, R. (2005). Application of the IWA Anaerobic Digestion Model (ADM1) for simulating full-scale anaerobic sewage sludge digestion. *Water Science and Technology*, 52(1-2):487–492.

Silva, A. M., Lima, R. M. F., and Leão, V. A. (2012). Mine water treatment with limestone for sulfate removal. *Journal of Hazardous Materials*, 221-222:45–55.

Snip, L. J. P., Flores-Alsina, X., Aymerich, I., Rodríguez-Mozaz, S., Barceló, D., Plósz, B. G., Corominas, L., Rodriguez-Roda, I., Jeppsson, U., and Gernaey, K. V. (2016). Generation of synthetic influent data to perform (micro)pollutant wastewater treatment modelling studies. *Science of the Total Environment*, 569-570:278–290.

Sobieszuk, P. and Szewczyk, K. W. (2006). Estimation of (c/n) ratio for microbial denitrification. *Environmental Technology*, 27(1):103–108.

Soda, S., Wada, K., Okuda, M., and Ike, M. (2011). Application of modified ADM1 to long-term experiments for methane/hydrogen production from model organic waste. *Water Practice & Technology*, 6(1):wpt2011009.

Solon, K., Flores-Alsina, X., Gernaey, K. V., and Jeppsson, U. (2015a). Effects of influent fractionation, kinetics, stoichiometry and mass transfer on CH4, H2 and CO2 production for (plant-wide) modelling of anaerobic digesters. *Water Science and Technology*, 71(6):870–877.

Solon, K., Flores-Alsina, X., Kazadi-Mbamba, C., Ikumi, D., Volcke, E. I. P., Vaneeckhaute, C., Ekama, G., Vanrolleghem, P. A., Batstone, D. J., Gernaey, K. V., and Jeppsson, U. (2017). Plant-wide modelling of phosphorus transformations in wastewater treatment systems: Impacts of control and operational strategies. *Water Research*, 113:97–110.

Solon, K., Flores-Alsina, X., Kazadi-Mbamba, C., Volcke, E. I. P., Tait, S., Batstone, D. J., Gernaey, K. V., and Jeppsson, U. (2015b). Effects of ionic strength and ion pairing on (plant-wide) modelling of anaerobic digestion. *Water Research*, 70:235–245.

Steyer, J. P., Buffière, P., Rolland, D., and Moletta, R. (1999). Advanced control of anaerobic digestion processes through disturbances monitoring. *Water Research*, 33(9):2059–2068.

Storck, T., Picioreanu, C., Virdis, B., and Batstone, D. J. (2014). Variable cell morphology approach for individual-based modeling of microbial communities. *Biophysical Journal*, 106(9):2037–2048.

Strömberg, S., Possfelt, M. O., and Liu, J. (2012). Computer simulation of control strategies for optimal anaerobic digestion. *Water Science & Technology*, 67(3):594.

Sun, J., Dai, X., Wang, Q., Pan, Y., and Ni, B. J. (2016). Modelling methane production and sulfate reduction in anaerobic granular sludge reactor with ethanol as electron donor. *Scientific reports*, 6:3531.

Suneethi, S., Sri Shalini, S., and Joseph, K. (2014). State of the art strategies for successful ANAMMOX startup and development : A review. *International Journal of Waste Resources*, 4(4).

Tait, S., Clarke, W. P., Keller, J., and Batstone, D. J. (2009). Removal of sulfate from high-strength wastewater by crystallisation. *Water Research*, 43(3):762–772.

van de Graaf, A. A., de Bruijn, P., Robertson, L. A., Jetten, M. S. M., and Kuenen, J. G. (1996). Autotrophic growth of anaerobic ammonium-oxidizing microorganisms in a fluidized bed reactor. *Microbiology*, 142(8):2187–2196.

van der Star, W. R. L., Abma, W. R., Blommers, D., Mulder, J. W., Tokutomi, T., Strous, M., Picioreanu, C., and van Loosdrecht, M. C. M. (2007). Startup of reactors for anoxic ammonium oxidation: Experiences from the first full-scale anammox reactor in Rotterdam. *Water Research*, 41(18):4149–4163.

Van Hulle, S. W. H., Vandeweyer, H. J. P., Meesschaert, B. D., Vanrolleghem, P. A., Dejans, P., and Dumoulin, A. (2010). Engineering aspects and practical application of autotrophic nitrogen removal from nitrogen rich streams. *Chemical Engineering Journal*, 162(1):1–20.

van Langerak, E., Hamelers, H., and Lettinga, G. (1997). Influent calcium removal by crystallization reusing anaerobic effluent alkalinity. *Water Science and Technology*, 36(6-7).

van Langerak, E. P. A., Gonzalez-Gil, G., van Aelst, A., van Lier, J. B., Hamelers, H. V. M., and Lettinga, G. (1998). Effects of high calcium concentrations on the development of methanogenic sludge in upflow anaerobic sludge bed (UASB) reactors. *Water Research*, 32(4):1255–1263.

van Langerak, E. P. A., Ramaekers, H., Wiecher, J., Veeken, A. H. M., Hamelers, H. V. M., and Lettinga, G. (2000). Impact of location of CaCO3 precipitation on the development of intact anaerobic sludge. *Water Research*, 34(2):437–446.

van Lier, J. B. (2008). High-rate anaerobic wastewater treatment: diversifying from end-of-the-pipe treatment to resource-oriented conversion techniques. *Water Science & Technology*, 57(8):1137.

van Lier, J. B., Tilche, A., Ahring, B. K., Macarie, H., Moletta, R., Dohanyos, M., Pol, L. W., Lens, P., and Verstraete, W. (2001). New perspectives in anaerobic digestion. *Water Science and Technology*, 43(1):1–18.

van Lier, J. B., van der Zee, F. P., Frijters, C. T. M. J., and Ersahin, M. E. (2015). Celebrating 40 years anaerobic sludge bed reactors for industrial wastewater treatment. *Reviews in Environmental Science and Biotechnology*, 14(4):681–702.

Vangsgaard, A. (2013). *Modeling, experimentation, and control of autotrophic nitrogen removal in granular sludge systems*. PhD thesis, DTU Chemical Engineering, Denmark.

Vangsgaard, A. K., Mauricio-Iglesias, M., Gernaey, K. V., Smets, B. F., and Sin, G. (2012). Sensitivity analysis of autotrophic N removal by a granule based bioreac-

tor: Influence of mass transfer versus microbial kinetics. *Bioresource Technology*, 123:230–241.

Vanhooren, H., Van Hulle, S. W. H., De Pauw, D. J. W., and Vanrolleghem, P. A. (2002). Monitoring and modelling a pilot-scale trickling filter using on-line off-gas analysis. *Proceedings of the International Specialized Conference on Biofilm Monitoring, Porto, Portugal, 2002*, pages 260–263.

Vázquez-Padín, J. R., Morales, N., Gutiérrez, R., Fernández, R., Rogalla, F., Barrio, J. P., Campos, J. L., Mosquera-Corral, A., and Méndez, R. (2014). Implications of full-scale implementation of an anammox-based process as post-treatment of a municipal anaerobic sludge digester operated with co-digestion. *Water Science and Technology*, 69(6):1151–1158.

Volcke, E. I. P., Picioreanu, C., Baets, B. D., and van Loosdrecht, M. C. M. (2012). The granule size distribution in an anammox-based granular sludge reactor affects the conversion-implications for modeling. *Biotechnology and Bioengineering*, 109(7):1629–1636.

Volcke, E. I. P., Picioreanu, C., De Baets, B., and Van Loosdrecht, M. C. M. (2010). Effect of granule size on autotrophic nitrogen removal in a granular sludge reactor. *Environmental Technology*, 31(11):1271–1280.

Wanner, O., Eberl, H., Morgenroth, E., Noguera, D., Picioreanu, C., Rittmann, B., and van Loosdrecht, M. (2006). Mathematical modeling of biofilms. IWA Scientific and Technical Report No. 18. London, UK: IWA Publishing.

Weron, R. (2014). Electricity price forecasting: A review of the state-of-the-art with a look into the future. *International Journal of Forecasting*, 30(4):1030–1081.

Wett, B. (2006). Solved upscaling problems for implementing deammonification of rejection water. *Water Science and Technology*, 53(12):121–128.

Wett, B., Schoen, M., Phothilangka, P., Wackerle, F., and Insam, H. (2007). Model-based design of an agricultural biogas plant: Application of anaerobic digestion model no. 1 for an improved four chamber scheme. *Water Science & Technology*, 55(10):21–28.

Wichern, M., Gehring, T., Fischer, K., Andrade, D., Lübken, M., Koch, K., Gronauer, A., and Horn, H. (2009). Monofermentation of grass silage under mesophilic conditions: Measurements and mathematical modeling with ADM1. *Bioresource Technology*, 100(4):1675–1681.

Winkler, M. K. H., Kleerebezem, R., Strous, M., Chandran, K., and van Loosdrecht, M. C. M. (2013). Factors influencing the density of aerobic granular sludge. *Applied Microbiology and Biotechnology*, 97(16):7459–7468.

Xavier, J. B., Picioreanu, C., and van Loosdrecht, M. C. M. (2005). A framework for multidimensional modelling of activity and structure of multispecies biofilms. *Environmental Microbiology*, 7(8):1085–1103.

Xing, B. S., Guo, Q., Zhang, Z. Z., Zhang, J., Wang, H. Z., and Jin, R. C. (2014). Optimization of process performance in a granule-based anaerobic ammonium oxidation (anammox) upflow anaerobic sludge blanket (UASB) reactor. *Bioresource Technology*, 170:404–412.

Zaher, U., Li, R., Jeppsson, U., Steyer, J. P., and Chen, S. (2009). GISCOD: General Integrated Solid waste co-digestion model. *Water Research*, 43(10):2717–2727.

Zhang, Y., Piccard, S., and Zhou, W. (2015). Improved ADM1 model for anaerobic digestion process considering physico-chemical reactions. *Bioresource Technology*, 196:279–289.

Zhao, J., Zuo, J., Lin, J., and Li, P. (2015). The performance of a combined nitritation-anammox reactor treating anaerobic digestion supernatant under various C/N ratios. *Journal of Environmental Sciences*, 30:207–214.

A Appendices

A.1 Supplemental information Chapter 2

Table A.1. Overview of the mass balance data of the corresponding figures (2.2, 2.3, 2.4, 2.5).

	Dataset #1		Dataset #2	
	ADin	ADout	ADin	ADout
COD soluble ($kg\,h^{-1}$)	1366	250	1596	219
COD particulate ($kg\,h^{-1}$)	261	166	642	634
CH_4	0	1209	0	1302
NH_4^+ ($kg\,h^{-1}$)	32.2	43.1	73.3	88.4
$N_{organic}$ (soluble) ($kg\,h^{-1}$)	19.6	13.9	37.2	25.9
$N_{organic}$ (particulate) ($kg\,h^{-1}$)	19.9	9.1	48.0	15.1
P particulate ($kg\,h^{-1}$)	15.0	5.4	33.5	30.3
P soluble ($kg\,h^{-1}$)	9.6	6.7	3.2	3.0
SO_4^{2-} ($kg\,h^{-1}$)	35.5	14.0	40.0	24.6
SO_3^{2-} ($kg\,h^{-1}$)	1.6	4.8	5.7	8.2
HS^- ($kg\,h^{-1}$)	3.7	13.8	10.2	21.6
S in proteins ($kg\,h^{-1}$)	2.1	0	0.34	0
H_2S ($kg\,h^{-1}$)	0	9.8	0	11.23

A.2 Supplemental information Chapter 3

Table A.2. Quantitative fits between model outputs and measured data for #D1 for Model I.

Compound	Deviation (%)	Correlation (R^2)
Methane	12.8	> 0.7
Carbon dioxide	6.4	> 0.7
Hydrogen sulfide	15.8	> 0.7
VFA	2.2	< 0.4
pH	0.39	0.4 – 0.7
$COD_{soluble}$	25.7	0.4 – 0.7
S_{SO4}	6.9	< 0.4
S_{IN}	16.5	< 0.4
S_{IP}	30.5	0.4 – 0.7
Average	13.0	

Table A.3. Quantitative fits between model outputs and measured data for #D2 for Model I.

Compound	Deviation (%)	Correlation (R^2)
Methane	12.9	0.4 – 0.7
Carbon dioxide	4.4	0.4 – 0.7
Hydrogen sulfide	8.6	< 0.4
VFA	28.9	< 0.4
pH	-	-
$COD_{soluble}$	10.4	< 0.4
S_{SO4}	17.6	< 0.4
S_{IN}	16.1	< 0.4
S_{IP}	19.7[1]	> 0.7
Average	14.8	

[1]The data had to be smoothened due to a large peak offset in the model caused by the reactor shut-down not being captured properly.

A.3 Supplemental information Chapter 5

Table A.4. ADM1 kinetic parameter values for #D1 and #D2.

Parameter	Description	Default	#D1	#D2	Units
k_{carb}	Hydrolysis rates for carbohydrates	0.3	30	1	d^{-1}
k_{prot}	Hydrolysis rate for proteins	0.3	30	1	d^{-1}
k_{lip}	Hydrolysis rate for lipids	0.3	30	1	d^{-1}
$k_{m,SRB,H2}$	Uptake rate for autolitotrophic SRBs	38.5	40	50	$kgCOD\,kgCOD^{-1}\,d^{-1}$
$k_{m,H2S,SRB}$	H_2S inhibition for autolitotrophic SRBs	0.50	0.0025	0.50	$kgCOD\,m^{-3}$
$k_{m,H2S,H2}$	H_2S inhibition for hydrogen degraders	0.40	0.0020	0.40	$kgCOD\,m^{-3}$
$k_{m,H2S,ac}$	H_2S inhibition for acetate degraders	0.46	0.0014	0.46	$kgCOD\,m^{-3}$
$k_{m,H2S,pro}$	H_2S inhibition for propionate degraders	0.50	0.0025	0.50	$kgCOD\,m^{-3}$
$k_{m,H2S,c4}$	H_2S inhibition for c4 degraders	0.50	0.0025	0.50	$kgCOD\,m^{-3}$
k_{CaCO3}	Precipitation rate for calcium carbonate	0.01	-	0.0075	d^{-1}

Table A.5. ADM1 stoichiometric parameter values for #D1 and #D2.

Parameter	Description	Default	#D1	#D2	Units
$N_{biomass}$	N content in biomass	0.0062	0.018	0.018	$kmol\,kgCOD^{-1}$
$P_{biomass}$	P content in biomass	0.0007	0.0006	0.0005	$kmol\,kgCOD^{-1}$
$S_{biomass}$	S content in biomass	0.000075	-	0.0001	$kmol\,kgCOD^{-1}$
$S_{proteins}$	S content in proteins	0.00013	-	0.0004	$kmol\,kgCOD^{-1}$

Process and Systems Engineering Centre (PROSYS)
Department of Chemical and Biochemical Engineering
Technical University of Denmark
Søltofts Plads, Building 229
DK - 2800 Kgs. Lyngby
Denmark

Phone: +45 45 25 28 00
Web: www.kt.dtu.dk/forskning/prosys